Proximity Operations of an Underwater Vehicle to a Host Vessel

by

Jess Eugene Riggle

B.S., Mechanical Engineering
California Polytechnic State University, San Luis Obispo, 1986

Submitted to the Department of Ocean Engineering
in Partial Fulfillment of the Requirements for the Degrees of

Naval Engineer
and
Master of Science in Naval Architecture

at the
Massachusetts Institute of Technology
May 1996

Signature of
Author_____

Certified
by_____
Jerome Milgram, Professor of Ocean Engineering
Thesis Advisor

Accepted by_____
A. Douglas Carmichael, Professor of Power Engineering
Chairman, Committee on Graduate Students, Department of Ocean Engineering

DISCLAIMER NOTICE

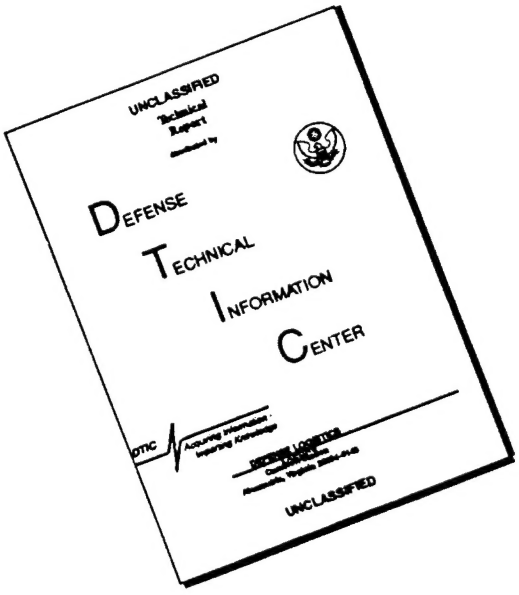

THIS DOCUMENT IS BEST QUALITY AVAILABLE. THE COPY FURNISHED TO DTIC CONTAINED A SIGNIFICANT NUMBER OF PAGES WHICH DO NOT REPRODUCE LEGIBLY.

DEPARTMENT OF THE NAVY

NAVAL RESERVE OFFICERS TRAINING CORPS CONSORTIUM
BOSTON UNIVERSITY-M.I.T.

Massachusetts Institute of Technology
77 Massachusetts Ave Room 20E-125
Cambridge MA 02139-4307

Boston University
116 Bay State Road
Boston MA 02215-1796

IN REPLY REFER TO:

1500
61:rjg
Ser 1079
29 Jul 1996

From: Comanding Officer, Boston University-MIT NROTC Consortium, Cambridge, MA
To: Director of Civilian Institutions Programs, Code 031, Naval Postgraduate School, 589 Dyer Road, Room 228, Root Hall, Monterey, CA 93943-5143

Ref: (a) NAVPGSCOLINST 1520.1D

Subj: END OF TOUR REPORTS

Encl: (1) End of Tour Reports
(2) Two Copies of Transcripts
(3) Two Copies of Thesis

1. The following students have graduated and completed the Educational Skill Requirements (ESR) necessary for award of a subspeciality code. Enclosures (1) - (3) are forwarded in accordance with reference (a).

Name	Curriculum	Subspeciality Code
LT Michael Amrozowicz	510	51N
LCDR John M. Barentine	510	51N
LCDR David R. Beckett	510	51N
LT Jess E. Riggle	510	51N
LT James E. Tatera	510	51N
LCDR Mark W. Thomas	510	51N
LCDR Bruce W. Brisson	520	52N
LCDR Thomas J. Moore	520	52N

M. S. WELSH
LCDR USN
By direction

Copy to:
Capt R. Tuddenham (SEA03R) w/ Encl (1) ,(Brisson, Moore)
PERS 445 w/o Encl
file

Proximity Operations of an Underwater Vehicle to a Host Vessel

by

Jess Eugene Riggle

Submitted to the Department of Ocean Engineering in Partial Fulfillment of the Requirements for the Degrees of Naval Engineer and Master of Science in Naval Architecture.

ABSTRACT

This paper presents a method for estimating the forces and moments on the six axes of an Unmanned Underwater Vehicle (UUV) operating in close proximity to a host vessel. Forces and moments encountered by the vehicle in the host vessel launchway, near the vessel and clear of the launchway, and far away from the host vessel, are modeled from experimental and theoretical sources. A quasi - steady approach to the vehicle launch dynamics allows coupling of experimental data, potential flow theory, and hydrodynamic maneuvering coefficients to develop an algorithm capable of modeling vehicle and host vessel interactions with any user defined trajectory.

A vehicle motion simulation study was performed using the Revised Standard Equations of Motion (EOM) augmented to incorporate the interaction force model for proximity effects of the UUV to a host. Application of the trajectory simulation and force and moment time history are developed for a underwater vehicle launching from a submerged host illustrating the hydrodynamic interaction of the vehicle to the host. The method is developed to account for host forward speed, UUV propulsor effects, and open water hydrodynamics. The robustness of the method is demonstrated for several launch trajectories.

Thesis Supervisor: Dr. Jerome Milgram

Table of Contents

List of Illustrations and Figures

List of Tables

List of Symbols

g	acceleration due to gravity [ft/sec^2]
m	mass of vehicle [slugs]
p	roll rate
q	pitch rate
r	yaw rate
u	surge velocity
v	sway velocity
w	normal velocity
x,y,z	position in inertia reference frame
x_B,y_B,z_B	position of center buoyancy in vehicle reference frame
x_C,y_C,z_C	position limits at launchway exit in host relative coordinate system
x_G,y_G,z_G	position of center of gravity in vehicle reference frame
ρ	density of water [slug/ft^3]
ϕ	roll angle
θ	pitch angle
ψ	yaw angle
B	buoyancy
CFX	axial non dimensional force coefficient
CFY	lateral non dimensional force coefficient
CMZ	lateral non dimensional moment coefficient
K	roll moment
L	vehicle length
M	pitch moment
N	yaw moment
PTF	non dimensional Propulsive Thrust Factor coefficient
$\vec{\Re}$	vector quantity in non inertial reference frame
$\vec{\Re}_0$	vector quantity in inertial reference frame
RPM	revolutions per minute
U	host vessel velocity
W	vehicle weight [lb]

With respect to equation of motion hydrodynamic coefficients, SNAME [16] established a symbolic convention which will be followed here where the subscript below the coefficient implies the slope or derivative relationship of the coefficient with respect to the indicated subscript.

Acknowledgments

There are many people who assisted me in my efforts as I prepared this thesis. Special recognition is due to the following:

Jerome Milgram, for his patience and continued support;

The men and women of the Marine Instrumentation Laboratory for their camaraderie, and Soren Jensen for laying the experimental groundwork for this effort;

Robert Hickey for his continued interest and willingness to entertain discussion and foster ideas.

The U. S. Navy, for the graduate education opportunity provided;

My parents, Roger and Billie, for their unfailing support and encouragement throughout my life;

My sisters, for seeing past and future;

And especially, Jennifer Lee, for teaching me a lesson in faith under adversity.

Chapter 1 INTRODUCTION

1.1 Motivation

Underwater vehicles find applications in an increasing number of diverse missions and roles. Recent uses of AUV's and ROV's both in commercial and military applications continue to outline the capabilities, and limitations of employing unmanned underwater vehicles (UUV). Integral to the use of a UUV, whether autonomous underwater vehicle (AUV) or remotely operated vehicle (ROV), is the process used for launch and recovery. This process is largely driven by the type of support ship, land based launch and recovery facility, or submerged host platform. Launch and recovery from a submerged host represents an opportunity to add flexibility to the vehicle mission, but adds complexity to vehicle design. The ability of a submerged host vessel, hereafter generically referred to as the host, to deploy a ROV or AUV to a mission commencement location in latitude, longitude and depth offers unique advantages in mission duration, real time interrogation, and covert mission accomplishment over other launch platforms. The ability to properly control a vehicle as it transitions from within the submarine launchway to a point far away from the host and back until finally rehoused represents a complex dynamic process for which improved models are necessary to investigate the forces, moments and trajectory of the vehicle during the course of its mission and through launch and recovery. The design of effective vehicle control is the goal of the hydrodynamic modeling of the launch and recovery process.

1.2 Research Objectives

Launch and recovery of a vehicle from a submarine is expected to represent the most demanding case for control effectiveness. The effect of the host body speed and launchway geometry on the hydrodynamic flow characteristics in and around the launchway have been documented by experiment [11]. Additionally, interaction effects between the UUV and the host have been quantified by experiment for specific cases [11]. One can foresee that the combined effects which in turn are coupled, lead to a complex hydrodynamic modeling problem.

The first objective of this thesis is to use experimental observations from a scale UUV within and in the vicinity of a launchway to develop a model to describe the forces and moments acting on a UUV as a function of hydrodynamic and geometric criteria relative to the host. Due to the specific nature of vehicle and host geometry on the forces experienced, the model will be tailored to the host and UUV. However this specificity is necessary only in so far as to proceed to the next objective, that of determining a reasonable simulation to determine the time dependent forces and moments acting upon the vehicle.

This second objective is to incorporate this force model into a form of the Revised Standard Submarine Equations of Motion [5] to determine the forces and moments acting upon the vehicle given a specified trajectory. This investigation relies upon mating experimental data in the complex region within the launchway, with inviscid flow code results external to the launchway and in proximity to the host "boundary", and accounting for viscous effects of cross flow drag associated with the vehicle transitioning through a region where the vehicle axis is not aligned with the mean free stream velocity. The resulting control force simulator is intended to be adaptable to alternate vehicle geometries.

Chapter 2 FORCE MODEL

2.1 Introduction

The forces acting upon a UUV operating in the open ocean differ from those experienced when operating in the vicinity of a boundary, such as the free surface, ocean bottom, or host vessel. For the purposes of this thesis, boundary interaction effects are limited to a plane rigid wall approximation of a host vessel except in the internal region of the launchway of the host. Interaction forces during launch and recovery, and through the transition to the "infinite fluid", are of direct interest in determining the feasibility of the control system and/or the operating envelope for launch and recovery. Significant work has been undertaken in the past, including computational modeling of these forces to assess the effects of high speed ejection of torpedoes from submarines [2]. In the region of interest for UUV launch and recovery, it will be necessary to operate within a different regime of slow forward speed of the host and slow relative speed of the UUV to the host. This combination of slow host and UUV relative speed indicates the plausibility of modeling the UUV launch and recovery interaction forces as quasi - steady, the UUV stationary with respect to the host and slowly changing with respect to its variation in geometric relation to the host. This approach allows use of experimental results to develop a model for the forces in this region. Steady flow potential based codes may then be used to model the interaction effects of the vehicle near the host to resolve areas where experimental data is incomplete.

2.1.1 Background

The determination of the hydrodynamic forces present on a vehicle transitioning from a submarine launchway is complicated by the number of parameters involved and the complexity of the fluid -body interactions. For a baseline case with no vehicle in the

launchway Sjoblom and Schwemin [15] showed that the flow in a typical submarine launchway is unsteady and turbulent, with turbulence intensities within the cavity ranging from 10 - 20% of free stream velocity. Experimental observations document average flow magnitudes 0 - 10% of the free stream at the aft end of the cavity and approximately 30% of free stream at the midpoint of the launchway shutter. They document a large recirculation region in mid - region of the cavity and a separated region approximately 30% of the cavity length forward. As reported, the turbulence shows a flow periodicity with frequency content between 1 and 4 Hz. External to the launchway and turbulent boundary layer potential flow predictions compare well with measurements.

In order to assess the force and moment characteristics of a vehicle in launch or recovery transition, both the region within the launchway and external to it require modeling. The model must be sophisticated enough to capture three dimensional geometry effects, body - to - body interactions, as well as viscous flow effects. Inviscid potential flow models capture the proximity interaction effects; however, they do not include viscous drag effects including cross flow drag or lift forces generated by control surfaces and vorticity shed into the wake from separation. Numerical potential and viscous flow techniques can not at present handle all these effects so a combination of experimental results, numerical techniques, and semi-empirical non linear motion derivatives are suggested for investigating the launch and recovery envelope.

2.1.2 Experimental Data

Launchway Zone

Jensen and Milgram [11] describe an experiment conducted using a 1/10 scale model of an UUV transitioning through a submarine launchway. Figure 2-1 illustrates the basic configuration and geometry associated with the vehicle and the host. Principle dimensions of the UUV vehicle are listed in table 2-1.

UUV Principle Dimensions	
Length (ft)	10.5
diameter (ft)	1.604

Table 2-1 Principle Vehicle Dimensions

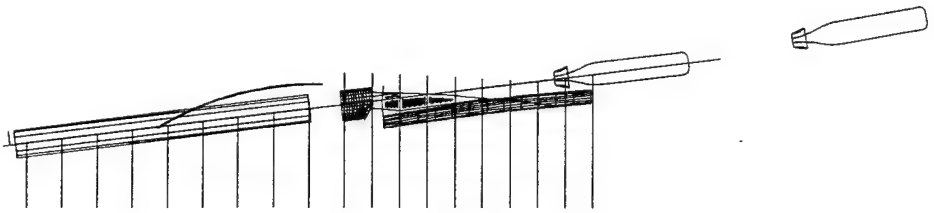

Figure 2-1

Data was obtained for the forces and moments at various points of advance along the launchway centerline. Reference to a "guide can" structure existing in the torpedo tube launchway is made in the model tests. The vehicle was advanced from a position farthest aft, corresponding to the aft end of the propulsor duct flush with the forward edge of the guide can, to a position 10 inches forward of this reference (100 inches full scale). This range of traverse starts with the vehicle fully within the launchway and extends to a position with the aft end of the propulsor duct approximately even with the forward most point of the launchway. Data in all six degrees of freedom were obtained at each position along the launchway for different onset flow conditions corresponding to the speed of the free stream past the host allowing the effect of forward speed on the host to be modeled. The UUV model was configured with a ducted propulsor which was operated during the tests at various RPM for each advance position and onset flow combination to simulate the influence of propulsor forces and race effects on the induced flow.

Near Boundary Zone

Once the vehicle is outside of the launchway, the geometry of the vehicle and the host can be approximated as a body in proximity to a plane rigid boundary. The approach taken here, utilizes results from a Boundary Integral Element Method (BIEM) panel code to determine the force and moment effects due to proximity operations external to the launchway. This method uses inviscid potential flow theory and does not include viscous effects. A description of the method and implementation is contained in [14]. The effect of the propulsor on the induced flow, and accompanying modification to the pressure integral is not captured by the BIEM in this application. An attempt to include these effects is made through use of experimental data obtained for the UUV at various onset flow speeds, propeller RPM, and clearance from the approximated plane boundary.

2.2 Modeling Results

2.2.1 Coordinate System

The force and moment models are referred to a right-hand orthogonal coordinate system of moving axes, fixed in the UUV with the origin located at the center of mass (CG) of the vehicle. The positive directions of the axes are x - forward, y - starboard, and z - downward in accordance with Standard Nomenclature [16].

2.2.2 Launchway Model

The experimental data lead to a model of the forces and moments experienced by the vehicle as a function of specific dependent variables. The parameters varied during the testing used to develop the model were:

(1) onset flow speed

(2) advance along the launchway axis

(3) propulsor rpm

(4) thruster flow and direction

The data runs with the thruster running were not used in this analysis in order to limit the force and moment effects to those induced by body and launchway geometry and propulsor effects. The forces and moments may be developed in accordance with the following dimensional form:

$$F = f(d, U, \rho, x, y, z)$$
$$M = f(d, U, L, \rho, x, y, z)$$

The following non-dimensional terms are defined for use in developing a model independent of scale.

$$\frac{Advance}{Length}$$

$$CFY = \frac{F}{\frac{1}{2}\rho U_{Of}^{\,2} A_f}$$

$$CMZ = \frac{M}{\frac{1}{2}\rho U_{Of}^{\,2} A_f L}$$

$$PTF = \frac{(PROPULSIVE\ FORCE)}{\frac{1}{2}\rho U_{Of}^{\,2} A_f}$$

where: $CF \equiv$ *Force Coefficient*
$CM \equiv$ *Moment Coefficient*
$PTF \equiv$ *Propulsive Thrust Factor*
$U_{Of} \equiv$ *Onset flow speed*
$A_f \equiv$ *Frontal Area*
$L \equiv$ *Vehicle Length*

For each data set the forces and moments recorded were converted to standard body coordinates with forces and moments limited to the horizontal plane being modeled in this case. A propulsion model was required which would allow robust modeling of propeller

effects. The non-dimensional Propulsive Thrust Factor (PTF) was used, with PTF determined for each data set by measuring the mean recorded thrust at zero RPM for each onset flow condition and advance to length position and subtracting this value from the axial force. The zero PTF data corresponds to the axial drag force experienced in the launchway due to the body position alone and was modeled as well. The procedure selected to arrive at a model recognized that significant variance existed in the experimental data. Figures 2.2 through 2.14 reflect the non dimensional data with associated best least squares linear regression fit.

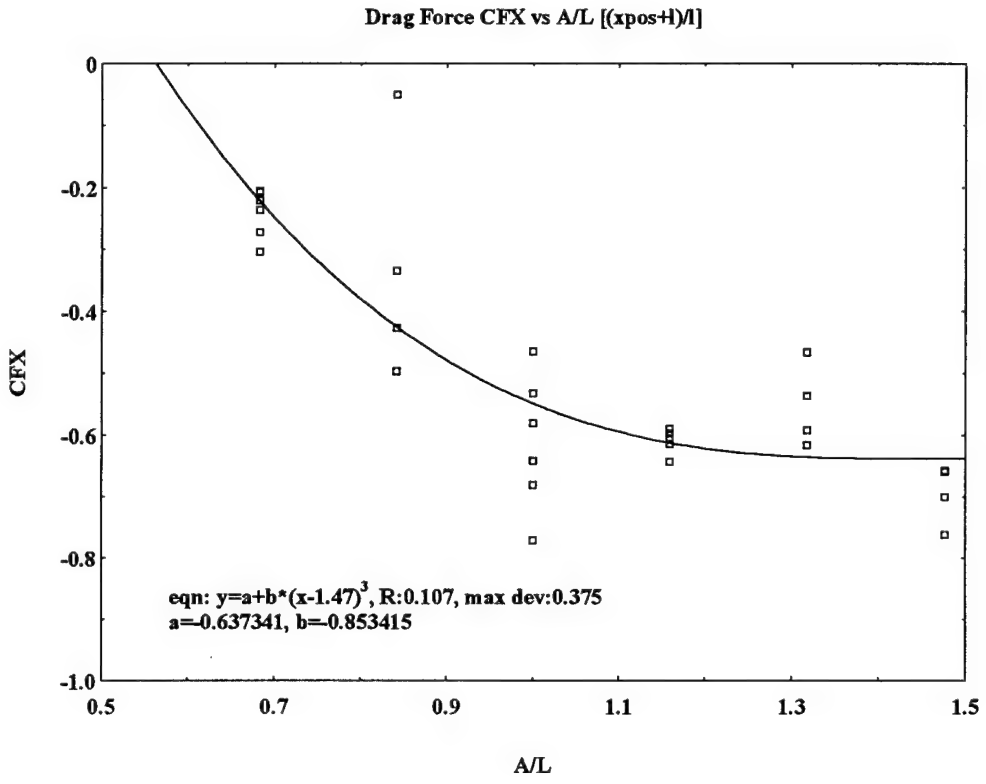

Figure 2.2 Drag Force

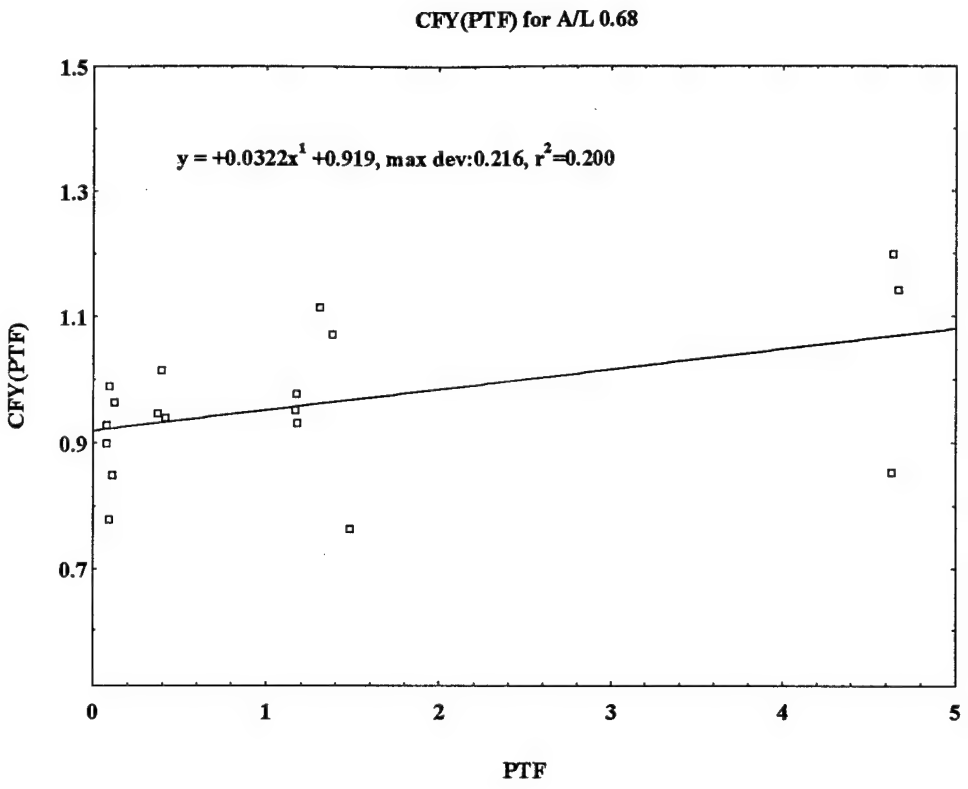

Figure 2.3 Lateral Force for A/L = 0.68

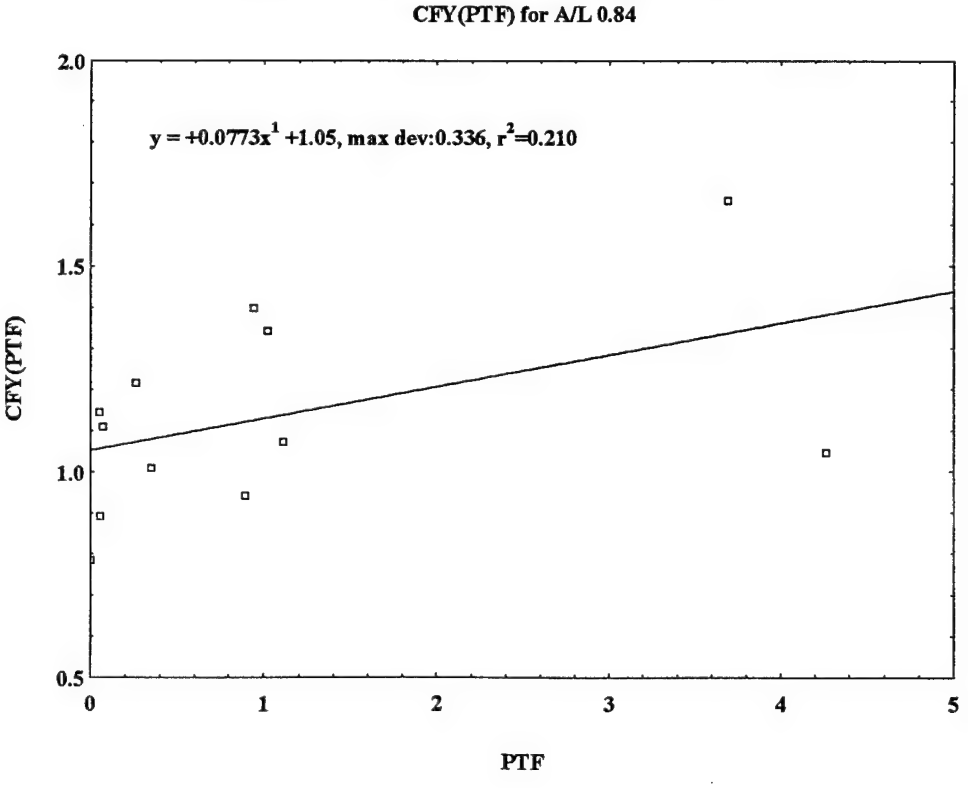

Figure 2.4 Lateral Force A/L = 0.84

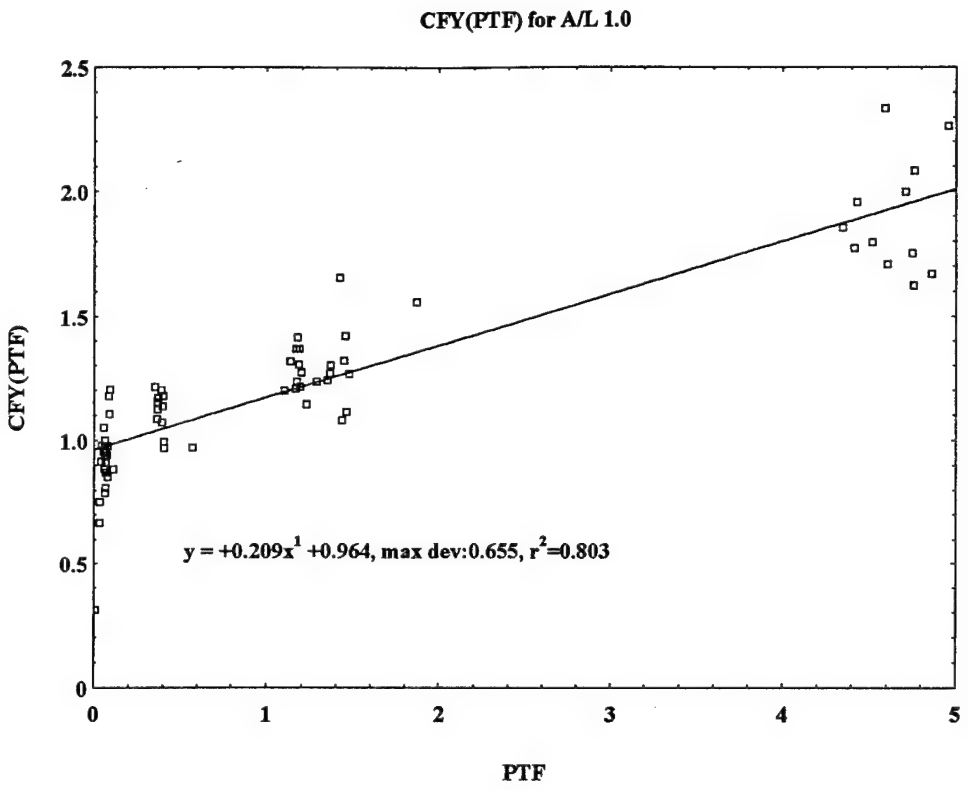

Figure 2.5 Lateral Force A/L = 1.0

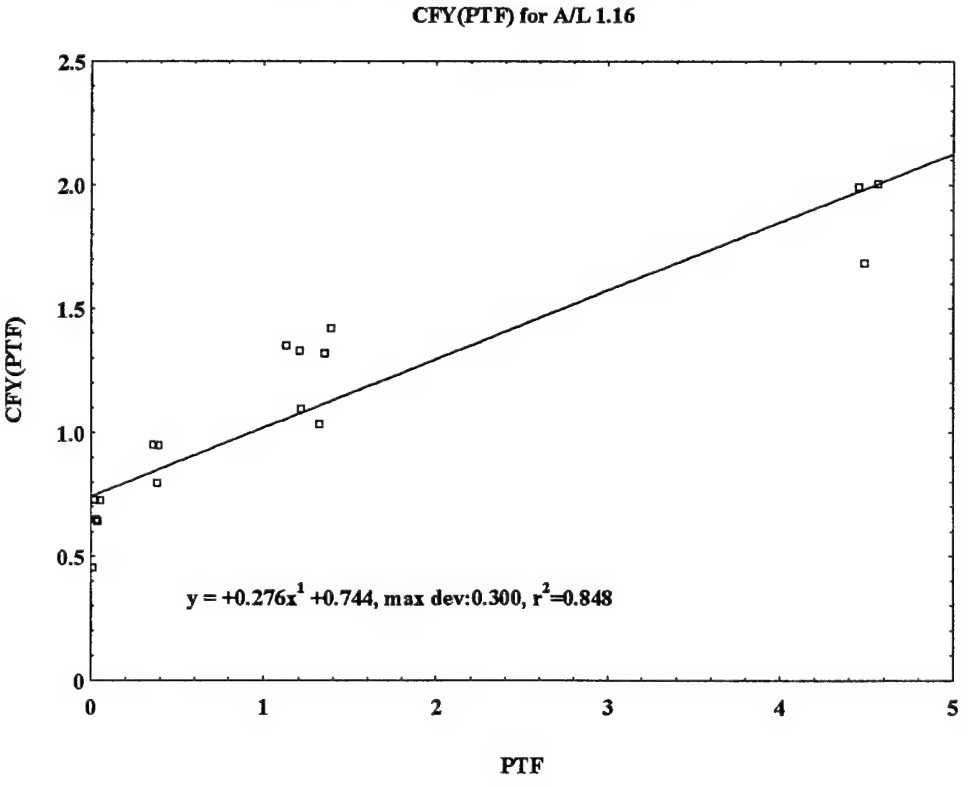

Figure 2.6 Lateral Force A/L = 1.16

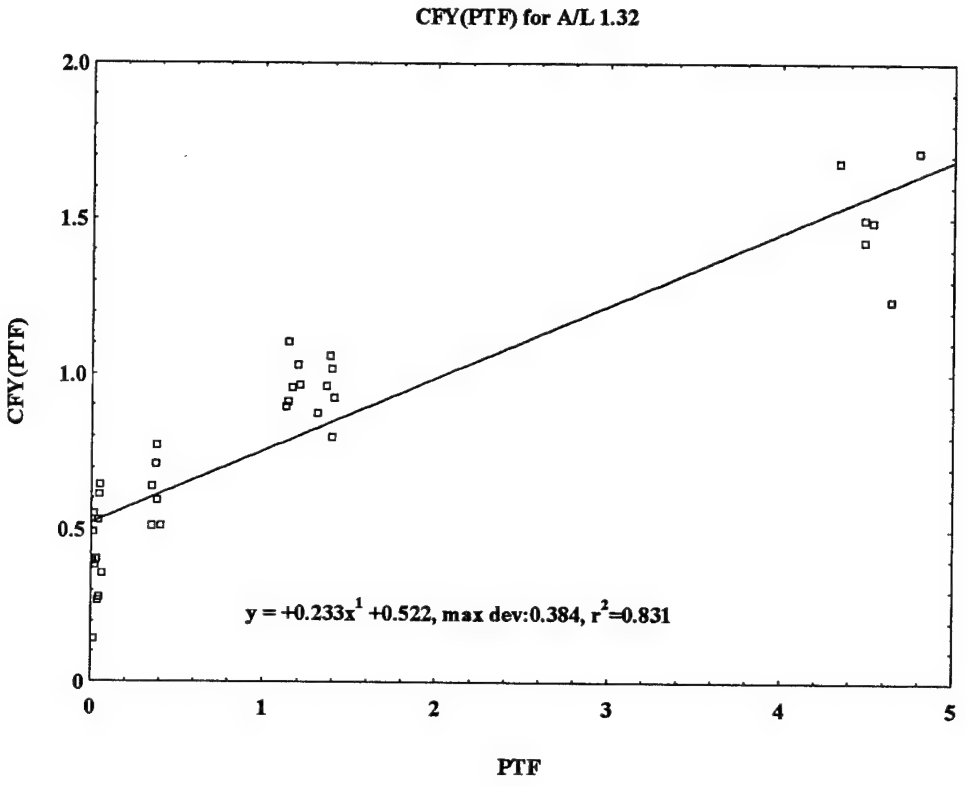

Figure 2.7 Lateral Force A/L = 1.32

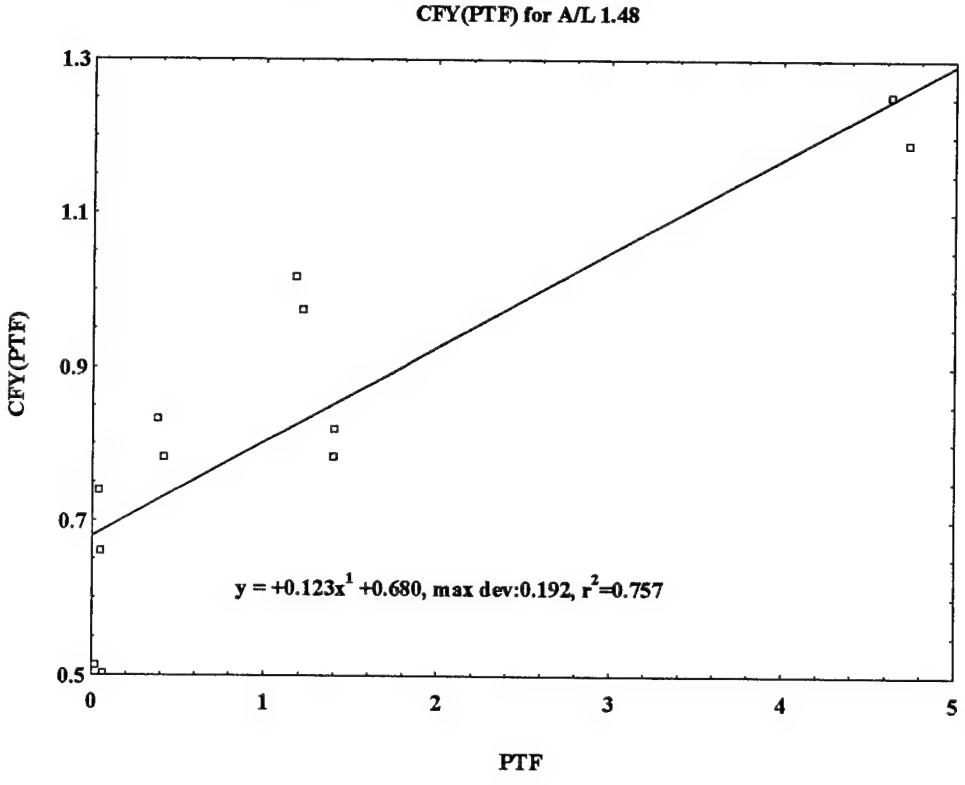

Figure 2.8 Lateral Force A/L = 1.48

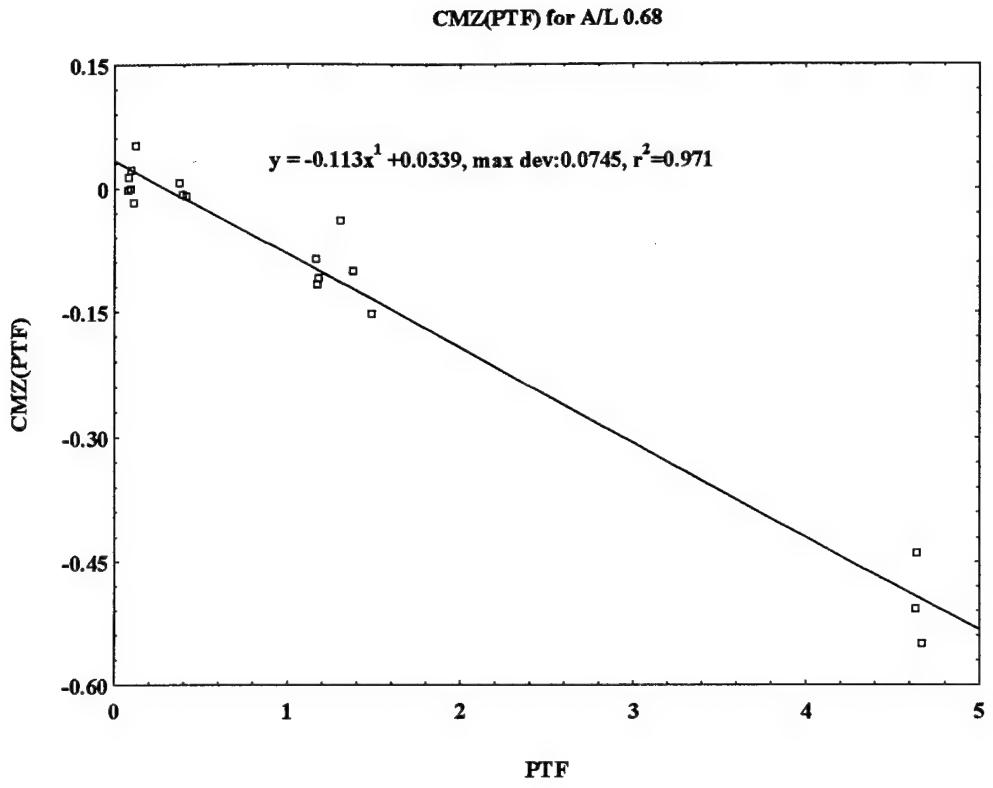

Figure 2.9 Lateral Moment A/L = 0.68

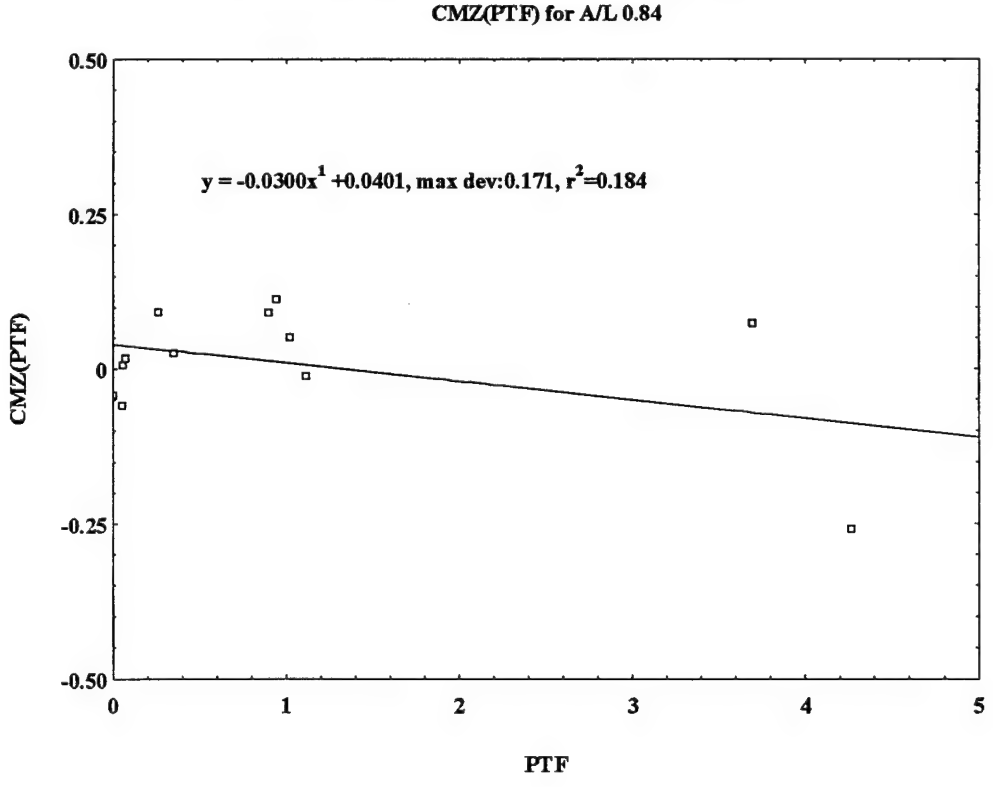

Figure 2.10 Lateral Moment A/L = 0.84

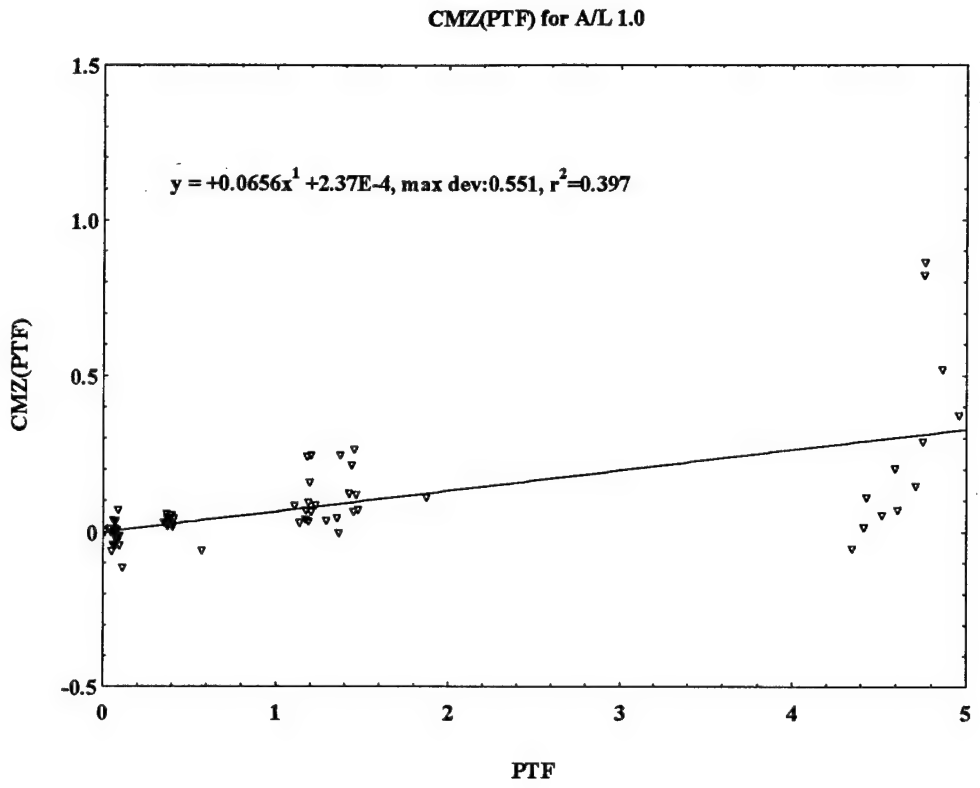

Figure 2.11 Lateral Moment A/L = 1.0

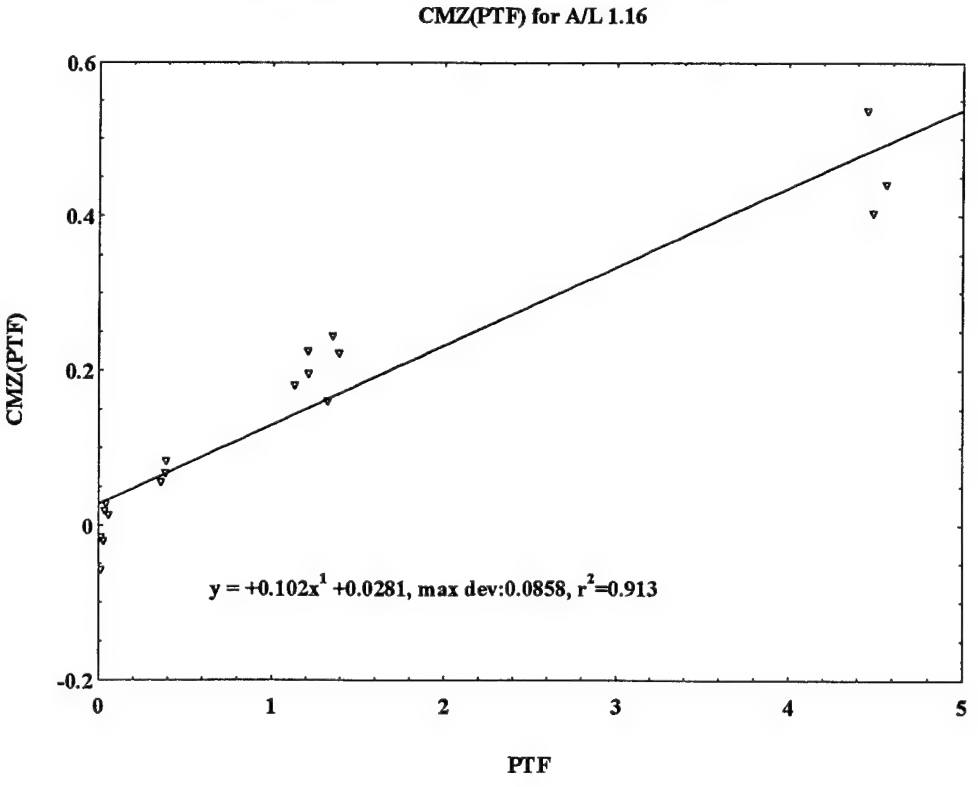

Figure 2.12 Lateral Moment A/L = 1.16

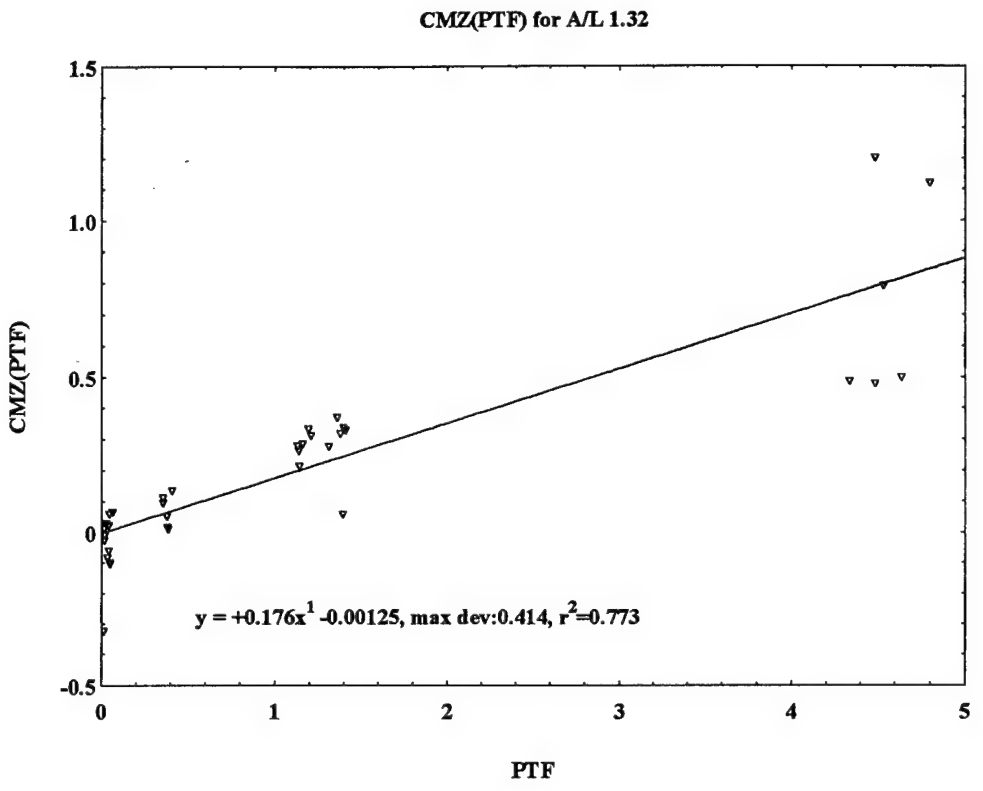

Figure 2.13 Lateral Moment A/L = 1.32

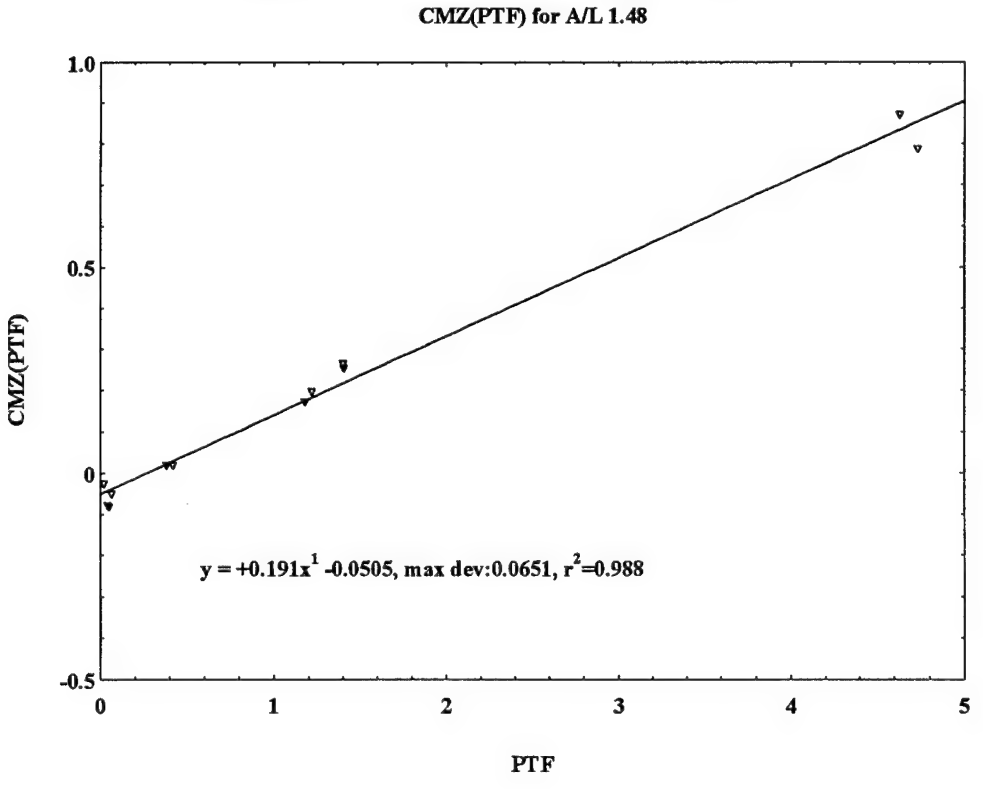

Figure 2.14 Lateral Moment A/L = 1.48

A One Way Analysis of Variance (ANOVA) was conducted on each data set of force and moment as a function of A/L and PTF. Table 2-2 summarizes the results.

A/L	Data	F Ratio	Prob > F	r^2
0.68	CFY	4.0022	0.0627	0.200087
	CMZ	539.6004	<0.0001	0.971202
0.84	CFY	2.6603	0.1339	0.210132
	CMZ	2.2577	0.1639	0.184186
1.0 †	CFY	276.3695	<0.0001	0.802538
	CMZ	44.7450	<0.0001	0.396869
1.16	CFY	88.9794	<0.0001	0.847589
	CMZ	167.6809	<0.0001	0.912892
1.32	CFY	166.9032	<0.0001	0.830764
	CMZ	116.0631	<0.0001	0.773429
1.47	CFY	31.1761	<0.0002	0.757141
	CMZ	857.6477	<0.0001	0.988475

† (2) outlying points omitted

Table 2-2 One Way ANOVA Results

In Table 2-2 , the F-ratio is a statistical measure indicating whether the model is a better fit than the response mean, as determined by

$$F\text{-}ratio = \frac{\left(\sum y_i^2 / Degrees\,of\,freedom\right)_{model}}{\left(\sum y_i^2 / Degrees\,of\,freedom\right)_{error}}$$

The r^2 category represents the amount of total variation accounted for by the model with the remaining variation attributed to random error and is determined as

$$r^2 = \frac{\left(\sum y_i^2\right)_{model}}{\left(\sum y_i^2\right)_{Ctotal}}$$

To conclude from Table 2-2 that the force and moment are dependent upon PTF the F-ratio must exceed an observed significance probability (P-Value) of 0.05. To determine the effectiveness of the model, r^2 is used in conjunction with the F-ratio. The case for A/L of 1.0 utilized the r^2 parameter to omit two outlying points from the model. The results indicate that for the majority of sample conditions the effect of PTF at each A/L is

present, and that a linear model is justified. Higher order models were not justified In order to arrive at a smooth model for force and moment as a function of PTF and A/L the $\partial C_{FY}(PTF)/\partial PTF_{A/L}$ is used to fit a 3rd order cubic function and the intercept is adjusted to make a best fit. Figure 2-15 and 2-16 reflect the best fit for force and moment within the launchway. It can be seen that a positive outboard force exists for a minimum A/L of 0.64 and remains positive throughout the vehicle transition along the launchway centerline with a maximum value at an A/L of 1.15 which corresponds to approximately one quarter of the stern shadowed by the launchway. The lateral force then diminishes to 50% of this force at the maximum A/L of 1.48. Lateral moment effects are quite different, showing an inboard moment at minimum A/L followed by a zero crossing at A/L = 0.9. From this position the moment shows a continual increase to a maximum with the vehicle fully emerged from the host, corresponding in magnitude but opposite sign its value at minimum A/L.

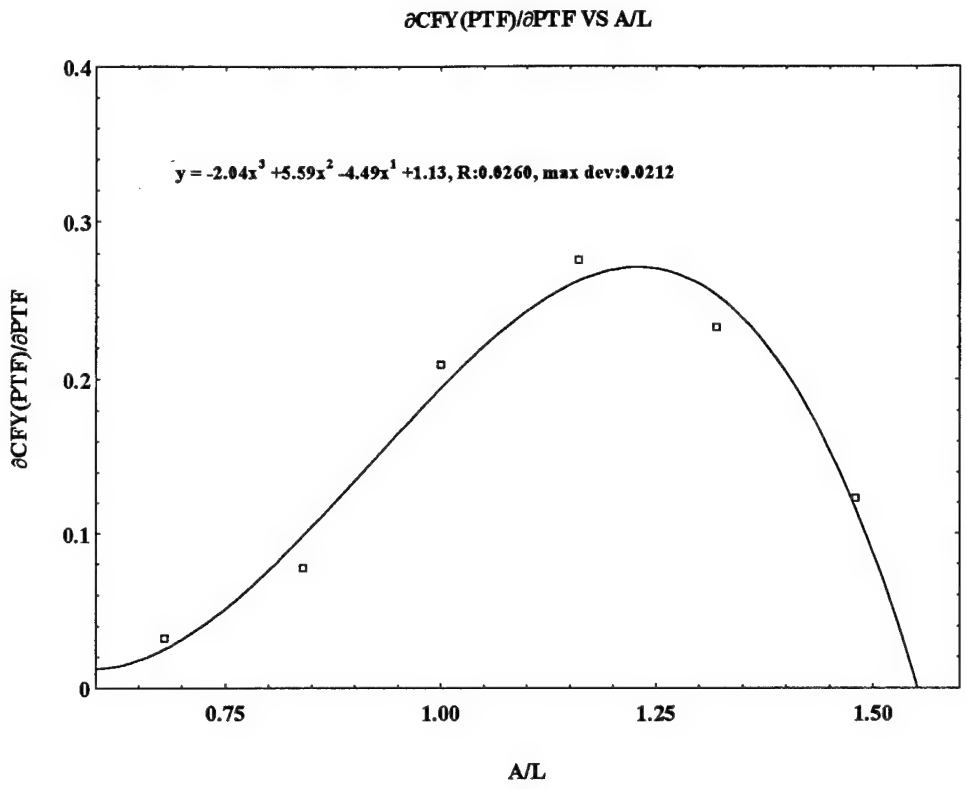

Figure 2.15 Fit of $\partial CFY(PTF)/\partial PTF_{A/L}$

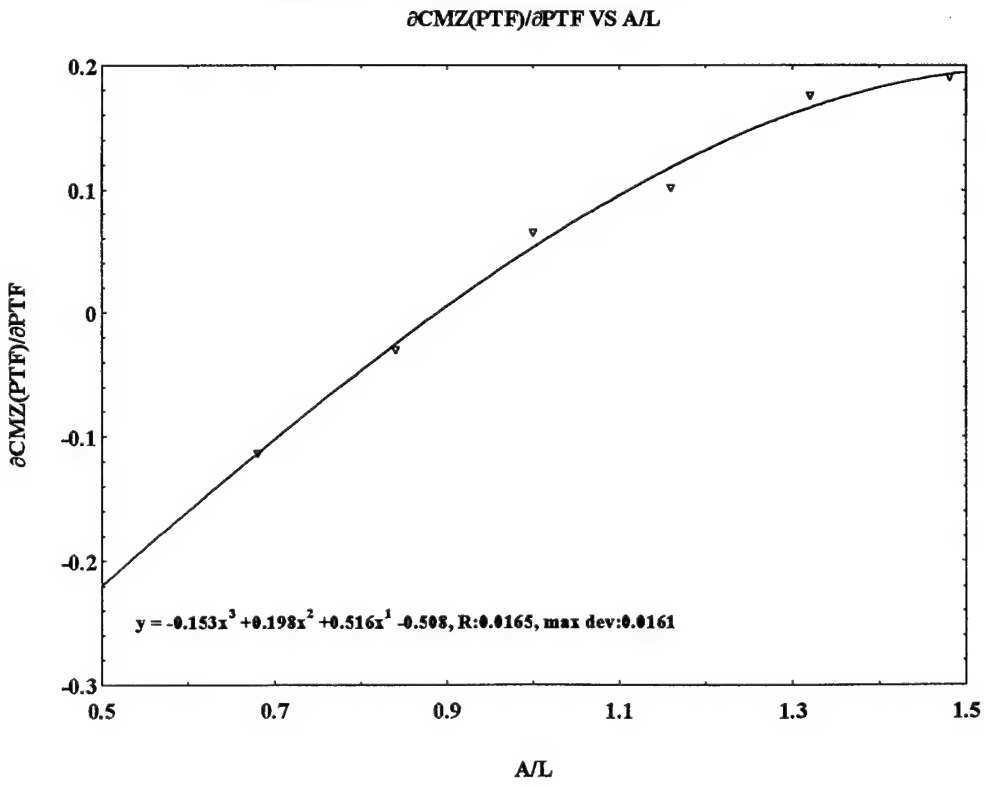

Figure 2.16 Fit of $\partial CMZ(PTF)/\partial PTF_{A/L}$

The resulting force and moment model in the launchway are expressed as

$$CFY = f_3\left(\partial CFY(PTF)/\partial PTF_{A/L}\right)A/L + f_1\left(CFY_{intercept}\right)$$

$$CMZ = f_3\left(\partial CMZ(PTF)/\partial PTF_{A/L}\right)A/L + f_1\left(CMZ_{intercept}\right)$$

where f_1 represents a linear fit

f_3 represents a third order polynomial fit

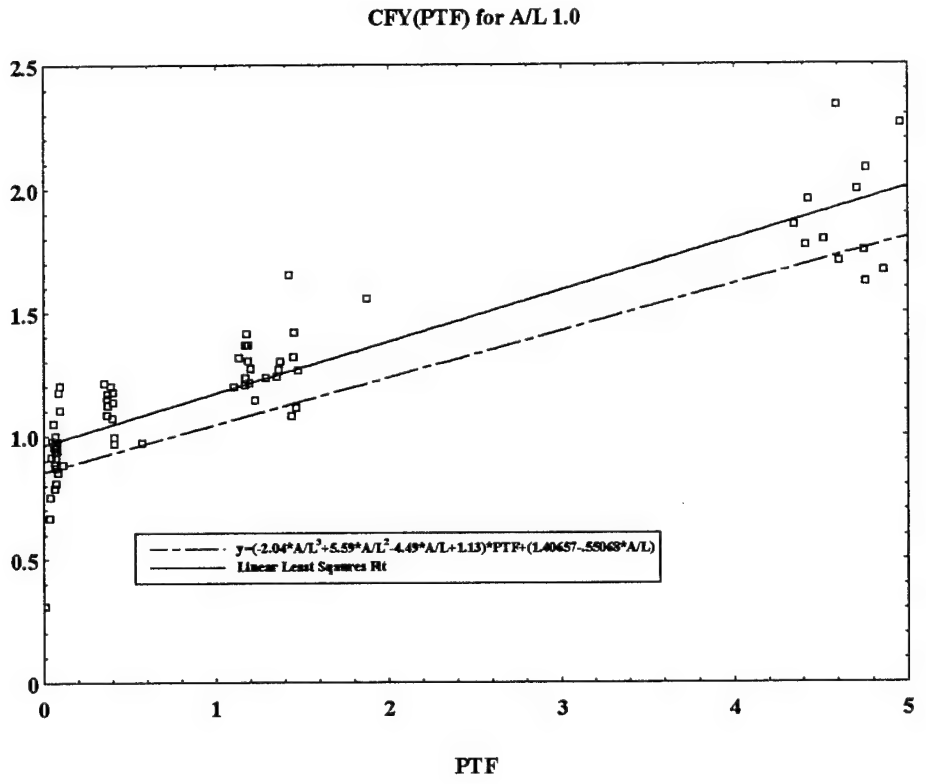

Figure 2.17 Sample of Lateral Force Model Fit A/L = 1.0

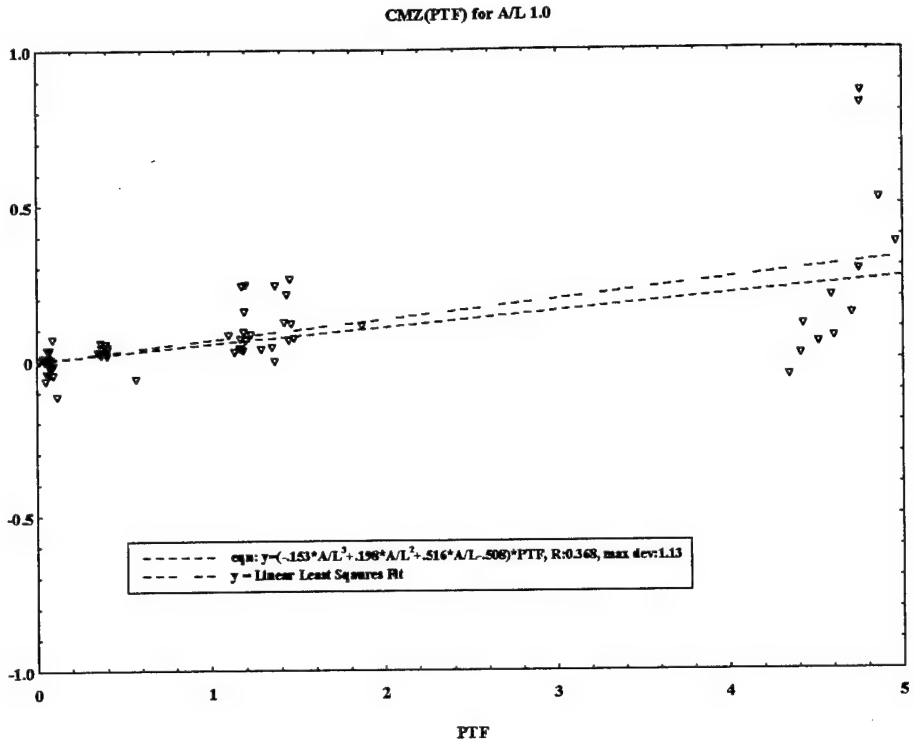

Figure 2.18 Sample of Lateral Moment Model Fit A/L = 1.0

2.2.2 Host Proximity

With the vehicle near the boundary but not in the launchway, insufficient data existed in [11] to predict the effects of relative pitch and clearance from the boundary. To develop this model, an inviscid potential flow panel code was resorted to, in order to determine the near host interaction effects. Difficulties in the numerical hydrodynamics were encountered in modeling due to the blunt forward end of the UUV geometry. Initial paneled models attempted to reflect the bow accurately, however the large change in sectional area vs. length resulted in a large negative pressure at the bow leading to excessive axial suction force instead of the zero drag condition expected. Modification of the model to blend the change in bow cross section over increased length provided a model which corresponded well with strip theory and experimental data to a similar vehicle [10]. The resulting panel geometry is illustrated in Figure 2.19.

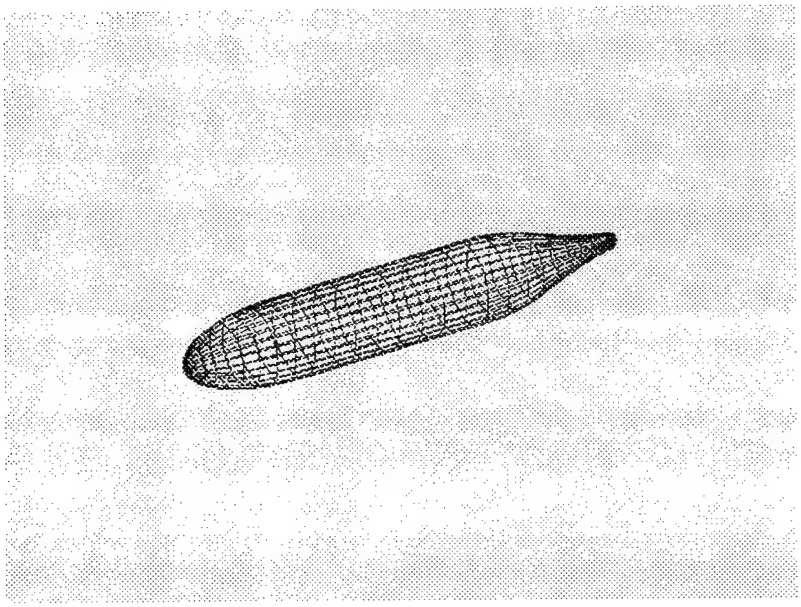

Figure 2.19 UUV Panel Geometry

The proximity model is obtained in two parts. First, investigating the effect of relative proximity to the boundary both with and without relative pitch including far field determination of the Munk moment using potential flow. And second, investigating the effect of PTF on force and moment from experimental data. Figure 2.20 shows the suction force and moment as a function of gap/diameter, where gap refers to the distance from the vehicle molded shell to the boundary. The effect of pitch and gap/diameter on the force and moment is illustrated for selected cases in Figures 2.21 through 2.23. The non linear least square fit is superimposed in Figures 2.21 and Figure 2.22 showing good agreement over the range of combinations of pitch and gap/diameter. Figure 2.23 represents the potential flow Munk moment determined with the vehicle in an unbounded fluid domain.

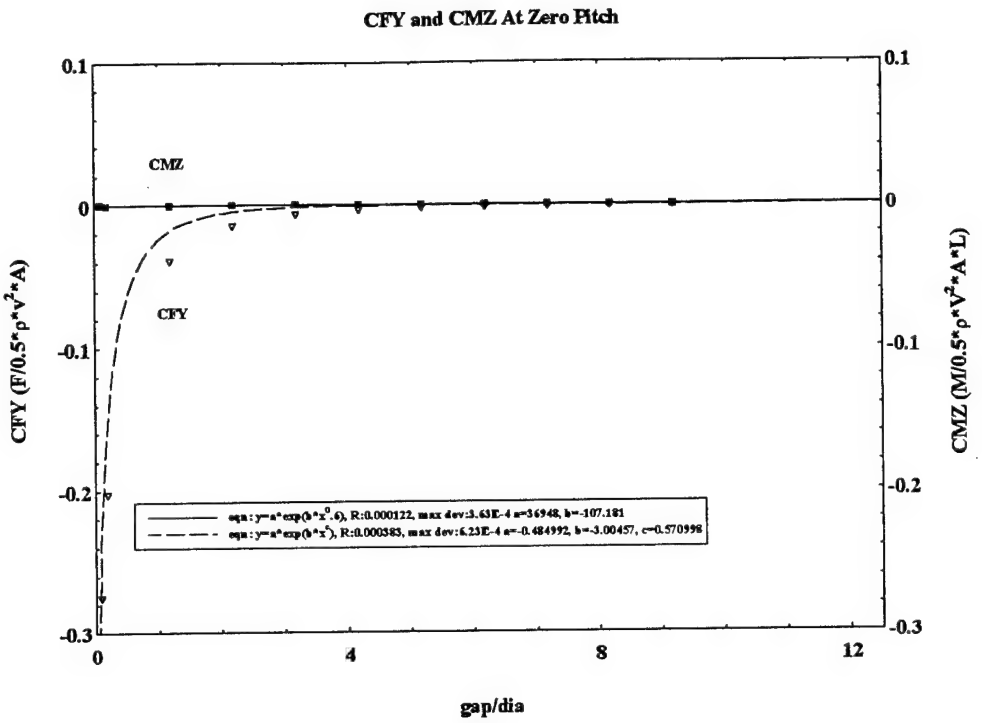

Figure 2.20 Boundary Interaction At Zero Pitch

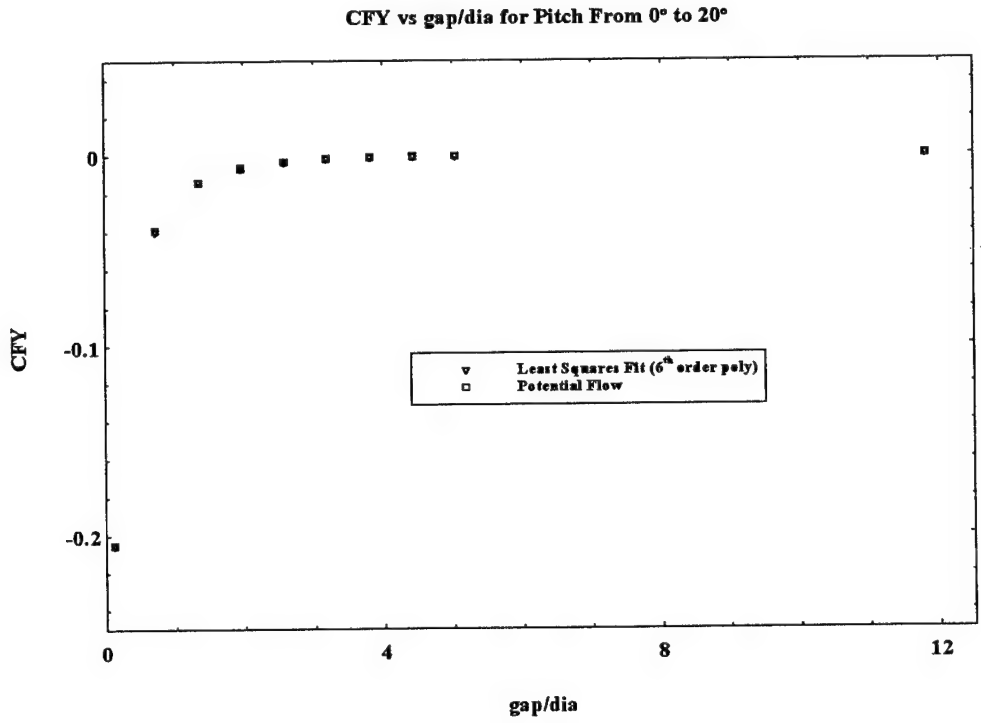

Figure 2.21 Lateral Force Near a Boundary

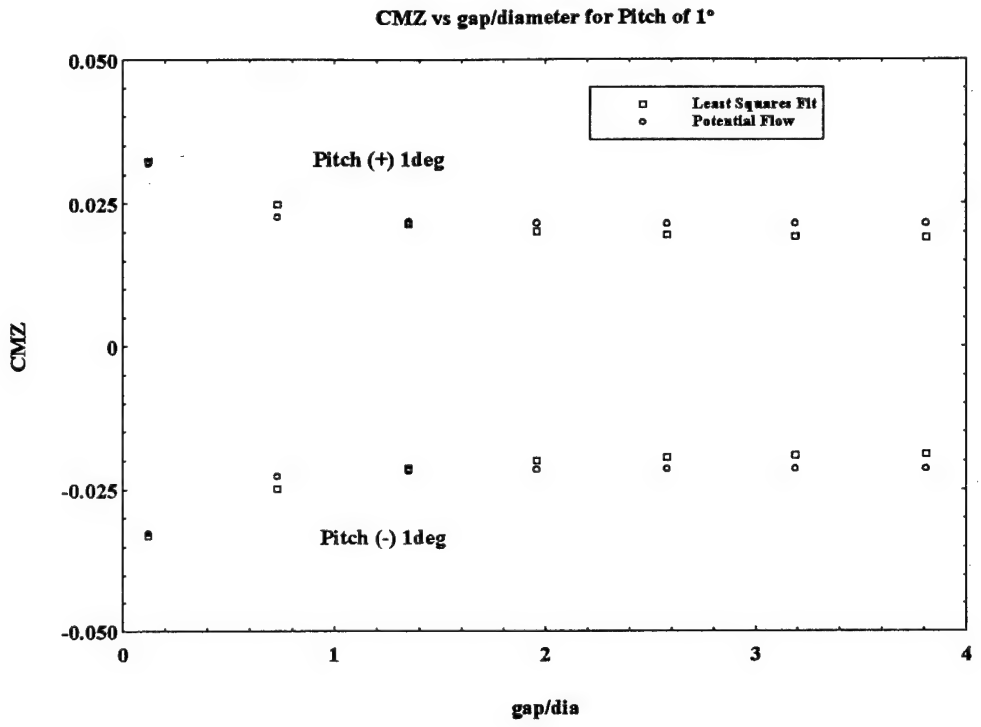

Figure 2.22 Lateral Moment Near a Boundary

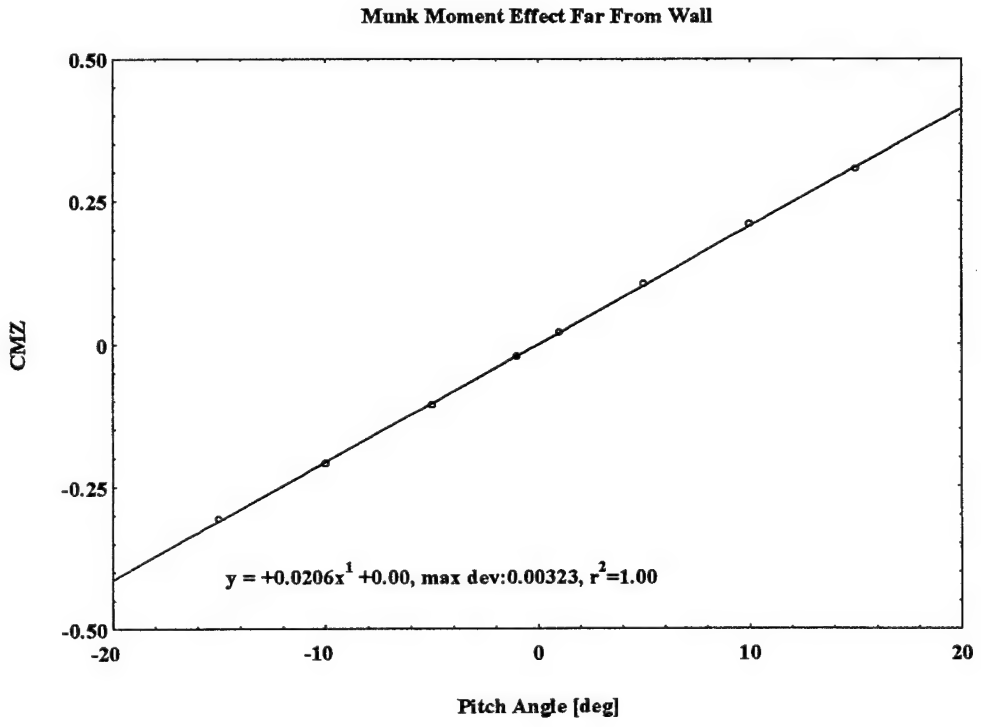

Figure 2.23 Open Water Munk Moment

The effect of PTF on the force and moment is captured by data obtained in [11]. Figures 2.24 and 2.25 represent the lateral force and moment effects due to a change in propulsive thrust factor. Significant scatter of experimental data was observed and several outlier points have been omitted in both curve fits, using the method described previously, to arrive at a model which makes physical sense and tends to the proper limit.

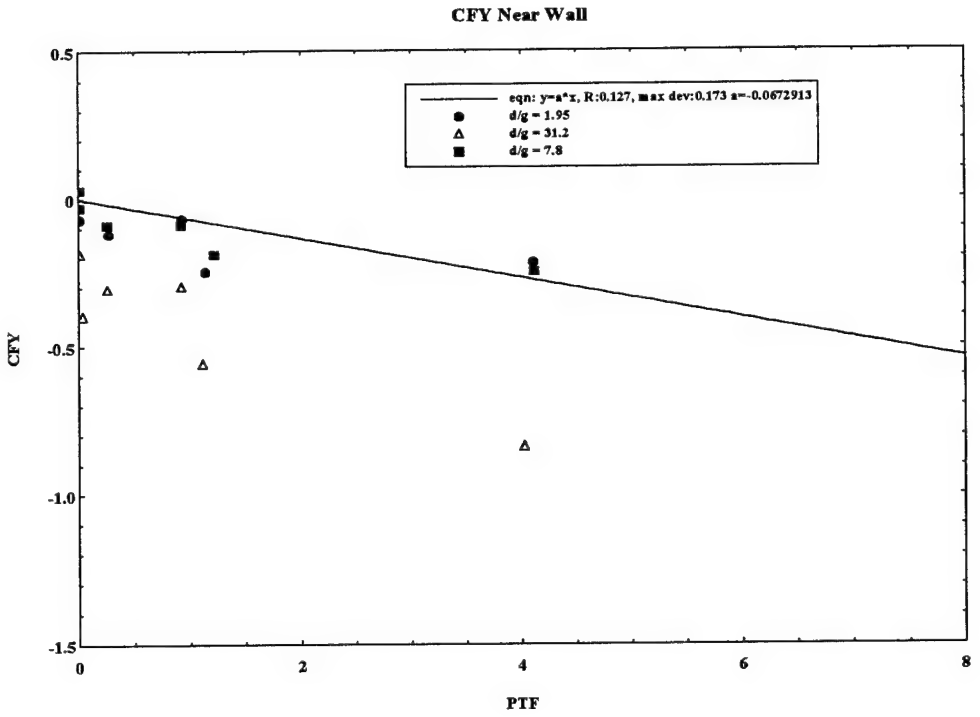

Figure 2.24 PTF Effect on Lateral Force

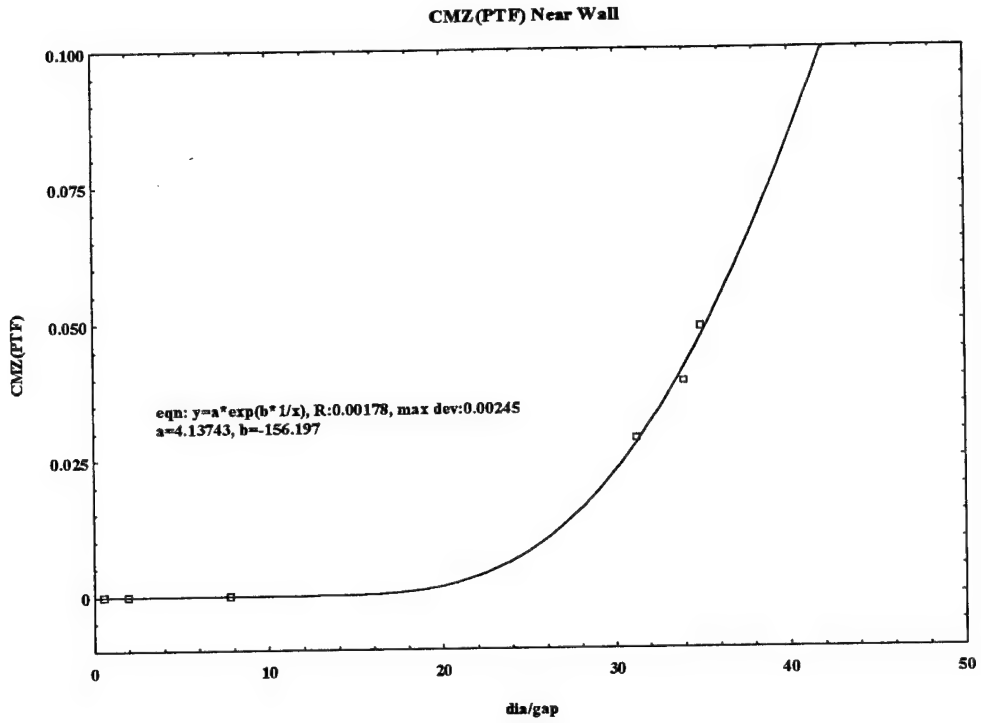

Figure 2.25 PTF Effect on Lateral Moment

Chapter 3 SIMULATION MODEL

3.1 Coordinate Systems

The forces acting on an underwater vehicle are normally referred to a non-inertial coordinate system fixed in the body, however, motion of the vehicle is most easily described in an inertial reference frame. For the purposes of this analysis, the inertial reference frame is translating at the constant velocity of the host, assumed to be along the positive X axis, and therefore represents a host fixed reference. The Z axis is directed positive downwards and the positive Y axis is to starboard in this frame of reference. To obtain the forces and moments in the non-inertial reference it is necessary to transform the vehicle motion to this frame. The vector transformation between the reference frames is uniquely determined by three angles: ϕ rotation about the X axis (roll), θ rotation about the Y axis (pitch), ψ rotation about the Z axis (yaw), which describe the angular orientation between the two frames and are termed the Euler angles. The order in which the transformation about these angular relations is observed is significant, and if taken in different sequence can produce a different vector result. In accordance with standard convention the transformation is accomplished by ordering the rotations as first yaw (ψ), then pitch (θ), and finally roll(ϕ). The transformation matrix describing the vehicle motion in translation in the non-inertial frame, given the inertial frame motion, is expressed by:

$$T_1(\phi,\theta,\psi)=\begin{bmatrix} \cos(\theta)\cos(\psi) & \cos(\theta)\sin(\psi) & -\sin(\theta) \\ -\sin(\psi)\cos(\phi)+\sin(\phi)\sin(\theta)\cos(\psi) & \cos(\phi)\cos(\psi)+\sin(\phi)\sin(\theta)\sin(\psi) & \sin(\phi)\cos(\theta) \\ \sin(\phi)\sin(\psi)+\cos(\phi)\cos(\psi)\sin(\theta) & -\sin(\phi)\cos(\psi)+\cos(\phi)\sin(\theta)\sin(\psi) & \cos(\phi)\cos(\theta) \end{bmatrix}$$

This transformation accounts for the rigid body rotation from host fixed reference to body fixed reference. The transformation of angular rate quantities follows the same Euler angle transformation convention and order of rotations.

The angular rate transformation is then:

$$T_2(\phi,\theta,\psi)=\begin{bmatrix}1 & 0 & -\sin(\theta)\\ 0 & \cos(\phi) & \sin(\phi)\cos(\phi)\\ 0 & -\sin(\phi) & \cos(\theta)\cos(\phi)\end{bmatrix}$$

The total transformation matrix may be represented as:

$$T(\phi,\theta,\psi)=\begin{bmatrix}T_1(\phi,\theta,\psi) & 0\\ 0 & T_2(\phi,\theta,\psi)\end{bmatrix}$$

With $\vec{\Re}_0$ representing a vector in the inertial frame consisting of scalar quantities of u (surge), v (sway), and w (heave) velocities , and p (roll rate), q (pitch rate) and r (yaw rate), or their respective time derivatives; the previously defined Euler angles ϕ, θ, and ψ are used to determine the vector $\vec{\Re}$, representing the same vector $\vec{\Re}_0$, but in the body reference frame changed only in orientation. The relation

$$\vec{\Re}=T(\phi,\theta,\psi)\vec{\Re}_0$$

is used to determine the body relative velocity and acceleration in the body reference frame translating with the velocity of the host in the host axial direction. Finally, the body velocities are corrected for this constant translation of the body fixed reference frame to arrive at the total body relative velocities independent of the host.

3.2 Equations of Motion and Implementation

The equations of motion of a rigid body may be expressed for arbitrary origin in matrix form as follows:

$$\begin{bmatrix}m-Y_{\dot{u}} & 0 & 0 & 0 & mz_G & -my_G\\ 0 & m-Y_{\dot{v}} & 0 & -mz_G-Y_{\dot{p}} & 0 & mx_G-Y_{\dot{r}}\\ 0 & 0 & m-Z_{\dot{w}} & my_G & -mx_G-Z_{\dot{q}} & 0\\ 0 & -mz_G-K_{\dot{v}} & my_G & I_{xx}-K_{\dot{p}} & -I_{xy} & -I_{xz}-K_{\dot{r}}\\ mz_G & 0 & -mx_G-M_{\dot{w}} & -I_{xy} & I_{yy}-M_{\dot{q}} & -I_{yz}\\ -my_G & mx_G-N_{\dot{v}} & 0 & -I_{zx}-N_{\dot{p}} & -I_{yz} & I_{zz}-N_{\dot{r}}\end{bmatrix}\begin{bmatrix}\dot{u}\\ \dot{v}\\ \dot{w}\\ \dot{p}\\ \dot{q}\\ \dot{q}\end{bmatrix}=\begin{bmatrix}X\\ Y\\ Z\\ K\\ M\\ N\end{bmatrix}$$

This expresses the Revised Standard Equations of Motion [5] with the acceleration terms isolated to the left hand side. The right hand side consists of the sum of the gyroscopic and centripetal acceleration effects as well as forces arising from the fluid hydrodynamic effects on the vehicle. These last include forces and moments accounted for by maneuvering coefficients including control forces, hydrostatics, crossflow and vortex effects. The hydrodynamic forces are calculated in accordance with the standard equations of motion. These are described for the hydrodynamic terms as:

$$X = X_{qq}q^2 + X_{rr}r^2 + X_{rp}rp + X_{vr}vr + X_{wq}wq + X_{vv}v^2 + X_{ww}w^2 + X_{w}uw + X_{q}uq + X_{uu}u^2$$

$$Y = Y_{p|p|}p|p| + Y_{pq}pq + Y_{r}ur + Y_{p}up + Y_{v}uv + Y_{v|uv|}v|uv| + Y_{vv}v^2 + Y_{wp}wp + Y_{v|uv|}v|uv| + Y_{r|r|}r|r| + Y_{*}uu + Y_{v|rv|}v\left|\sqrt{v^2 + w^2}\right|$$

$$Z = Z_{q}uq + Z_{w}uw + Z_{|w|}u|w| + Z_{vp}vp + Z_{*}uu + Z_{q|q|}q|q| + Z_{w|w|}w|w| + Z_{rp}rp + Z_{ww}w\left|\sqrt{v^2 + w^2}\right|$$

$$K = K_{p}up + K_{r}ur + K_{qr}qr + K_{wp}wp + K_{wr}wr + K_{v}uv + K_{p|p|}p|p| + K_{*}u^2$$

$$M = M_{q}uq + M_{q|q|}q|q| + M_{w|w|}w|w| + M_{vp}vp + M_{rp}r + M_{*}u^2 + M_{w}uw + M_{ww}w\sqrt{v^2 + w^2}$$

$$N = N_{pq}pq + N_{p}up + N_{wp}wp + N_{*}u^2 + N_{r}ur + N_{v}uv + N_{v|vr|}r\left|\sqrt{v^2 + w^2}\right| + N_{|v|}u|v| + N_{vv}v^2 + N_{v|v|}v|v| + N_{r|r|}r|r|$$

The body terms, including coriolis, centripetal, and hydrostatic effects are calculated separately. Neglecting cross products of inertia these terms may be expressed in the form:

$$X_{body} = -m\left(wq - vr - x_G(q^2 + r^2) + y_G pq + z_G(pr)\right) - (W - B)\sin(\theta)$$

$$Y_{body} = -m\left(ur - wp + x_G pq + z_G qr\right) + (W - B)\cos(\theta)\sin(\phi)$$

$$Z_{body} = -m\left(vp - uq + x_G pr - z_G(p^2 + q^2)\right) + (W - B)\cos(\theta)\cos(\phi)$$

$$K_{body} = (I_{yy} - I_{zz})qr - m\left(y_G(vp - wq) + z_G(ur - wp)\right) + (y_G W - y_B B)\cos(\theta)\cos(\phi) - (z_G W - z_B B)\cos(\theta)\sin(\phi)$$

$$M_{body} = (I_{zz} - I_{xx})pr - m\left(x_G(vp - uq) - z_G(wq - vr)\right) - (x_G W - x_B B)\cos(\theta)\cos(\phi) - (z_G W - z_B B)\sin(\theta)$$

$$N_{body} = (I_{xx} - I_{yy})pq - m\left(x_G(ur - wp) - y_G(wq - vr)\right) + (x_G W - x_B B)\cos(\theta)\sin(\phi) + (y_G W - y_B B)\sin(\theta)$$

The hydrodynamic maneuvering coefficients may be obtained by experiment, or predicted by numerous methods [1], [9], [12]. These relations do not include the propulsive thrust model forces or control forces in order to prevent redundancy of these terms with the interaction force model.

The right hand side forces on the vehicle may be expressed as a partition of the total right hand side in the following fashion:

$$\vec{F}_{total} = \vec{F}_H + \vec{F}_I + \vec{F}_C$$

where $\vec{F}_{total}$ may be equated to the acceleration and mass product terms , $\vec{F}_H$ represents the forces and moments acting on the body due to open water hydrodynamic, centripetal, gyroscopic, and hydrostatic effects. The term $\vec{F}_I$ accounts for the interaction effects due to the operation in a restricted fluid e.g. in the launchway and host vicinity. $\vec{F}_C$ accounts for the control force and moment required to effect the selected trajectory. $\vec{F}_C$ may be solved for directly:

$$\vec{F}_C = \vec{F}_{total} - (\vec{F}_H + \vec{F}_I)$$

This relation is adapted for implementation in a six degree of freedom motion simulation program for which a general description of the method employed follows.

The desired trajectory of the vehicle must be known a - priori and specified as input to the algorithm. It is important in the launch and recovery of the vehicle to know the relative position , velocity, and acceleration of the vehicle with respect to the moving host, therefore the trajectory is specified in a host fixed inertial frame. The vehicle accelerations and velocities are determined by a coordinate transformation from the moving inertial frame to the body fixed frame with the effect of forward speed of the host accounted for in the transformation. The total force at each time step is determined from the vehicle accelerations by solving the product of the mass matrix and body relative acceleration vector directly. A word of explanation is warranted with respect to the use of a motion simulation program. For the aspect of this thesis, with the specification of a trajectory known explicitly over time along with acceleration, and velocity, there is no

need to invert the mass matrix and integrate over each time step. The forces and moments may be computed directly at each time step allowing the algorithm to run very fast without growing errors due to a integration scheme. The hydrodynamic forces and moments including the body terms are calculated at each time step without consideration to the host presence. A separate subroutine implements the interaction force model previously developed, where forces and moments when the vehicle is located within the launchway are determined completely from the launchway model and include hydrodynamic and interaction effects. Once the vehicle has transitioned to a position outside of the launchway the interaction effects alone are determined. This condition reflects only a portion of the forces acting upon the vehicle, therefore to arrive at the total right hand side force vector when the vehicle is outside of the launchway, the hydrodynamic derivative based forces are added to the interaction effects.

In order to achieve a smooth transition between the experimental data representing the total force on the vehicle to the force calculated by the hydrodynamic derivative based force vector, it is necessary to employ a smoothing procedure to blend the differences between the two. In order to accomplish this, a zone structure is defined with the following description:

Zone 1 Inside the host launchway $F(x,y,z) = \text{Hydrodynamic}_e + \text{Interaction}_e$

Zone 2 Within the transition region $F(x,y,z) = \text{Hydrodynamic}_i + \text{Interaction}_i$

Zone 3 Outside of the transition region $F(x,y,z) = \text{Hydrodynamic}_d + \text{Interaction}_e$

Where $F(x,y,z)$ is the force calculated by the force model and subscripts e, i, and d refer to experiment, interpolated, and coefficient based semi-empirical data respectively.

Zone 2 is where the smoothing routine operates. This zone is defined by a hemisphere with the center located at the launchway exit defined by x_c,y_c,z_c with the diameter of this

zone a user defined input. The projection of the chosen trajectory of the UUV origin onto the sphere defines the demarcation between Zone 2 and Zone 3. The force vector in the transition zone is then obtained by a linear interpolation between Zone 1 relative to $x_C y_C z_C$ and Zone 3 relative to the specific trajectory intersection with the defining spherical transition surface. It is important that the transition zone be kept as small as possible to prevent dynamic force effects from being hidden by the interpolating scheme. For the purposes of this preliminary analysis a transition radius of 0.8 L was selected. The effect of host hull curvature on the interaction effect when the transition sphere intersection point is off the $z_C = 0$ radial from the launchway exit is modeled. With respect to these interaction forces, the interaction effects are assumed to act at the relative pitch angle to the hull normal surface, which depends upon the vehicle orientation in the inertial reference frame, pitch (θ) angle and yaw (ψ) angle, at this x,y,z location. With the total hydrodynamic force vector calculated, including host interaction effects, the control force vector is determined. The difficulty of determining lack of clearance is overcome by stipulating that the desired trajectory selected be a non crash trajectory. However within the bounds of the launchway and host geometry, significant flexibility in three dimensional space is provided.

The program input consists of the following files:

1) Revised Standard EOM simulation input file with control surface deflections selected to zero, and providing vehicle initial conditions relative to the host.
2) A model input file containing the open water hydrodynamic coefficients for solving the right hand side vector within the EOM hydrodynamic force routine.
3) A force model input file containing the coefficients for the potential flow model portion of the interaction effects.

4) A geometry limitation file containing the position information with regard to launchway geometry, host geometry and host speed.

5) A trajectory file which includes vehicle acceleration and velocity scaling parameters and trajectory modification commands versus time.

A linear interpolation scheme is used to determine the body position, velocity and acceleration changes over time from the commanded trajectory inputs. A partial list of the subroutines implementing the trajectory, force model and coordinate transformation is included as Appendix A.

Chapter 4 SIMULATION RESULTS

4.1 Trajectory Runs

Four different trajectories were selected for evaluation of the simulation. A copy of the input files is included in Appendix B. The trajectories were selected to test the blending between the force and moment models between Zone 1 and Zone 3. The trajectories selected were not intended to reflect in all cases the trajectory that would be optimal or would represent the real vehicle desired course but would illustrate the model.

4.2 Straight Launch

The first trajectory simulated was a straight ahead motion of the vehicle. Using an exponential time function acceleration described by:

$$\dot{x}(t) = 2\left(1 - e^{-0.04t^2}\right)$$

$$\ddot{x}_{Body}(t) = (4 * 0.04te^{\left(-0.04t^2\right)})$$

The vehicle is directed out of the launchway and away from the host at a constant heading angle. The trajectory in host reference is illustrated in Figure 4.1. Figure 4.2 through 4.7 show the resulting accelerations, velocities, forces and moments for this maneuver in the vehicle reference frame.

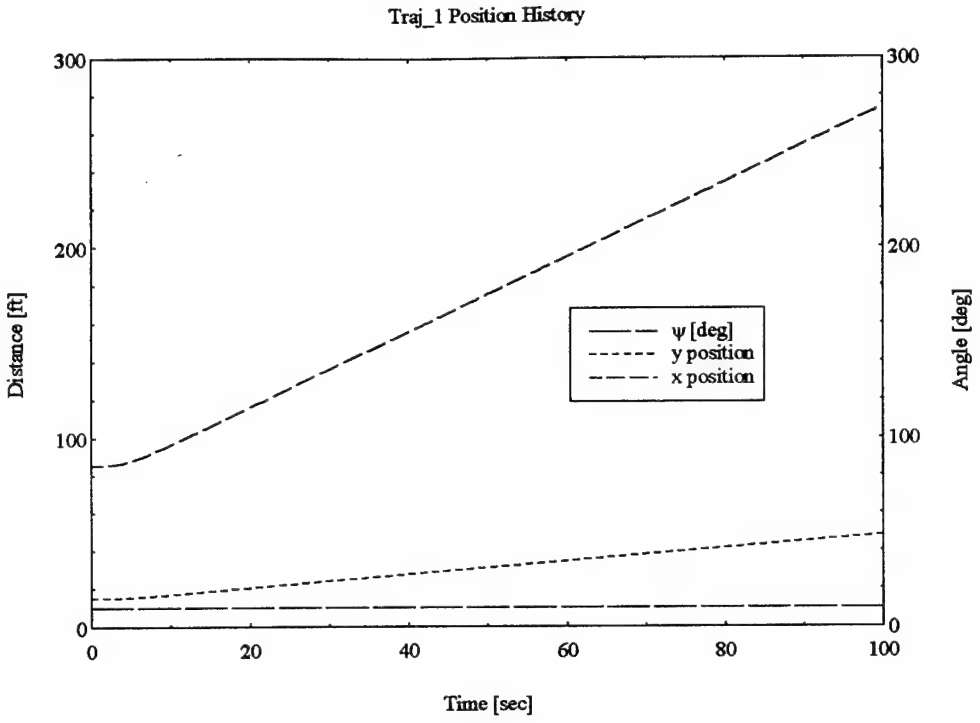

Figure 4.1 Vehicle Trajectory

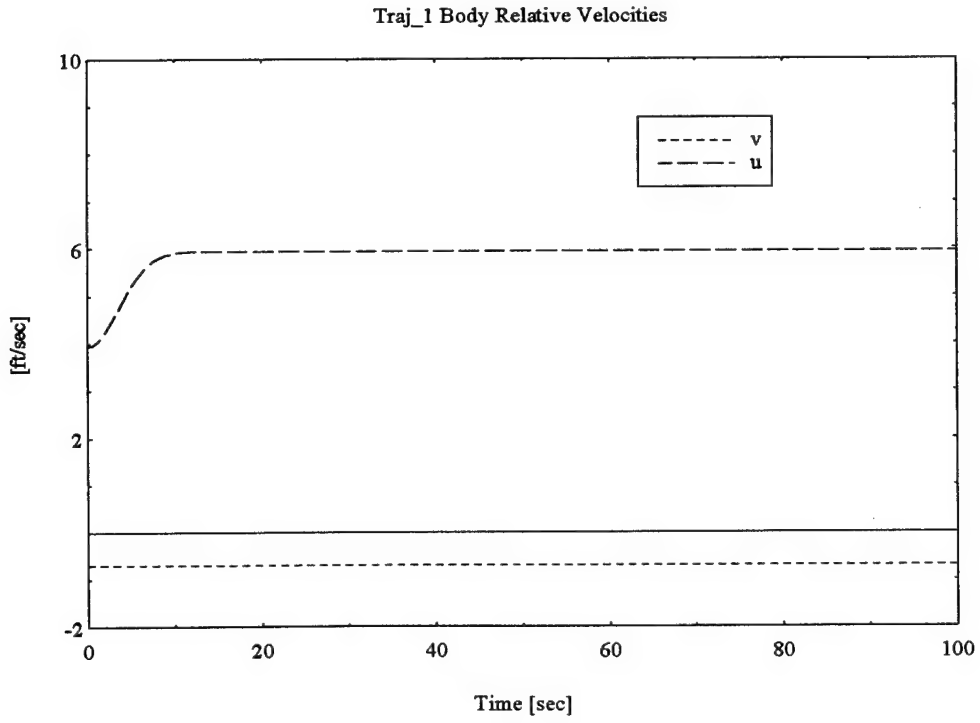

Figure 4.2 Velocity Profile

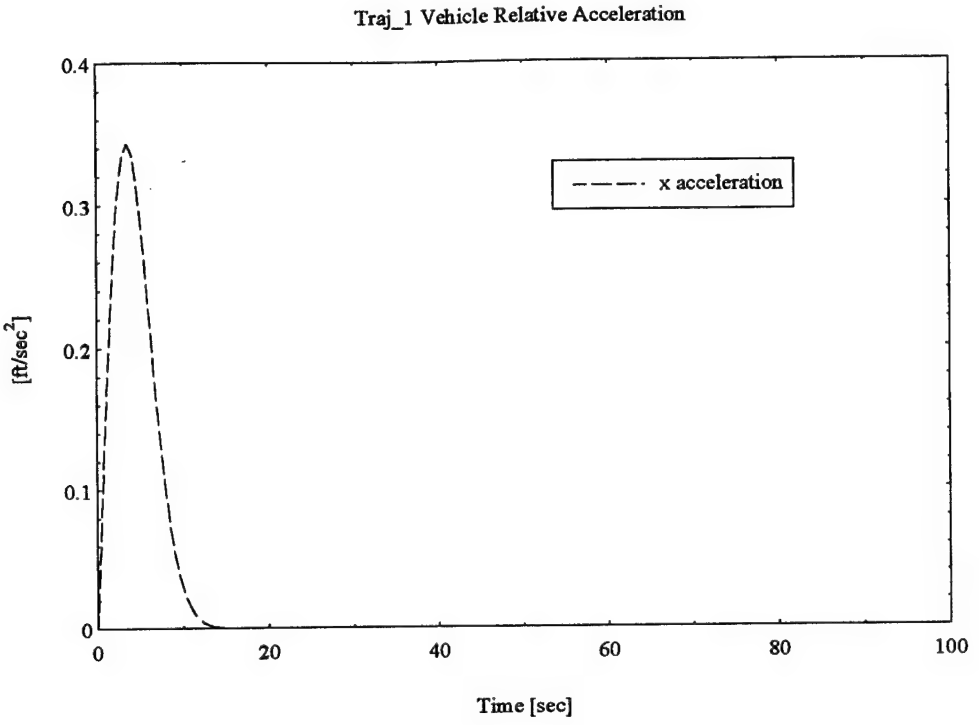

Figure 4.3 Acceleration Profile

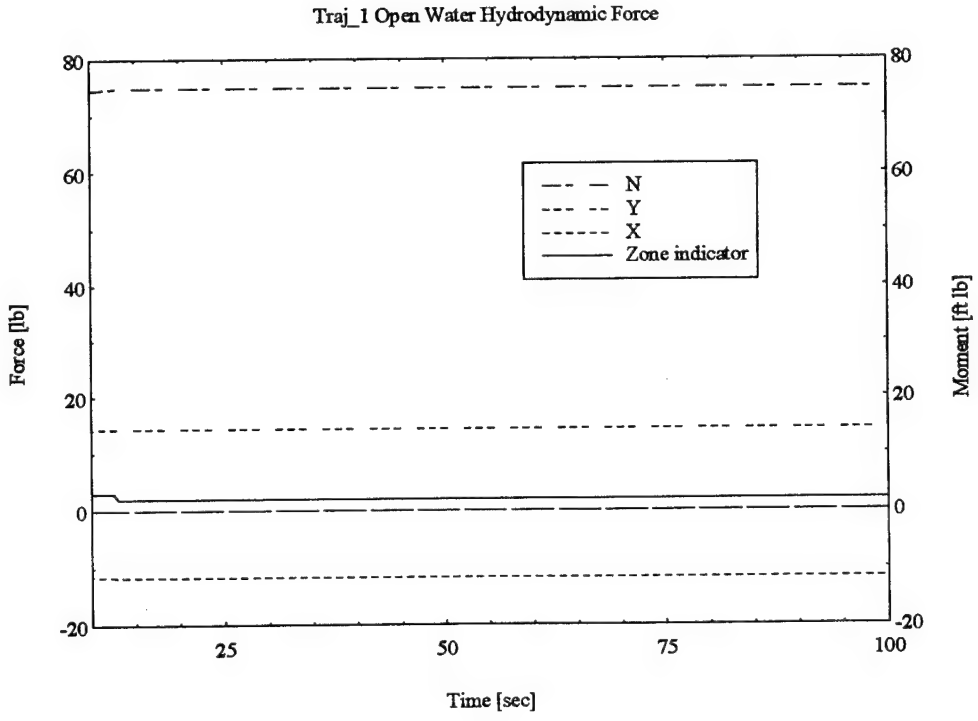

Figure 4.4 Hydrodynamic Forces in Open Water

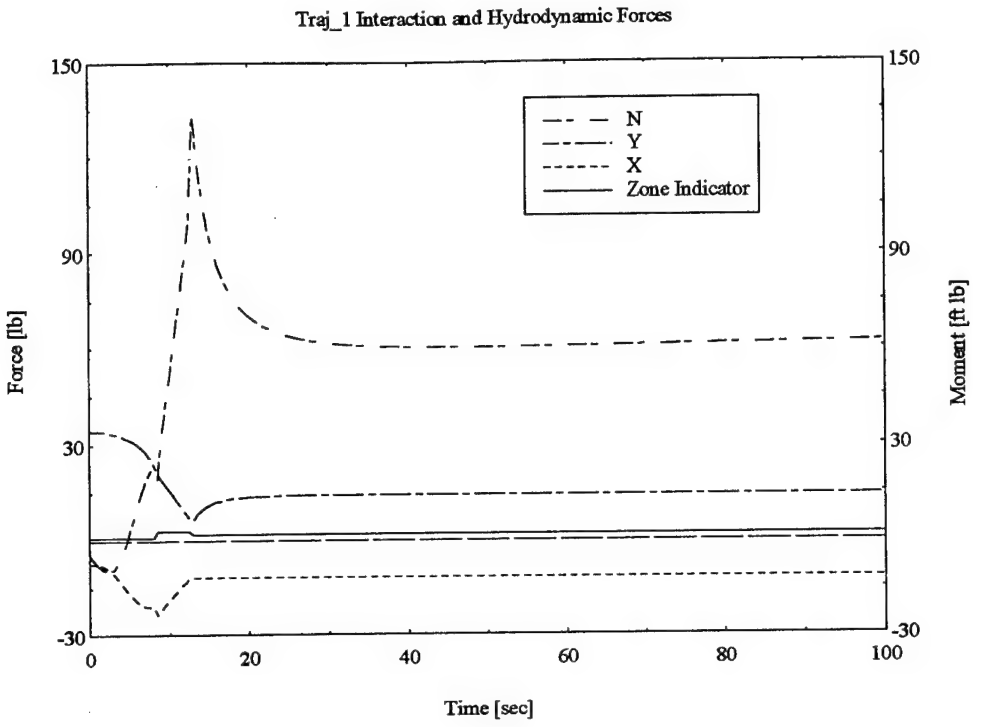

Figure 4.5 Hydrodynamic Forces Including Vehicle Interactions

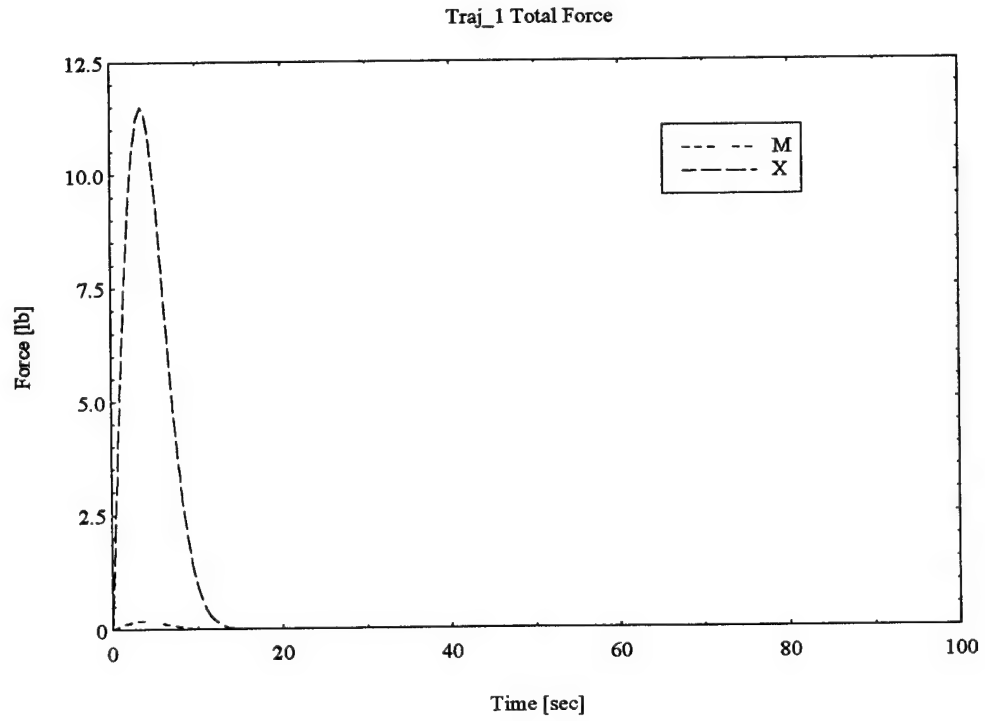

Figure 4.6 Total Force

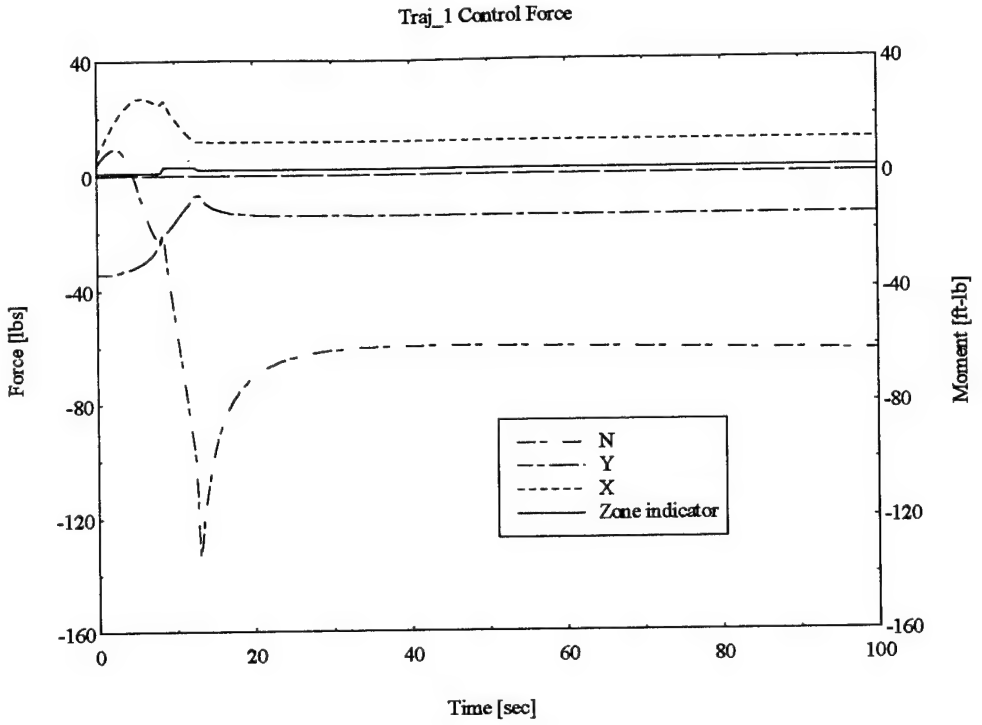

Figure 4.7 Control Forces

Although unrealistic as a desired maneuver due to the large sustained crossflow drag resulting from the constrained yaw angle, this trajectory is illustrative of the interaction effects and transition from a region where interaction effects play a role to the region in the far field where the interaction effects are small. As such it is useful as a baseline condition. The location of the vehicle relative to the zones previously defined is indicated in the figures, where pertinent, by a zone indicator line which takes a value of 1, 2, or 3 respective to the appropriate zone.

The interaction effects of the launchway and host vehicle are apparent in the figures. As the vehicle nose passes the launchway exit (occurring very early in the trajectory at ~ 4 sec) the lateral force can be seen to decrease as the nose proceeds into the transition zone. The effect on the lateral moment indicates an almost impulsive effect turning the moment from a negative value when the vehicle is fully within the launchway to a large positive moment as the vehicle fully exits. The magnitude of this moment depends upon the

interaction due to the boundary as well as the effect of PTF on the accelerated flow between the vehicle and the interacting boundary. As the boundary recedes, the moment decreases to the open water Munk moment due to the imposed angle of attack of the vehicle in this trajectory simulation.

4.3 Launch with Yaw Maneuver

The second trajectory for simulation yaws the vehicle to a zero relative heading angle after the vehicle has cleared the launchway. This represents a more realistic maneuver intended to investigate the effect of maneuvering to remove crossflow. The vehicle is yawed to a zero heading angle at time {t = 25 sec} and proceeds along a path parallel to the host for the rest of the simulation. This trajectory is illustrated in Figure 4.8. Figures 4.9 through 4.14 illustrate the velocities, forces and moments.

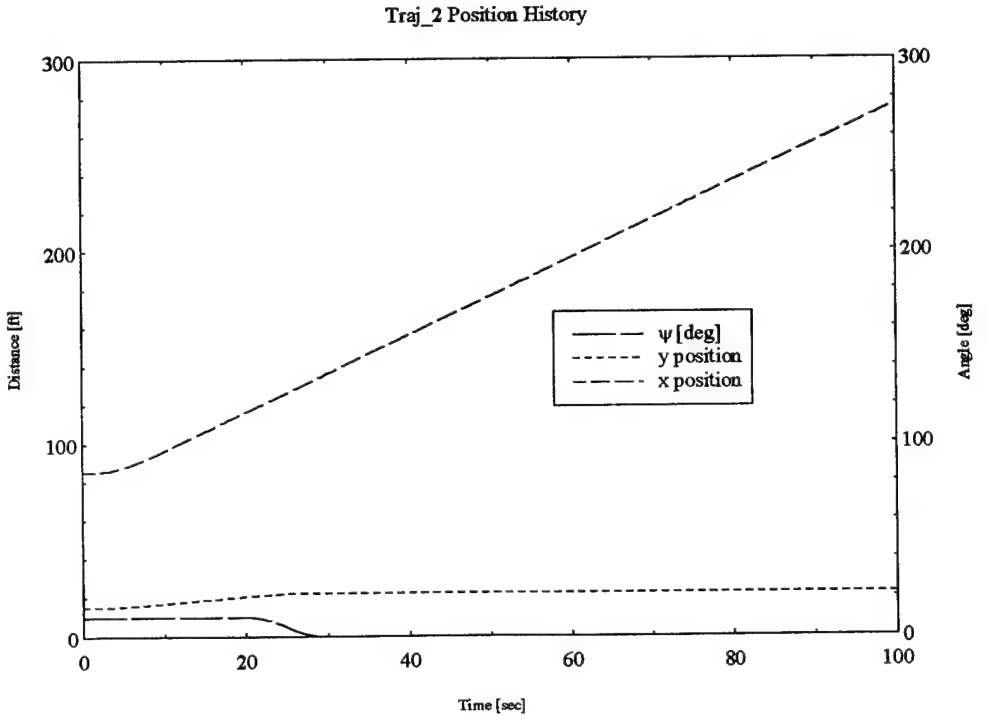

Figure 4.8 Vehicle Trajectory

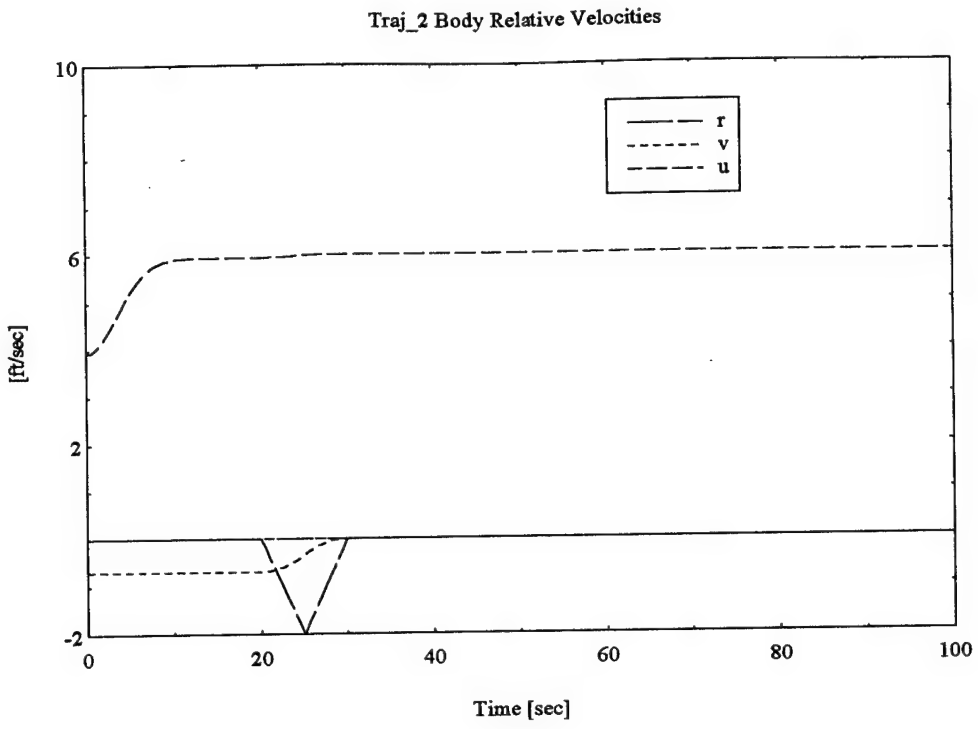

Figure 4.9 Velocity Profile

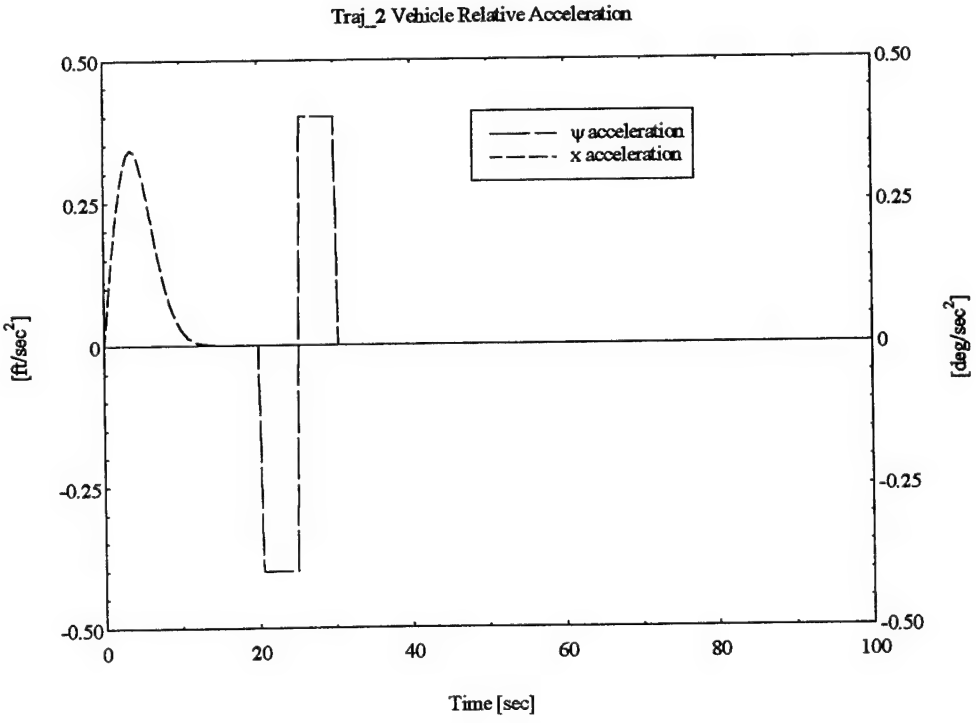

Figure 4.10 Acceleration Profile

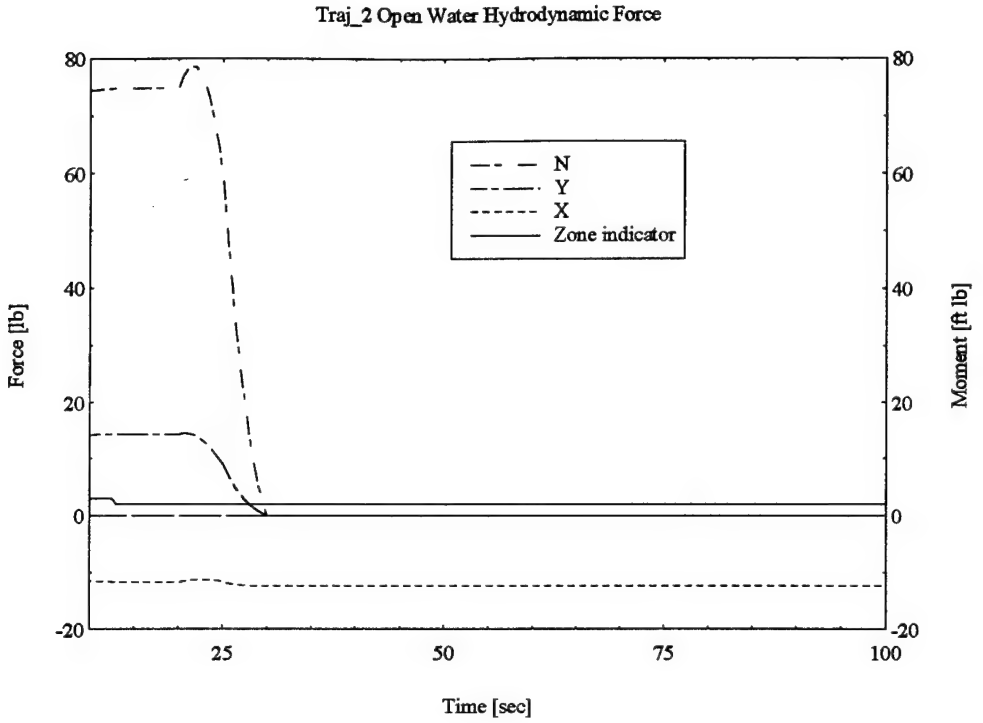

Figure 4.11 Hydrodynamic Forces in Open Water

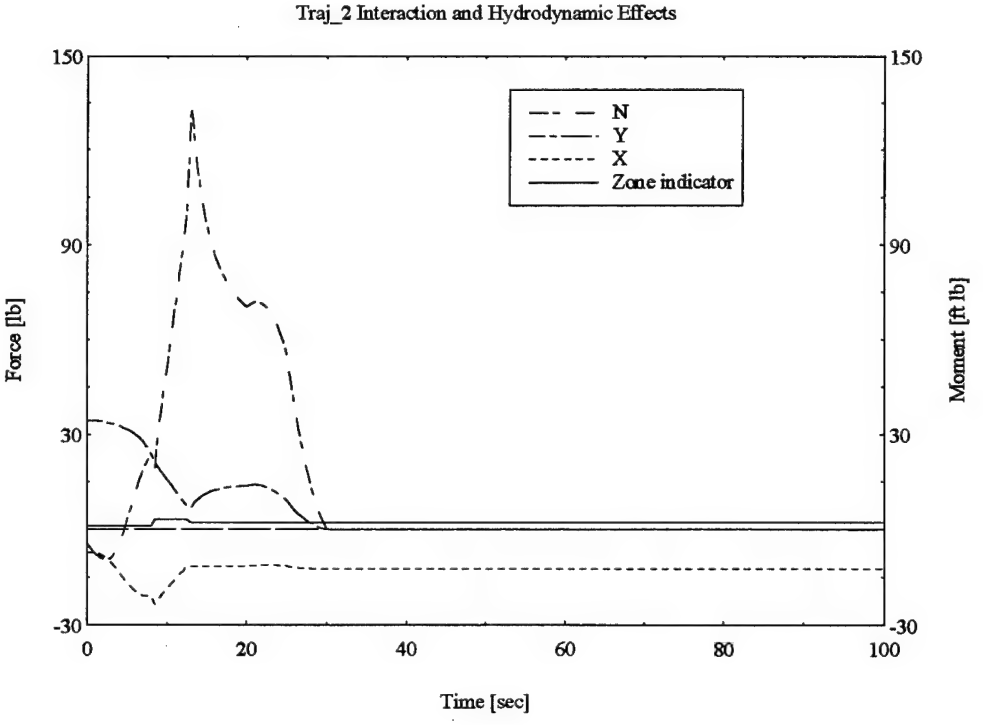

Figure 4.12 Hydrodynamic Forces Including Vehicle Interactions

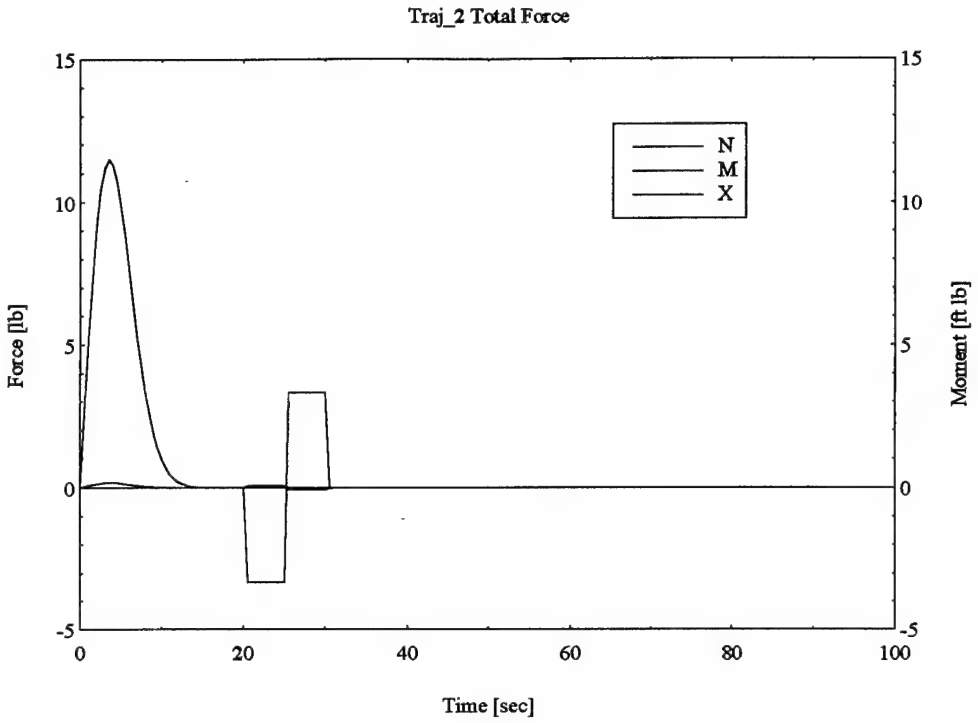

Figure 4.13 Total Force

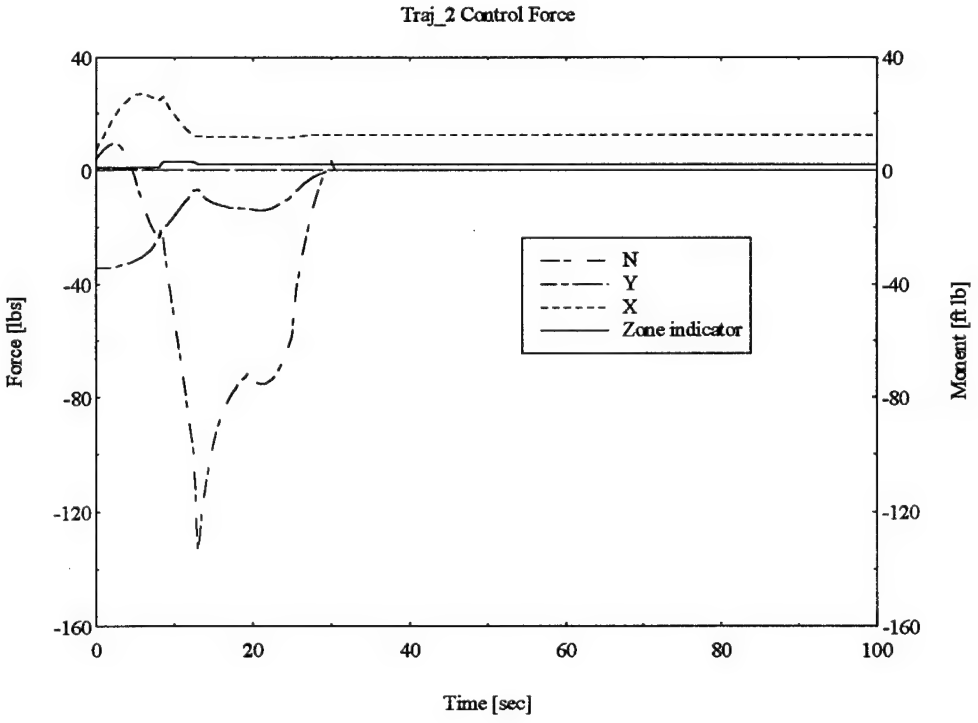

Figure 4.14 Control Force

The interaction effects near the host are apparent in the lateral force and moment as they were in the straight launch trajectory. In addition, acceleration effects during the maneuver can be seen to affect the required control forces, specifically in this instance the contribution of $N_{\dot{r}}$ to the lateral moment.

4.4 Launch with Yaw and Deceleration Maneuver

The third trajectory selected for simulation illustrates a maneuver intended to reflect a realistic vehicle maneuver. In this simulation the vehicle transitions out of the launchway and subsequently decelerates to the desired speed once clear of the host. Figure 4.15 shows the trajectory history. Figures 4.16 through 4.21 illustrate the velocities, forces and moments.

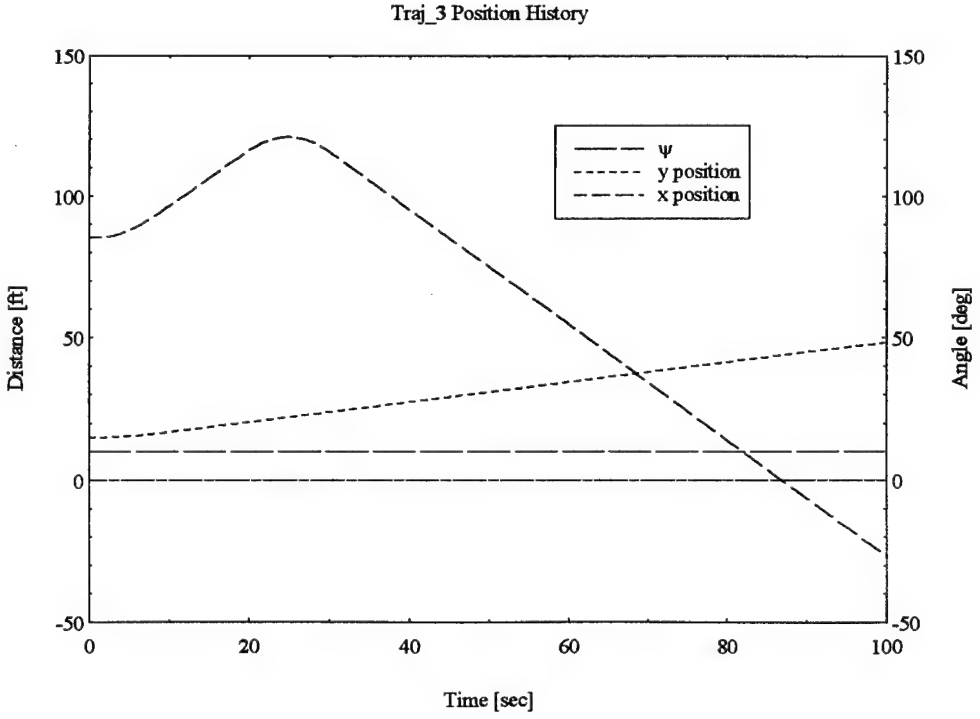

Figure 4.15 Vehicle Trajectory

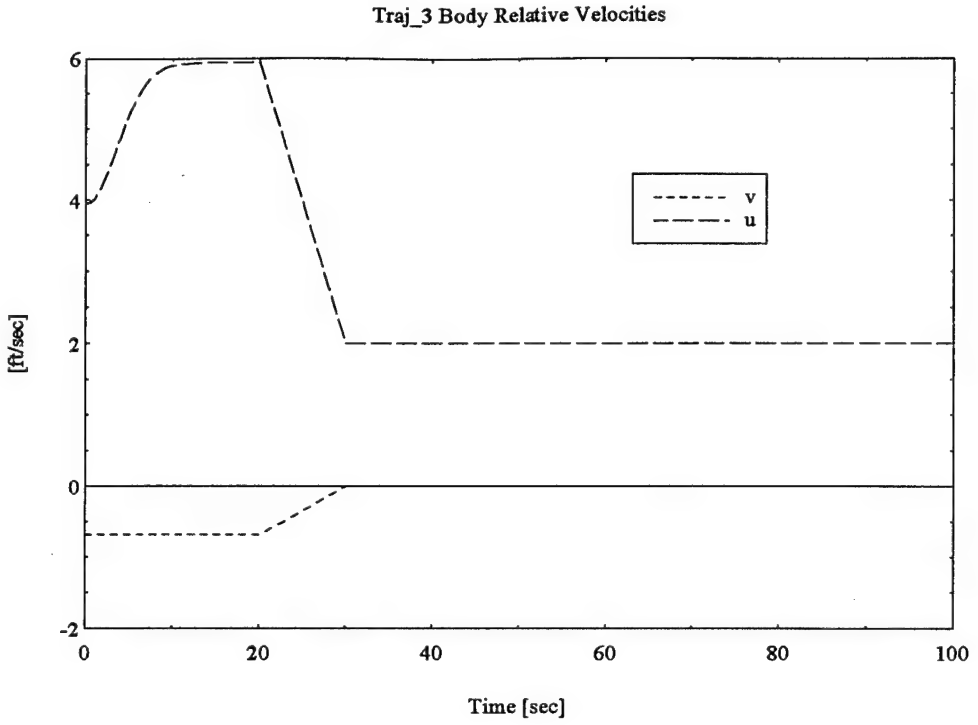

Figure 4.16 Velocity Profile

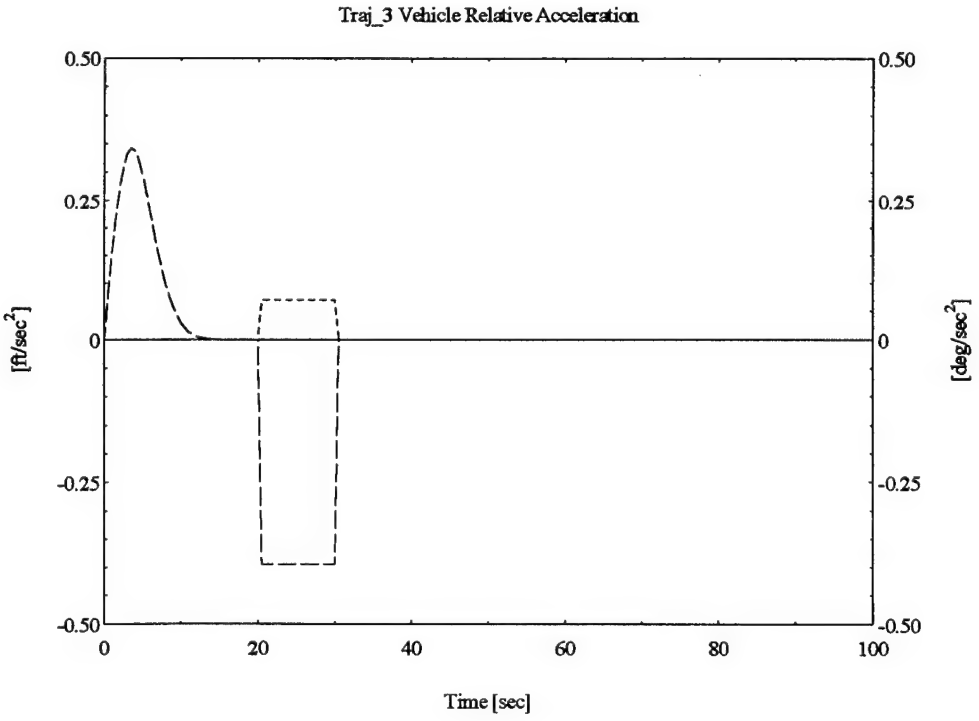

Figure 4.17 Acceleration Profile

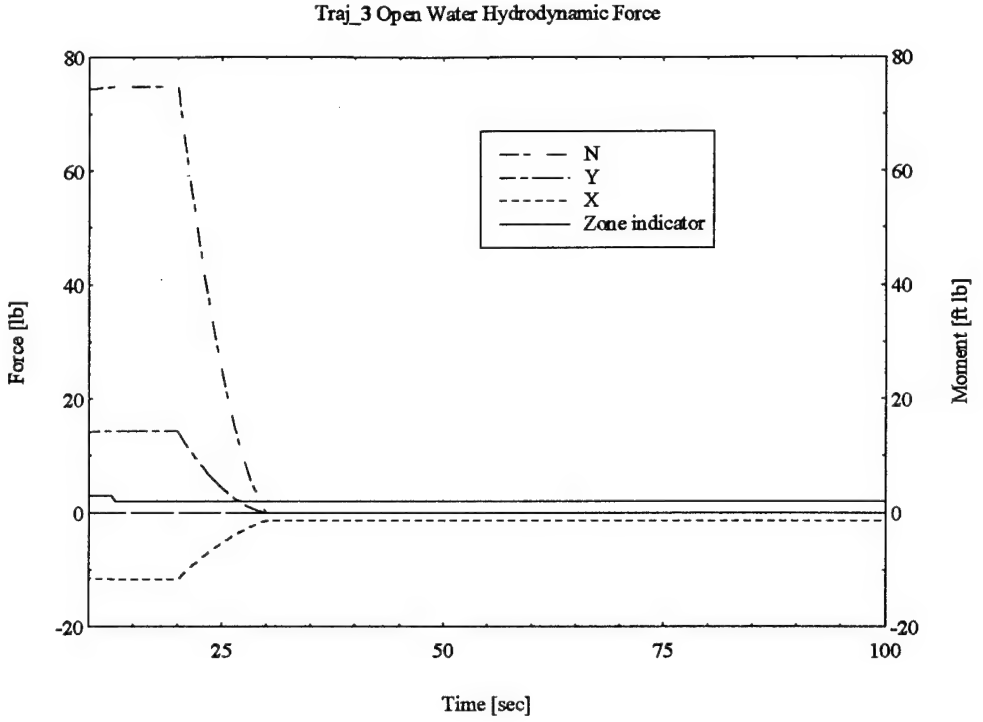

Figure 4.18 Hydrodynamic Forces in Open Water

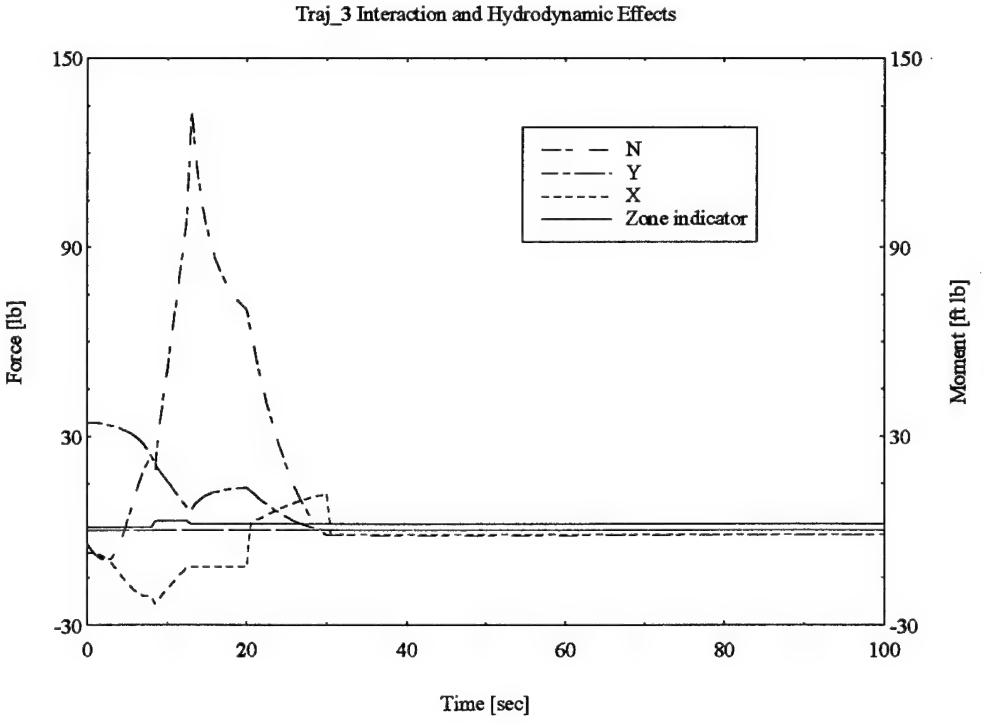

Figure 4.19 Hydrodynamic Forces Including Vehicle Interactions

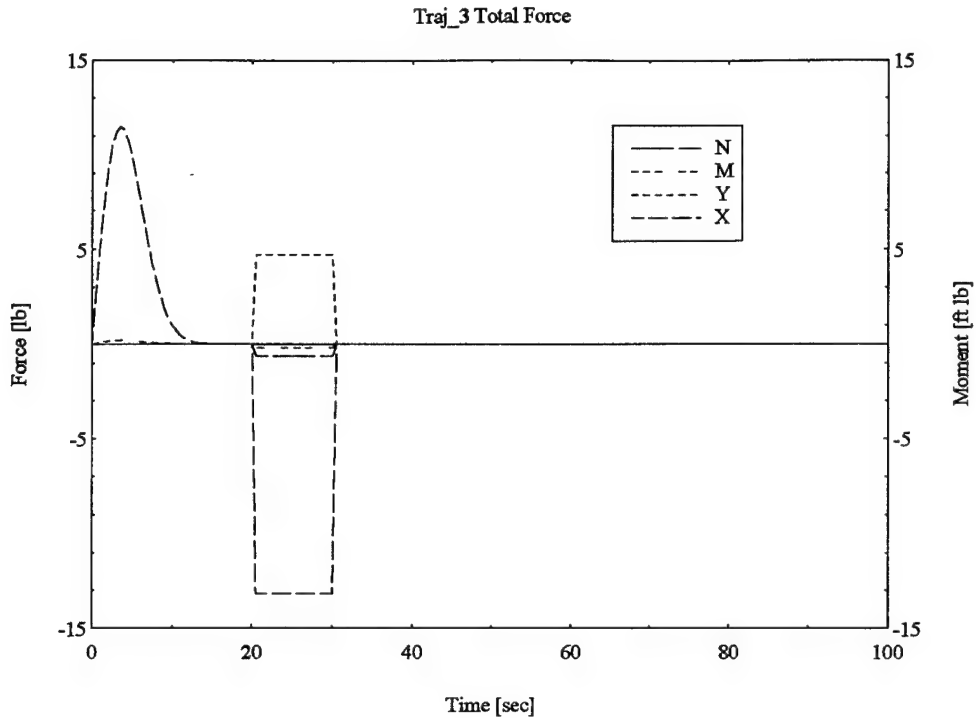

Figure 4.20 Total Force

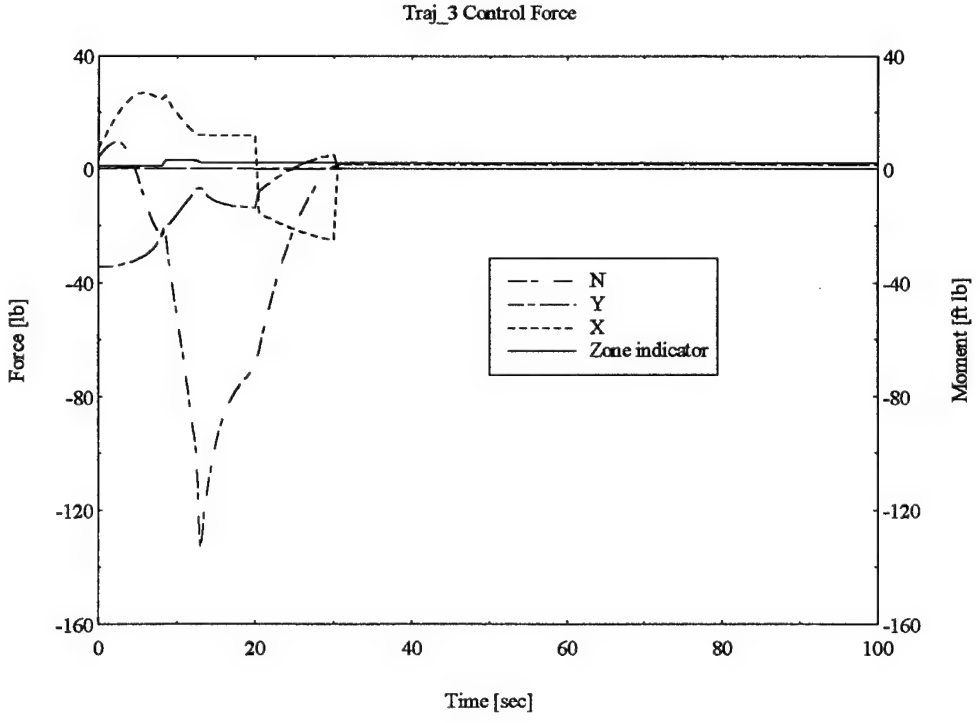

Figure 4.21 Control Force

Again as in the previous trajectory the significance of the acceleration effects are evident in the axial and lateral body forces during deceleration. The lateral moment peak occurs just after the vehicle has cleared the launchway and experiences the maximum interaction effect of the planar boundary in proximity to the vehicle in this configuration.

4.5 Straight Launch At Zero Host Speed

The fourth trajectory selected for simulation illustrates a launch from a stationary host. In this simulation the vehicle transitions out of the launchway maintaining a straight course and speed without onset flow. Figure 4.22 shows the trajectory history. Figures 4.23 through 4.28 illustrate the velocities, forces and moments.

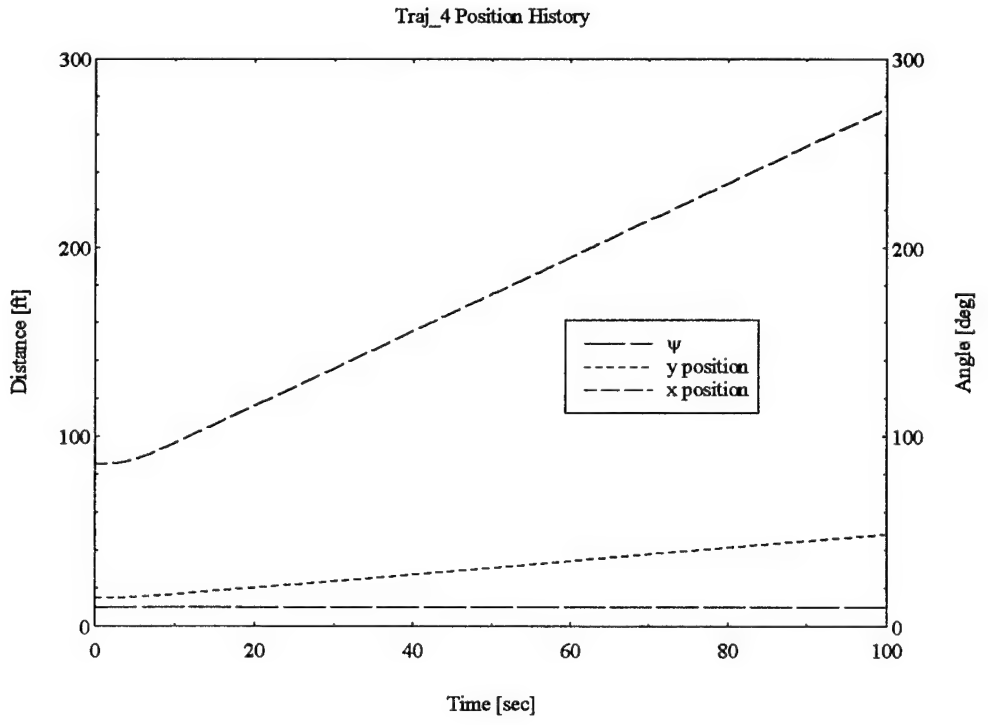

Figure 4.22 Vehicle Trajectory

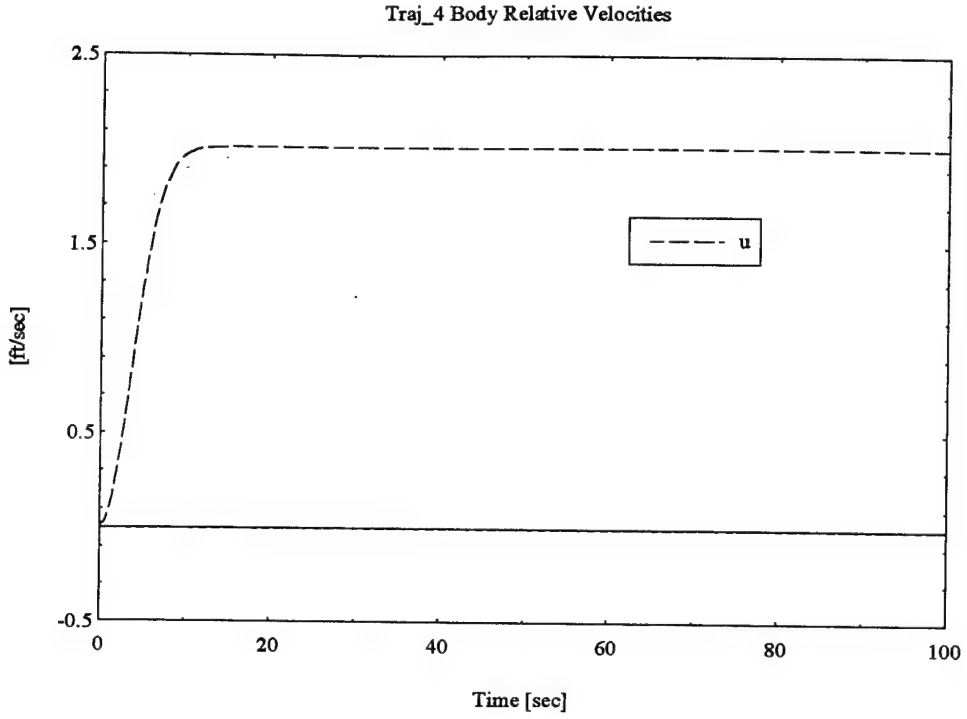

Figure 4.23 Velocity Profile

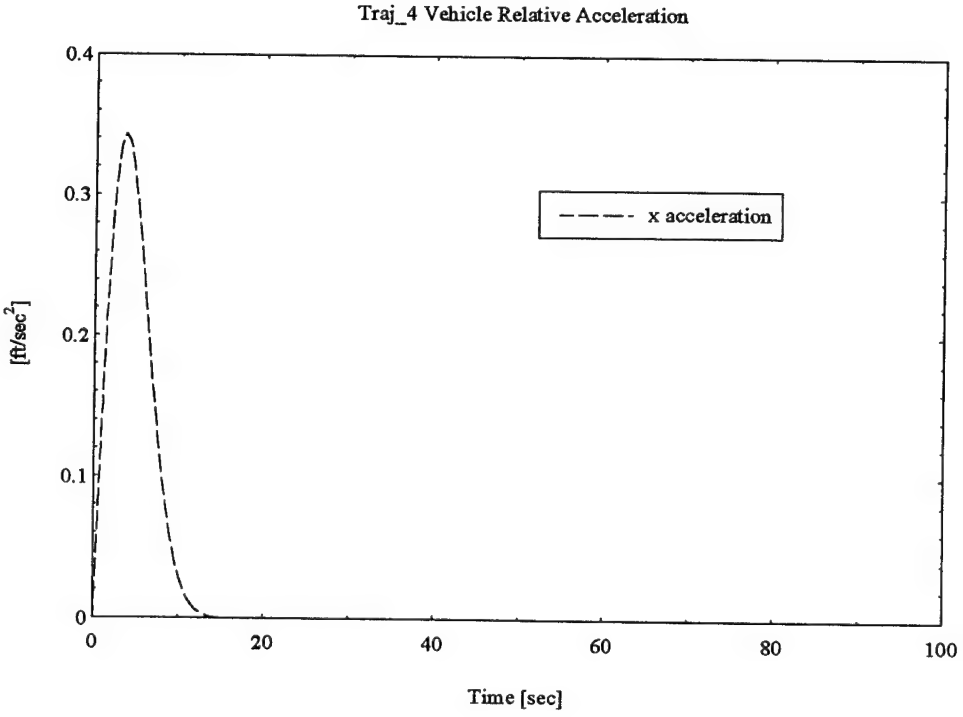

Figure 4.24 Acceleration Profile

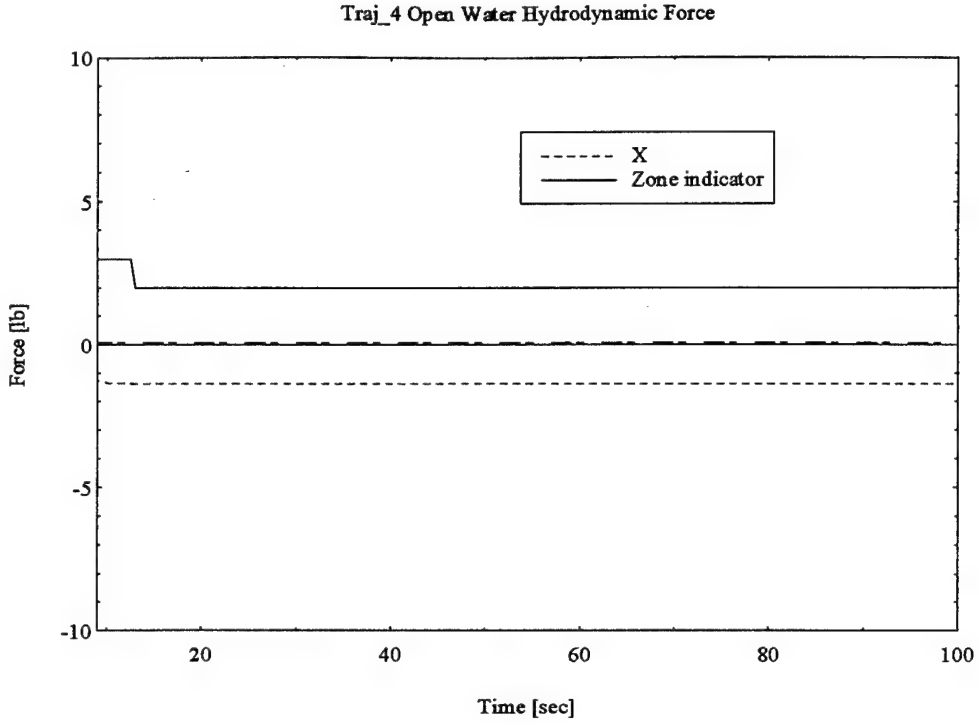

Figure 4.25 Hydrodynamic Forces in Open Water

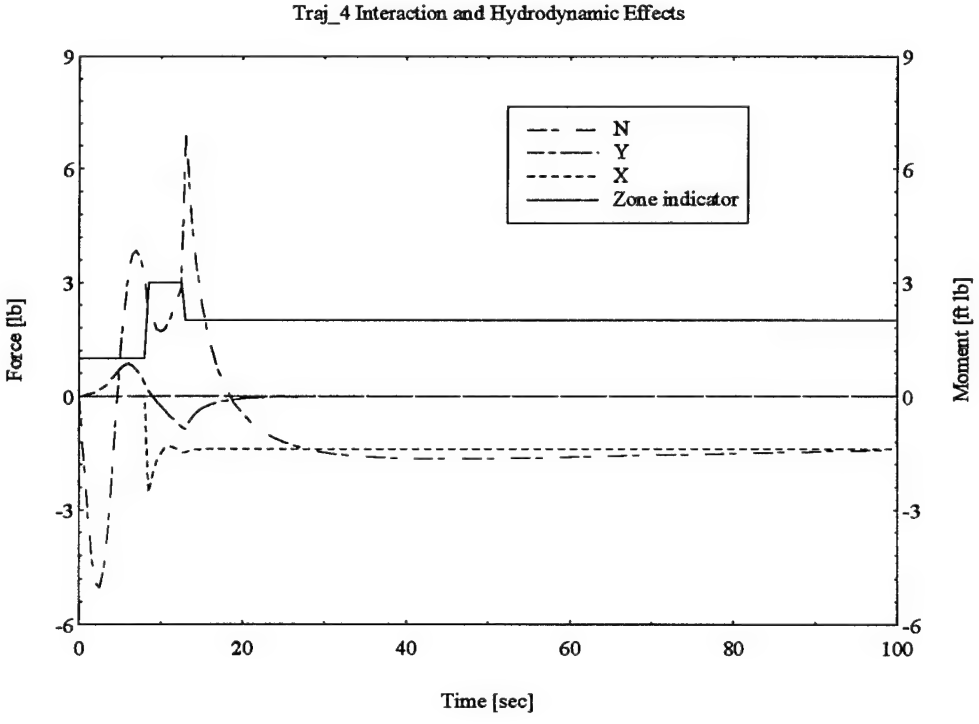

Figure 4.26 Hydrodynamic Forces Including Vehicle Interactions

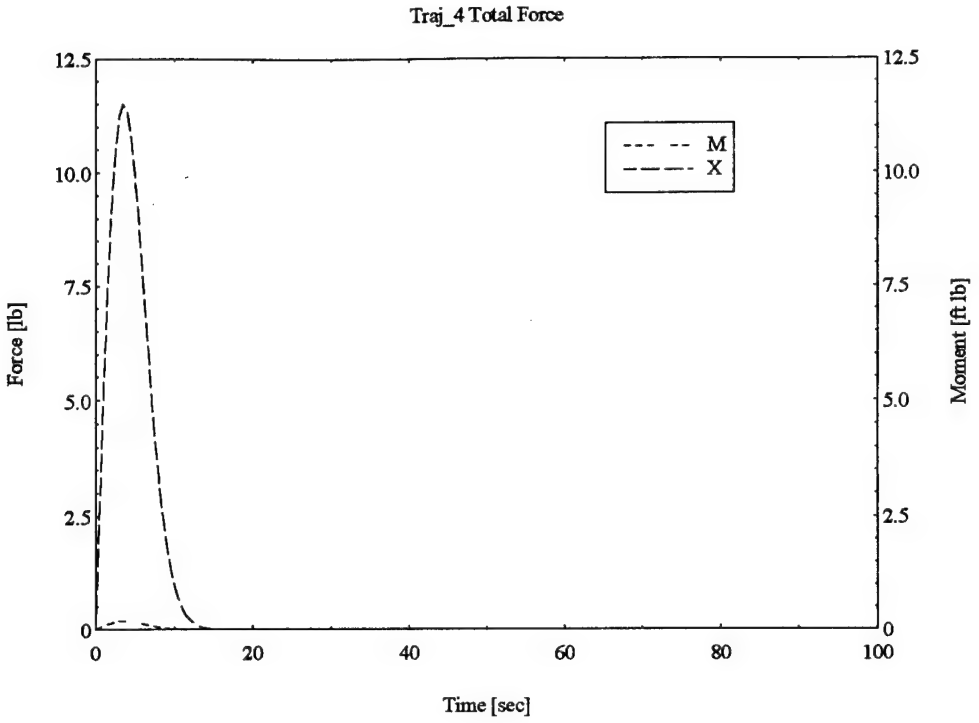

Figure 4.27 Total Force

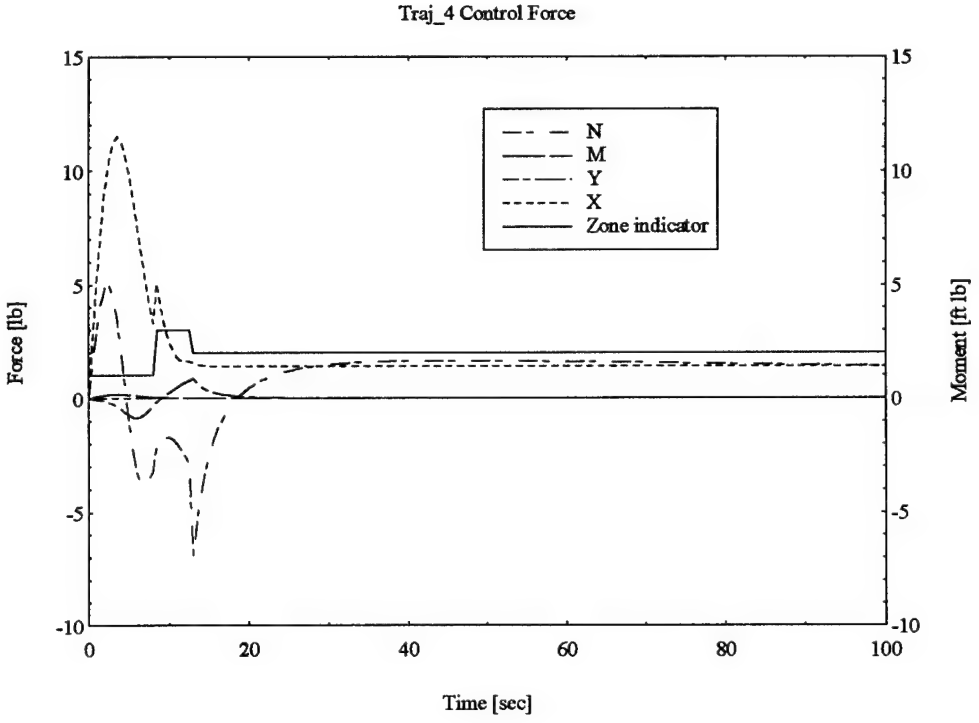

Figure 4.28 Control Force

It is of interest to note the differences between this launch and the previous launches, with forward host speed. In this launch the interaction effects are clearly seen; the lateral force changing sign from an outward force when the vehicle is mostly within the launchway to a inward suction force once clear. The lateral moment also changes sign from a bow in moment when the vehicle is mostly within the launchway to an outward moment due to boundary interaction and suction region acting on the aft portion of the vehicle. The axial force reflects the acceleration to constant velocity with corresponding constant axial hydrodynamic drag, while the lateral moment approaches asymptotically to a value dependent upon PTF. The effect of forward host speed has a marked effect on the force and moment on the vehicle, from commencement of launch with the vehicle fully within the launchway, to its transition to open water. With a 4 feet per second onset flow velocity due to the host forward speed, the lateral force does not achieve sign reversal, and an outward force dominates throughout the maneuver sequence. The effect on moment is pronounced as well, reflecting a twenty fold increase in peak moment over the zero forward speed case.

The small perturbation of the lateral moment observed as the vehicle becomes fully emerged from the launchway is qualitatively similar to the moment profile results described in [2] for a high speed torpedo ejection from a submarine launchway. This comparison is not intended to validate the results here but is offered for completeness. Due to the disimilar nature of the ejection dynamics compared to vehicle swimout, a quantitative comparison was not conducted.

Chapter 5 CONCLUSION

5.1 Summary

From the comparison of trajectory runs it is clear that the force and moment model implemented into a six degree of freedom motion algorithm can solve for control forces versus time for any desired trajectory. The mathematical model successfully makes non dimensional and integrates experimental data with potential flow panel code results, and with a parametric based non linear mathematical model, to span the trajectory regime from launchway to open water. Host vessel speed effects are incorporated. The smoothing technique accounts for the inevitable mismatch between the experimentally derived interaction model to the parametric, coefficient based, hydrodynamic forces in open water and allows for geometrically similar models to be tested using the existing experimental results.

Based upon trajectories with changing accelerations, acceleration effects add significant information to the force simulation. Vehicle motion gain evaluation is enabled through the trajectory input file.

The magnitudes of the required control forces are broken down in such a way so as to enable the contributing interaction forces, open water hydrodynamic forces, or body mass forces, to be compared and their dependence upon trajectory evaluated.

5.2 Recommendations for Future Work

The control force output from the model represents, in a sense, the magnitude of control actuated force to maintain the selected trajectory. A shortcoming in the model

exists in that it ignores interaction effects between the control surface or thruster, the vehicle, and proximity boundary. The fidelity of the simulation would be improved by incorporating control effects on the uncontrolled vehicle interaction force model.

For a vehicle with a different propulsor, a means of effectively adapting the thrust model and resulting thrust, moment and torque effects would be useful.

The basis for a maneuvering workbench exists which can be used to assist in control appendage sizing, control system design, and free swimming motion simulation in one simulation environment.

The accuracy of the simulation and its representation of the real world can only be determined by comparing its output to full scale tests. These would indicate those areas captured by the model as well as areas requiring improvement. Additional scale testing should be conducted to provide a more robust mathematical model, and should incorporate thruster, propeller, and launchway off - axis effects.

Bibliography

[1] Abkowitz, Martin., *Stability and Motion Control of Ocean Vehicles*, MIT Press, Cambridge, Ma. 1969.

[2] Crisalli, A. J., and T. L. Thorsen, *A Three Dimensional Model for the Dynamics of a Torpedo Emerging from a Submarine*, Technical Note TN-82-370, Westinghouse Electric Corporation Marine Division, Sunnyvale, Ca.

[3] Daniel, C. and F. S. Wood, *Fitting Equations to Data*, Wiley-Interscience, NY,1955.

[4] Draper, N. R., and H. Smith, *Applied Regression Analysis*, Wiley, NY, 1966.

[5] Feldman, Jerome, *DTNSRDC Revised Standard Submarine Equations of Motion*, DTNSRDC/SPD-0393-09, June 1979.

[6] Gertler, Morton and Hagen, Grant R., *Standard Equations of Motion for Submarine Simulation*, Naval Ship Research and Development Center Report 2510, June 1967.

[7] Hickey, Robert I., *Submarine Motion Simulation Including Zero Forward Speed and Propeller Race Effects*, MIT Masters Thesis, February 1990.

[8] Hoerner, Sighard F., *Fluid Dynamic Drag*, 1965.

[9] Humphreys, D. E., and N. S. Smith, *Background Discussion of the GEORGE Hydrodynamic Model and the TRJv Trajectory Simulation*, Titan Research and Technology Corporation, September 1993.

[10] Jensen, Soren, T., *Forces on Underwater Vehicles*, Masters Thesis, MIT, January 1995.

[11] Jensen, Soren, T., and Jerome H. Milgram, *Model Scale Tests of an Underwater Vehicle*, MIT unpublished, 1995.

[12] Landweber, L., and J. L. Johnson, *Prediction of Dynamic Stability Derivatives of an Elongated Body of Revolution*, Navy Department DTMB Report C-359, May 1951.

[13] Newman, J. N., *Marine Hydrodynamics*, MIT Press, Cambridge, Ma, 1977.

[14] Ramsey, W., Phd Thesis, MIT, June 1996.

[15] Sjoblom, B., and John A. Schwemin, One-Tenth-Scale Flow Field Measurements for an SSN 688 Class Submarine Torpedo Tube Launchway, NUWC-NPT TM 932129, September 1993

[16] *Nomenclature for Treating the Motion of a Submerged Body Through a Fluid*, Technical and Research Bulletin 1-5, American Towing Tank Conference, SNAME, April 1950.

Appendix A. Source Code Listing for Trajectory Simulation and Force Model

This appendix includes source code for the implementation of the trajectory, and force model. Also included is a portion of the Equation of Motion (EOM) program used to calculate the hydrodynamic open water forces.

```
C ***********************************************************************
      SUBROUTINE TRJ
C ***************************************************4/96*****************

      IMPLICIT NONE
      REAL*8 CTRN(6,6),RHS(6),EDOT(6),E(6),PDOT(6)
      REAL*8 P(6),DT,TA,PDOTO,PDDOTO
      REAL*8 DS4,DC4,DS5,DC5,DS6,DC6,DT5,DS5DC6,DS5DS6
      REAL*8 PDDOT(6),RHSTOT(6),RHSC(6)
      REAL*8 A(6,6),WORK(6,6),ACOF(6),BCOF(6)
      REAL*8 ACP(3),BCP(3),RHSFM(6),RTD,DTR
      REAL*8 XC,YC,ZC,XMIN,XMAX,YMIN,YMAX,ZMIN,ZMAX,D2,HRAD
      REAL*8 VRAD,UHOST,DIA,RHOC,ATLMAX,VLEN
      REAL*8 FX,FY,FZ,MX,MY,MZ,AEDOT1,RHS1,PTF
      REAL*8 ATL,VEX(2),TEMP1,TEMP2
      REAL*8 P1A,P1T,P2A,P2T,P3A,P3T
      REAL*8 P4A,P4T,P5A,P5T,P6A,P6T
      REAL*8 P1DOT,P2DOT,P3DOT
      REAL*8 P4DOT,P5DOT,P6DOT
      REAL*8 P1DDOT,P2DDOT,P3DDOT
      REAL*8 P4DDOT,P5DDOT,P6DDOT
      INTEGER*2 I,J,JJ,K,JJJ,II,KODE,JR,JJR,JP,JJP,JYA,JJYA
      INTEGER*2 JX,JJX,JY,JJY,JZ,JJZ
      CHARACTER*15 LABEL

      REAL*8 DD(1800)
      COMMON /COMDD/ DD
      COMMON/FGEOM/ XC,YC,ZC,XMIN,XMAX,YMIN,YMAX,ZMIN,ZMAX,
     1 D2,HRAD,VRAD,UHOST,DIA,RHOC,ATLMAX,VLEN
     1 ACP,ACOF,BCP,BCOF
      SAVE J,JJ,JR,JJR,JP,JJP,JYA,JJYA,JX,JJX,JY,JJY,JZ,JJZ
      DATA J,JJ,JR,JJR,JP,JJP,JYA,JJYA /9,9,2,0,2,0,2,0/
      DATA JX,JJX,JY,JJY,JZ,JJZ /2,0,2,0,2,0/

      EQUIVALENCE (DD(  1),      DT)
      EQUIVALENCE (DD( 11),     JJJ),(DD(  4),     RTD)
      EQUIVALENCE (DD( 10),      TA),(DD(  5),     DTR)
      EQUIVALENCE (DD( 31),EDOT(1))
      EQUIVALENCE (DD( 55),     E(1))
      EQUIVALENCE (DD( 61),     P(1))
      EQUIVALENCE (DD( 71),   RHS(1))
      EQUIVALENCE (DD( 77),PDOT(1))
      EQUIVALENCE (DD(107),A(1,1))
      EQUIVALENCE (DD(83),PDDOT(1))
```

```
      DIMENSION P1A(10),P1T(10),P2A(10),P2T(10),P3A(10),P3T(10)
      DIMENSION P4A(10),P4T(10),P5A(10),P5T(10),P6A(10),P6T(10)

      IF (TA .EQ. 0.) THEN

C READ IN THE GEOMETRY CONSTRAINTS

      WRITE(6,*) ' OPENING AND READING GEOMETRY LIMITATION FILE'
      OPEN(11,FILE='GEOM.LIM',STATUS='OLD')
      READ(11,*) XC,YC,ZC
      READ(11,*) XMIN,YMIN,ZMIN
      READ(11,*) XMAX,YMAX,ZMAX
      READ(11,*) D2,HRAD,VRAD,VLEN
      READ(11,*) UHOST,DIA,RHOC,ATLMAX
      CLOSE (11)

C READ IN FORCE MODEL COEFFICIENTS

      WRITE(6,*) ' OPENING AND READING LEAST SQUARES COEFFICIENT
FILE'
      OPEN(12,FILE='Z2COEF.EXP', STATUS='OLD')
      READ (12,*) (ACP(II), II = 1,3)
      READ (12,*) (BCP(II), II = 1,3)
      READ (12,*) (ACOF(II), II = 1,6)
      READ (12,*) (BCOF(II), II = 1,6)
      CLOSE (12)

C READ IN TRAJECTORY MODIFICATIONS

      WRITE(6,*) ' OPENING AND READING TRAJECTORY COMMAND FILE'
      OPEN(14,FILE='TRAJ.CM', STATUS='OLD')
      READ (14,*) (VEX(II), II = 1,2)
      READ (14,*)
      READ (14,*)
       DO 20 I = 1,10
       READ(14,*) P1A(I),P1T(I),P2A(I),P2T(I),P3A(I),P3T(I)
   20  CONTINUE
      READ(14,*)
      READ(14,*)
       DO 30 I = 1,10
       READ(14,*) P4A(I),P4T(I),P5A(I),P5T(I),P6A(I),P6T(I)
       P4A(I) = P4A(I) * DTR
       P5A(I) = P5A(I) * DTR
       P6A(I) = P6A(I) * DTR
   30  CONTINUE
```

```
      CLOSE (14)

C COMPLETE MODEL ENTRY
      ELSE
      ENDIF

C USE STANDARD INITIAL VELOCITY PROFILE
C MODIFY TRAJECTORY BY SCALING OF U,V, AND W RELATIVE
C TO THE HOST FOLLOWED BY ROLL,PITCH,YAW RATE COMMANDS

      IF (TA .LT. P1T(JX)) THEN
      JJX = JX - 1
      P1DDOT = (P1A(JX) - P1A(JJX))/(P1T(JX) - P1T(JJX))
      P1DOT = P1DOT + P1DDOT*DT
      ELSE
      P1DDOT = (P1A(JX) - P1A(JJX))/(P1T(JX) - P1T(JJX))
      P1DOT = P1DOT + P1DDOT*DT
      JX = JX + 1
      ENDIF

C     WRITE(6,*) TA,P1DOT,P1DDOT

      IF (TA .LT. P2T(JY)) THEN
      JJY = JY - 1
      P2DDOT = (P2A(JY) - P2A(JJY))/(P2T(JY) - P2T(JJY))
      P2DOT = P2DOT + P2DDOT*DT
      ELSE
      P2DDOT = (P2A(JY) - P2A(JJY))/(P2T(JY) - P2T(JJY))
      P2DOT = P2DOT + P2DDOT*DT
      JY = JY + 1
      ENDIF

      IF (TA .LT. P3T(JZ)) THEN
      JJZ = JZ - 1
      P3DDOT = (P3A(JZ) - P3A(JJZ))/(P3T(JZ) - P3T(JJZ))
      P3DOT = P3DOT + P3DDOT*DT
      ELSE
      P3DDOT = (P3A(JZ) - P3A(JJZ))/(P3T(JZ) - P3T(JJZ))
      P3DOT = P3DOT + P3DDOT*DT
      JZ = JZ + 1
      ENDIF

      IF (TA .LT. P4T(JR)) THEN
      JJR = JR - 1
      P4DDOT = (P4A(JR) - P4A(JJR))/(P4T(JR) - P4T(JJR))
```

```
P4DOT = P4DOT + P4DDOT*DT
ELSE
P4DDOT =  (P4A(JR) - P4A(JJR))/(P4T(JR) - P4T(JJR))
P4DOT = P4DOT + P4DDOT*DT
JR = JR + 1
ENDIF

IF (TA .LT. P5T(JP)) THEN
JJP = JP - 1
P5DDOT = (P5A(JP) - P5A(JJP))/(P5T(JP) - P5T(JJP))
P5DOT = P5DOT + P5DDOT*DT
ELSE
P5DDOT = (P5A(JP) - P5A(JJP))/(P5T(JP) - P5T(JJP))
P5DOT = P5DOT + P5DDOT*DT
JP = JP + 1
ENDIF

IF (TA .LT. P6T(JYA)) THEN
JJYA = JYA - 1
P6DDOT = (P6A(JYA) - P6A(JJYA))/(P6T(JYA) - P6T(JJYA))
P6DOT = P6DOT + P6DDOT*DT
ELSE
P6DDOT = (P6A(JYA) - P6A(JJYA))/(P6T(JYA) - P6T(JJYA))
P6DOT = P6DOT + P6DDOT*DT
JYA = JYA + 1
ENDIF

C    ESTABLISH THE BODY POSITION, VELOCITY, AND ACCELERATION
C    OVER TIME IN INERTIAL REFERENCE FRAME COORDINATES
C    RELATIVE TO THE HOST

     PDOTO = VEX(1)*(1.- DEXP(-(VEX(2))*(TA**2)))
      PDOT(1) = PDOTO*DCOS(P(6)) + P1DOT
      PDOT(2) = PDOTO*DSIN(P(6)) + P2DOT
      PDOT(3) = PDOTO*DTAN(P(5)) + P3DOT
      PDOT(4) = P4DOT
      PDOT(5) = P5DOT
      PDOT(6) = P6DOT

        PDDOTO = VEX(1)*(2.*VEX(2)*TA*DEXP(-(VEX(2))*(TA**2)))
        PDDOT(1) = PDDOTO*DCOS(P(6)) + P1DDOT
        PDDOT(2) = PDDOTO*DSIN(P(6)) + P2DDOT
        PDDOT(3) = PDDOTO*DTAN(P(5)) + P3DDOT
        PDDOT(4) = P4DDOT
        PDDOT(5) = P5DDOT
```

```
      PDDOT(6) = P6DDOT

      P(1) = P(1) + PDOT(1)*DT + PDDOT(1)*DT**2
      P(2) = P(2) + PDOT(2)*DT + PDDOT(2)*DT**2
      P(3) = P(3) + PDOT(3)*DT + PDDOT(3)*DT**2
      P(4) = P(4) + PDOT(4)*DT + PDDOT(4)*DT**2
      P(5) = P(5) + PDOT(5)*DT + PDDOT(5)*DT**2
      P(6) = P(6) + PDOT(6)*DT + PDDOT(6)*DT**2

C CALCULATE COORDINATE TRANSFORM FROM INERTIA FRAME (HOST)
C TO VEHICLE FRAME
C TRANSPOSE OF THE SNAME 1950 CONVENTION (IAW ABKOWICZ)
C ORDER IS YAW, PITCH, ROLL

      DS4 = DSIN(P(4))
      DC4 = DCOS(P(4))
      DS5 = DSIN(P(5))
      DC5 = DCOS(P(5))
      DS6 = DSIN(P(6))
      DC6 = DCOS(P(6))
C
      CTRN(1,1) =  DC5*DC6
      CTRN(1,2) =  DC5*DS6
      CTRN(1,3) = -DS5
      CTRN(2,1) = -DS6*DC4 + DS4*DS5*DC6
      CTRN(2,2) =  DC4*DC6 + DS4*DS5*DS6
      CTRN(2,3) =  DS4*DC5
      CTRN(3,1) =  DS4*DS6 +DC4*DC6*DS5
      CTRN(3,2) = -DS4*DC6 + DC4*DS5*DS6
      CTRN(3,3) =  DC4*DC5
C
      CTRN(4,4) =  1.0
      CTRN(4,5) =  0.0
      CTRN(4,6) = -DS5
      CTRN(5,4) =  0.0
      CTRN(5,5) =  DC4
      CTRN(5,6) =  DS4*DC5
      CTRN(6,4) =  0.0
      CTRN(6,5) = -DS4
      CTRN(6,6) =  DC5*DC4

C  XFORM INERTIA RELATIVE VELOCITIES AND ACCELERATIONS
C  TO VEHICLE RELATIVE
C     CTRN (6X6) * PDOT (6X1) = E (6X1)
C     CTRN (6X6) * PDDOT (6X1) = EDOT (6X1)
```

```
C INITIALIZE THE E AND EDOT MATRICE TO ZERO AT EACH TIME STEP

    DO 110 I=1,6
    E(I) = 0.0
    EDOT(I) = 0.0
  110 CONTINUE

    DO 120 I=1,6
    DO 130 K=1,6
    E(I) = E(I) + PDOT(K)*CTRN(I,K)
    EDOT(I) = EDOT(I) + PDDOT(K)*CTRN(I,K)
  130 CONTINUE
  120 CONTINUE

C CONVERT BODY VELOCITIES TO ADD IN HOST VESSEL SPEED EFFECTS
C HOST SPEED IN (-) P(1) DIRECTION ONLY. ADD AS A POSITIVE SCALAR

    E(1) = E(1) + UHOST*DCOS(P(6))*DCOS(P(5))
    E(2) = E(2) - UHOST*DSIN(P(6))
    E(3) = E(3) + UHOST*DCOS(P(6))*DSIN(P(5))

C SOLVE FOR THE RIGHT HAND SIDE VECTOR WITH TOTAL FORCE
C EDOT (6X1) * LHS (6X6) = RHS (6X1)

C INITIALIZE THE RHSTOT TO ZERO AT EACH TIME STEP
    DO 140 I=1,6
    RHSTOT(I) = 0.0
  140 CONTINUE

    IF (JJ .EQ. 9) THEN

    WRITE(25,178) (acp(I),I=1,3)

    LABEL = 'CTRN'
    CALL MPRINT1(CTRN,6,6,9,LABEL)

    LABEL = 'LHS'
    CALL MPRINT1(A,6,6,9,LABEL)
    ENDIF
    JJ = JJ + 1

    DO 200 I=1,6
    DO 220 K=1,6
    RHSTOT(I) = RHSTOT(I) +A(I,K)*EDOT(K)
```

```
 220 CONTINUE
 200 CONTINUE
    AEDOT1 = RHSTOT(1)

C CALCULATE THE RIGHT HAND SIDE OF THE HYDRODYNAMIC
EQUATIONS
C WITH NO CONTROL FORCE OR INTERACTION FORCE

C SET CROSSFLOW SWITCH JJJ TO 1

    JJJ = 1
    CALL HYDRO

C CALCULATE THE INTERACTION FORCES IN FORCE MODEL ROUTINE

    CALL FM (FX,FY,FZ,MX,MY,MZ,AEDOT1,PTF,ATL,KODE)

C CALCULATE THE CONTROL FORCES TO EFFECT THE
C CHOSEN TRAJECTORY. ADD IN HYDRO FORCE

    RHSFM(1) = FX
    RHSFM(2) = FY
    RHSFM(3) = FZ
    RHSFM(4) = MX
    RHSFM(5) = MY
    RHSFM(6) = MZ

    DO 240 I=1,6
    RHSC(I) = RHSTOT(I) - RHSFM(I)
 240 CONTINUE

C PRINT OUTPUT EVERY 10 DELTA T

    J = J+1
    IF (J .EQ. 10.) THEN
    J = 0

    WRITE(21,176) TA, (RHSTOT(I),I=1,6)
    WRITE(22,178) TA, KODE, (RHS(I),I=1,6)
    WRITE(23,178) TA, KODE, (RHSFM(I),I=1,6)
    WRITE(24,177) TA, KODE, (RHSC(I),I=1,6)
    WRITE(25,176) TA,(P(I),I=1,3),(RTD*P(I),I=4,6)
    WRITE(26,176) TA,(PDOT(I),I=1,3),(RTD*PDOT(I),I=4,6)
    WRITE(27,176) TA,(PDDOT(I),I=1,3),(RTD*PDDOT(I),I=4,6)
    WRITE(28,176) TA,(E(I),I=1,3),(RTD*E(I),I=4,6)
```

```
   WRITE(29,176) TA,(EDOT(I),I=1,3),(RTD*EDOT(I),I=4,6)
176 FORMAT(F5.1,1X,6(E11.4E3,1X))
177 FORMAT(F6.1,1X,I2,1X,6(E11.3E3,1X))
178 FORMAT(F6.1,1X,I2,1X,6(E9.3,1X))
   ENDIF

   RETURN
   END
```

```
C ***********************************************************************
 SUBROUTINE FM (FX,FY,FZ,MX,MY,MZ,
   1                AEDOT1,PTF,ATL,KODE)
C ***********************************************4/96*****************
C  SUBTOUTINE FORCE MODEL -- VEHICLE SPECIFIC FORCE AND MOMENT
C  MODELS ARE PLACED HERE
C
C  CENTER OF X,Y,Z, COORDINATE SYSTEM IS ON HOST AXIS
C  IN THIS VERSION, IT IS PRESUMED THAT A NON-CRASH TRAJECTORY
C  SPECIFIED
C  MODEL IS VALID FOR THE STARBOARD HALF PLANE
C  (ALPHA CALCULATION)
C ***************************************** 4/96 ******************

    REAL*8 MX,MY,MZ,MYC,MZC,MS,MTOT
    REAL*8 P(6),E(6),XC,YC,ZC,XMIN,YMIN,ZMIN
    REAL*8 XMAX,YMAX,ZMAX,D2,HRAD,VRAD,UHOST,DIA
    REAL*8 RHOC,ATLMAX,VLEN,ACP(3),ACOF(6),BCP(3)
    REAL*8 BCOF(6),FX,FY,FZ,DOGS,PTF,PTFS,PTFC
    REAL*8 UZ1LF,UZ1LM,UZ1VF,UZ1VM,FACC,FACS,GAPS
    REAL*8 FYC,FZC,GAP,DOG,PT,SG,FTOT,POSRAD
    REAL*8 UZ2LF,UZ2LM,X,Y,Z,ATL,ATLINV,AXDRAG
    REAL*8 U,V,W,PHI,THETA,PSI,ALPHA,FAREA,C1,C2,C4,C5
    REAL*8 D1,RAT,XS,YS,ZS,AEDOT1,RHS1,TA
    REAL*8 RHS(6)
    REAL*8 DD(1800)

    REAL*4 FOO,FOO1,FOO2,PTF2

    INTEGER KODE
    COMMON /COMDD/ DD
    COMMON /FGEOM/ XC,YC,ZC,XMIN,XMAX,YMIN,YMAX,ZMIN,ZMAX,
   1 D2,HRAD,
    VRAD,UHOST,DIA,RHOC,ATLMAX,VLEN,ACP,ACOF,BCP,BCOF
    EQUIVALENCE (DD( 55),   E(1)),(DD( 61),   P(1))
    EQUIVALENCE (DD( 10),     TA),(DD( 71), RHS(1))


    PI = 3.14159
    DPR = 180.0/pi
    X = P(1)
    Y = P(2)
    Z = P(3)
    U = E(1)
    V = E(2)
```

```
      W = E(3)
      PHI = P(4)
      THETA = P(5)
      PSI = P(6)
      ALPHA = ATAN2(Z,Y)
      FX = 0.0
      FY = 0.0
      FZ = 0.0
      MX = 0.0
      MY = 0.0
      MZ = 0.0
      FAREA = PI/4.*DIA**2
      C1 = .5*RHOC*(UHOST**2)*FAREA
      C2 = C1*VLEN
      C4 = .5*(RHOC*U**2)*FAREA
      C5 = C4*VLEN
      C6 = C5/12.

C IN THIS SUBROUTINE, THE HOST IS TREATED AS A CYLINDER OF RADIUS
HRAD.
C POSRAD IS RADIUS FROM HOST AXIS TO SMALL VEHICLE ORIGIN.

      POSRAD = SQRT(Y*Y + Z*Z)
      D1 = SQRT( (X-XC)**2 + (Y-YC)**2 + (Z-ZC)**2 )

      IF ((Z .LE. ZC) .AND. (Y .LE. YMAX) .AND. (Y .GE. YMIN) .AND.
     1    (X .LE. XMAX) .AND. (X .GE. XMIN)) THEN

C*********************************************************************
C          VEHICLE IS IN THE LAUNCHWAY - ZONE 1                  *
C*********************************************************************

      ATL = ATLMAX-(SQRT( (X-XC)**2 + (Y-YC)**2 + (Z-ZC)**2))/VLEN
      ATLINV = ATL - ATLMAX
      AXDRAG = (.637341 +.853415*(ATLINV)**3)*C1
      IF (AXDRAG .lt. 0.0) AXDRAG = 0.0
      FTOT = AEDOT1 + AXDRAG
      PTF = .5*(FTOT)/C1

      FX = -AXDRAG

      UZ1LF = ((-2.04*ATL**3+5.59*ATL**2-4.49*ATL+1.13)*PTF +
     1 (1.40657-.55068*ATL))

      FY = UZ1LF*C1
```

```
      UZ1LM = -((.153*ATL**3 -.198*ATL**2 - .516*ATL +.508)*PTF)

      MZ = UZ1LM*C2

      KODE = 1


      ELSEIF ( (Z .LE. ZC) .AND. (Y .GE. YMAX) .AND. (X .GE. XMAX)
     1     .AND. (D1 .LT. D2)) THEN

C ***************************************************************
C         VEHICLE IS IN TRANSITION ZONE - HEMI-SPHERE ZONE 2    *
C                                                               *
C ***************************************************************

        IF (D1 .LT. 0.001) D1 = 0.001
        RAT = D2/D1
        XS = XC + RAT*(X-XC)
        YS = YC + RAT*(Y-YC)
        ZS = ZC + RAT*(Z-ZC)
        FACC = (D2-D1)/D2
        FACS = D1/D2
        GAPS = SQRT(YS*YS + ZS*ZS) - HRAD - VRAD
        IF (GAPS .lt. 0.001) GAPS = 0.001
        DOGS = DIA/GAPS
        ATL =  ATLMAX
        ATLINV = 0.0
        AXDRAG = (.637341)*C1
        FXC = AEDOT1 + AXDRAG

C AT LAUNCHER EXIT

        PTFC = .5*(FXC)/C1


        FYC = UZ1LF*C1

        UZ1LF = ((-2.04*ATL**3+5.59*ATL**2-4.49*ATL+1.13)*PTFC +
     1   (1.40657-.55068*ATL))

        UZ1LM = -((.153*ATL**3 -.198*ATL**2 - .516*ATL +.508)*PTFC)

        MZC = UZ1LM*C2
```

```
C PTF EFFECT AT SPHERE INTERSECTION POINT

      FXS = -RHS(1) + AEDOT1
      PTFS = .5*(FXS)/C4
      UZ2LF = -(0.004*DOGS*PTFS)

      UZ2LM = (4.13743*DEXP(-156.197*(1./DOGS)))*PTFS

      Z2LMPTF = UZ2LM*C5

C ADD WALL RELATIVE PITCH AND GAP EFFECT

C APPLY EFFECTIVE PITCH ANGLE DUE TO LAUNCHWAY GEOMETRY

      PTEFF = ((-THETA*SIN(ALPHA) + PSI*COS(ALPHA)) * DPR)
      PT = PTEFF* (XS-XC)/(2.5*VLEN)
CDBG     WRITE(6,*) PTEFF,PT

      SG = SQRT(DOGS)

      UZ2LF = UZ2LF
     1  -((ACP(1)*DEXP(ACP(2)*(1./DOGS)**ACP(3)))+
     1  (ACOF(1)*PT*SG+ACOF(2)*PT*SG*SG+ACOF(3)*PT*SG**3 +
     1  ACOF(4)*PT*PT*SG+ACOF(5)*PT*PT*SG*SG+ACOF(6)*PT*PT*SG**3))

      FS = UZ2LF*C4

      UZ2LM =
     1  (BCOF(1)*PT*SG+BCOF(2)*PT*SG*SG+BCOF(3)*PT*SG**3 +
     1  BCOF(4)*PT*PT*SG+BCOF(5)*PT*PT*SG*SG+BCOF(6)*PT*PT*SG**3)

      MS = UZ2LM*C5+Z2LMPTF

      FX = FACC*(-FXC) + FACS*(-FXS)

      FY = FACC*FYC - FACS*FS*COS(ALPHA) + FACS*RHS(2)
      FZ = FACC*FZC - FACS*FS*SIN(ALPHA) + FACS*RHS(3)

      MY = FACC*MYC - FACS*MS*SIN(ALPHA) + FACS*RHS(5)

      MZ = FACC*MZC + FACS*MS*COS(ALPHA) + FACS*RHS(6)

      PTF = FACC*PTFC + FACS*PTFS

      KODE = 3
```

```
C
      ELSE

C ***************************************************************
C   ZONE IS ZONE 2                                          *
C ***************************************************************

        GAP = SQRT(Y*Y + Z*Z) - HRAD - VRAD
        IF (GAP .LT. 0.001) GAP = 0.001
        DOG = DIA/GAP
        FX = -RHS(1) + AEDOT1

C PTF EFFECT

        PTF = .5*(-RHS(1) + AEDOT1)/C4

        UZ2LF = -(0.004*DOG*PTF)

        UZ2LM = (4.13743*DEXP(-156.197*(1./DOG)))*PTF

        Z2LMPTF = UZ2LM*C5

C ADD WALL RELATIVE PITCH AND GAP EFFECT

        PT = (-THETA*SIN(ALPHA) + PSI*COS(ALPHA)) * DPR
        SG = SQRT(DOG)

        UZ2LF = UZ2LF
     1  -((ACP(1)*DEXP(ACP(2)*(1./DOG)**ACP(3)))+
     1  (ACOF(1)*PT*SG+ACOF(2)*PT*SG*SG+ACOF(3)*PT*SG**3 +
     1  ACOF(4)*PT*PT*SG+ACOF(5)*PT*PT*SG*SG+ACOF(6)*PT*PT*SG**3))

        FTOT = UZ2LF*C4

        UZ2LM =
     1  (BCOF(1)*PT*SG+BCOF(2)*PT*SG*SG+BCOF(3)*PT*SG**3 +
     1  BCOF(4)*PT*PT*SG+BCOF(5)*PT*PT*SG*SG+BCOF(6)*PT*PT*SG**3)

        MTOT = UZ2LM*C5 + Z2LMPTF

        FX =  - FX

        FY =  - FTOT*COS(ALPHA) + RHS(2)

        FZ =  - FTOT*SIN(ALPHA) + RHS(3)
```

```
      MY =  - MTOT*SIN(ALPHA) + RHS(5)

      MZ =    MTOT*COS(ALPHA) + RHS(6)

      KODE = 2

   ENDIF
   RETURN
   END
```

```
C ***********************************************************************
      SUBROUTINE HYDRO
C ***********************************************************************
C DTRC 2510 HYDRODYNAMIC COEFFICIENTS
C NOW INCLUDES ZERO FORWARD SPEED COEFFICIENTS
C ----------------------------------------------------------------------
      IMPLICIT NONE
      INTEGER*2 JJJ,II,J
      INTEGER*2 IDTAR
      REAL*8 TEMP1,TEMP2,TEMP3,TEMP
      REAL*8 UPFRAC,LOFRAC,URACER,URACER0,URACES,URACES0
      REAL*8 DRE3,DSPE3,DSSE3,DRE,DSPE,DSSE
      REAL*8 DRHS1,DRHS2,DRHS3,DRHS4,DRHS5,DRHS6
      REAL*8 ZRHS1,ZRHS2,ZRHS3,ZRHS4,ZRHS5,ZRHS6
      REAL*8 BRHS1,BRHS2,BRHS3,BRHS4,BRHS5,BRHS6
C
      REAL*8 DD(1800)
      COMMON /COMDD/ DD
C
      REAL*8 URUR,USUS,DELRCR,DELRCS,ACOF(8),BCOF(8),acp(4),bcp(4)
      REAL*8 DSP,DSS,DR,DB,UC,DT,RHS(6),E(6),P(6),QPROP,TA,YG,YB
      REAL*8 PHISTERN,VATS,WATS,ETA,CETA,ETAM1,BETAS
      REAL*8 KBETA,WT,BOUY
      REAL*8 ARAPPHI2,ARAPPHI4,CROSSLIM,SINTHETA
      REAL*8 COSTHETA,SINPHI,COSPHI
      REAL*8 UU,VV,WW,PP,QQ,RR,PR,PQ,QR,UV,UW,UP
      REAL*8 UQ,UR,VATTAIL,UUDB
      REAL*8 VP,VR,WP,WQ,SQRVVWW,VSQRVVWW
      REAL*8 WSQRVVWW,CROSS(6),VORT(6)
      REAL*8 DRDR,DSDS,UUDS,UUDR,UABW,UABV,WABW
      REAL*8 QABQ,VABV,RABR,FXP
      REAL*8 PABP,DPDP,UUDP,UT,BETA,ALPHA,WR
      REAL*8 ARRAY(6),WTINH2O,DBDB
C
      REAL*8 XUDOT,XQQ,XRP,XVR,XWQ,XVV,XDRDR,XDSSDSS
      REAL*8 XDSPDSP,XDBDB
      REAL*8 XW,XQ,XWDSP,XWDSS,XQDSS,XQDSP,XVDR,XRDR,XWW,XRR
      REAL*8 XDRE2,XDSSE2,XDSPE2
      REAL*8 YVDOT,YRDOT,YRU,YVU,YVABVU,YVV
      REAL*8 YDR,YDRN,YRABR,YVABV
      REAL*8 YPU,YWP,YPABP,YPQ,YSTAR,YVABVR,YHVABV,YDRE,YDRE3
      REAL*8 ZWDOT,ZQDOT,ZQU,ZWU,ZABWU,ZWW
      REAL*8 ZDSS,ZDSSN,ZQABQ,ZWABW
      REAL*8 ZVP,ZSTAR,ZPR,ZDSP,ZDSPN,ZHWABW,ZDB
      REAL*8 ZDSSE,ZDSPE,ZDSPE3,ZDSSE3
```

```
      REAL*8 KPDOT,KVDOT,KRDOT,KQR,KPU,KRU,KWP,KVU,K4S
      REAL*8 K8S,KI,KDSP,KDSS
      REAL*8 KPABP,KWR,KDR,KDRN,KSTAR
      REAL*8 KDRE,KDRE3,KDSSE,KDSPE,KDSSE3,KDSPE3
      REAL*8 MQDOT,MWDOT,MQU,MWU,MWABWR,MABWU,MWW,MDSS
      REAL*8 MDSSN,MQABQ,MWABW
      REAL*8 MRP,MSTAR,MVP,MDSP,MDSPN,MHWABW,MDB
      REAL*8 MDSSE,MDSPE,MDSSE3,MDSPE3
      REAL*8 NRDOT,NVDOT,NRU,NVU,NVABVR,NABVU,NVV,NDR
      REAL*8 NDRN,NVABV,NRABR
      REAL*8 NWP,NPQ,NSTAR,NPU,NHVABV,NDRE,NDRE3
      REAL*8 IYY,IZZ,IXX,SLEN,MASS,ZB,ZG,XB,XG,XSTERN
      REAL*8 XFORWARD,KTAINF,UAINF,IXZ,IXY,IYZ,YPDOT,NPDOT
      EQUIVALENCE (DD(  1),    DT), (DD( 10),    TA)
      EQUIVALENCE (DD( 11),   JJJ), (DD( 16),  BETA)
      EQUIVALENCE (DD( 15),  ALPHA)
      EQUIVALENCE (DD( 17),   FXP ),(DD( 18),  QPROP)
      EQUIVALENCE (DD( 19),   ETA ),(DD( 20),   CETA)
      EQUIVALENCE (DD( 55),   E(1)),(DD( 61),   P(1))
      EQUIVALENCE (DD( 67),    DSS),(DD( 68),    DSP)
      EQUIVALENCE (DD( 69),     DR),(DD( 71), RHS(1))
      EQUIVALENCE (DD(179),     DB)
      EQUIVALENCE (DD(260),CROSS(1)),(DD(266), VORT(1))
      EQUIVALENCE (DD(272),VATTAIL)
C
      EQUIVALENCE (DD(301),XUDOT  ),(DD(303),XW    )
      EQUIVALENCE (DD(305),XQ     ),(DD(307),XQQ   )
      EQUIVALENCE (DD(309),XRR    ),(DD(311),XRP   )
      EQUIVALENCE (DD(313),XVR    ),(DD(315),XWQ   )
      EQUIVALENCE (DD(317),XVV    ),(DD(319),XWW   )
      EQUIVALENCE (DD(321),XDBDB  ),(DD(323),XDRDR )
      EQUIVALENCE (DD(325),XDSSDSS ),(DD(327),XDSPDSP )
      EQUIVALENCE (DD(329),XDRE2  ),(DD(331),XDSSE2 )
      EQUIVALENCE (DD(333),XDSPE2 )
      EQUIVALENCE (DD(1703),XWDSP ),(DD(1705),XWDSS )
      EQUIVALENCE (DD(1707),XQDSP ),(DD(1709),XQDSS )
      EQUIVALENCE (DD(1711),XVDR  ),(DD(1713),XRDR  )
C
      EQUIVALENCE (DD(338),YVDOT  ),(DD(340),YPDOT  )
      EQUIVALENCE (DD(342),YRDOT  ),(DD(344),YPABP  )
      EQUIVALENCE (DD(346),YPQ    ),(DD(348),YRU    )
      EQUIVALENCE (DD(350),YPU    ),(DD(352),YVU    )
      EQUIVALENCE (DD(354),YVABVR ),(DD(356),YVABVU )
      EQUIVALENCE (DD(358),YVV    ),(DD(360),YDR    )
      EQUIVALENCE (DD(362),YDRN   ),(DD(364),YRABR  )
```

```
      EQUIVALENCE (DD(366),YVABV  ),(DD(368),YWP    )
      EQUIVALENCE (DD(370),YSTAR  ),(DD(372),YHVABV )
      EQUIVALENCE (DD(374),YDRE3  ),(DD(376),YDRE   )
C
      EQUIVALENCE (DD(390),ZWDOT  ),(DD(392),ZQDOT  )
      EQUIVALENCE (DD(394),ZQU    ),(DD(396),ZVP    )
      EQUIVALENCE (DD(398),ZSTAR  ),(DD(400),ZWU    )
      EQUIVALENCE (DD(402),ZABWU  ),(DD(404),ZWW    )
      EQUIVALENCE (DD(406),ZDB    ),(DD(408),ZDSS   )
      EQUIVALENCE (DD(410),ZDSSN  ),(DD(412),ZDSP   )
      EQUIVALENCE (DD(414),ZDSPN  ),(DD(416),ZQABQ  )
      EQUIVALENCE (DD(418),ZWABW  ),(DD(420),ZHWABW )
      EQUIVALENCE (DD( 422),ZDSSE3 ),(DD( 424),ZDSPE3 )
      EQUIVALENCE (DD( 426),ZDSSE  ),(DD( 428),ZDSPE  )
      EQUIVALENCE (DD(1717),ZPR    )
C
      EQUIVALENCE (DD(440),KVDOT  ),(DD(442),KPDOT  )
      EQUIVALENCE (DD(444),KRDOT  ),(DD(446),KQR    )
      EQUIVALENCE (DD(448),KPABP  ),(DD(450),KPU    )
      EQUIVALENCE (DD(452),KRU    ),(DD(454),KWP    )
      EQUIVALENCE (DD(456),KSTAR  ),(DD(458),KVU    )
      EQUIVALENCE (DD(460),KI     ),(DD(462),K4S    )
      EQUIVALENCE (DD(464),K8S    ),(DD(466),KDR    )
      EQUIVALENCE (DD(468),KDRN   ),(DD(470),KDSS   )
      EQUIVALENCE (DD(472),KDSP   ),(DD(474),KDRE   )
      EQUIVALENCE (DD(476),KDRE3  ),(DD(478),KDSSE  )
      EQUIVALENCE (DD(480),KDSPE  ),(DD(482),KDSSE3 )
      EQUIVALENCE (DD(484),KDSPE3 )
      EQUIVALENCE (DD(1721),KWR   )
C
      EQUIVALENCE (DD(494),MWDOT  ),(DD(496),MQDOT  )
      EQUIVALENCE (DD(498),MRP    ),(DD(500),MQU    )
      EQUIVALENCE (DD(502),MWU    ),(DD(504),MSTAR  )
      EQUIVALENCE (DD(506),MWABWR ),(DD(508),MABWU  )
      EQUIVALENCE (DD(510),MWW    ),(DD(512),MDSS   )
      EQUIVALENCE (DD(514),MDSSN  ),(DD(516),MDSP   )
      EQUIVALENCE (DD(518),MDSPN  ),(DD(520),MDB    )
      EQUIVALENCE (DD(522),MQABQ  ),(DD(524),MWABW  )
      EQUIVALENCE (DD( 526),MHWABW ),(DD( 528),MDSSE3 )
      EQUIVALENCE (DD( 530),MDSPE3 ),(DD( 532),MDSSE  )
      EQUIVALENCE (DD( 534),MDSPE  )
      EQUIVALENCE (DD(1723),MVP    )
C
      EQUIVALENCE (DD(546),NVDOT  ),(DD(548),NPDOT  )
      EQUIVALENCE (DD(550),NRDOT  ),(DD(552),NPQ    )
```

```
      EQUIVALENCE (DD(554),NPU    ),(DD(556),NRU    )
      EQUIVALENCE (DD(558),NSTAR  ),(DD(560),NVU    )
      EQUIVALENCE (DD(562),NVABVR ),(DD(564),NABVU  )
      EQUIVALENCE (DD(566),NVV    ),(DD(568),NDR    )
      EQUIVALENCE (DD(570),NDRN   ),(DD(572),NVABV  )
      EQUIVALENCE (DD(574),NRABR  ),(DD(576),NWP    )
      EQUIVALENCE (DD(578),NHVABV ),(DD(580),NDRE3  )
      EQUIVALENCE (DD(582),NDRE   )
C
      EQUIVALENCE (DD(593),SLEN   ),(DD(596),IYY    )
      EQUIVALENCE (DD(598),IZZ    ),(DD(600),IXX    )
      EQUIVALENCE (DD(602),IXZ    ),(DD(604),IYZ    )
      EQUIVALENCE (DD(606),IXY    ),(DD(608),MASS   )
      EQUIVALENCE (DD(610),WT     ),(DD(612),BOUY   )
      EQUIVALENCE (DD(614),ZB     ),(DD(616),ZG     )
      EQUIVALENCE (DD(618),XB     ),(DD(620),XG     )
      EQUIVALENCE (DD(622),XSTERN ),(DD(624),XFORWARD)
      EQUIVALENCE (DD(626),YG     ),(DD(628),YB     )
      EQUIVALENCE (DD(629),WTINH2O )
      EQUIVALENCE (DD(630),CROSSLIM)
      EQUIVALENCE (DD(631),LOFRAC ),(DD(632),UPFRAC )
C
      EQUIVALENCE (DD(848),KTAINF ),(DD(849),UAINF  )
      EQUIVALENCE (DD(850),URACER0 ),(DD(851),URACES0 )
      EQUIVALENCE (DD(858),URACER ),(DD(859),URACES )
      EQUIVALENCE (DD(866),DRE    ),(DD(867),DSSE   )
      EQUIVALENCE (DD(868),DSPE   )
      EQUIVALENCE (DD(1758),ARRAY(1)),(DD(1764),ACOF(1))
      EQUIVALENCE (DD(1800),botdep), (DD(1772),BCOF(1))
      EQUIVALENCE (DD(1780),acp(1)), (DD(1788), bcp(1))

C
C FOR EFFICIENCY THE FOLLOWING VARIABLES ARE CALCULATED
C
      UU = E(1)*E(1)
      VV = E(2)*E(2)
      WW = E(3)*E(3)
      UT = DSQRT(UU+VV+WW)
      PP = E(4)*E(4)
      QQ = E(5)*E(5)
      RR = E(6)*E(6)
      PR = E(4)*E(6)
      PQ = E(4)*E(5)
      QR = E(5)*E(6)
      UV = E(1)*E(2)
```

```
      UW = E(1)*E(3)
      UP = E(1)*E(4)
      UQ = E(1)*E(5)
      UR = E(1)*E(6)
      VP = E(2)*E(4)
      VR = E(2)*E(6)
      WP = E(3)*E(4)
      WQ = E(3)*E(5)
      WR = E(3)*E(6)
      URUR = URACER*URACER
      USUS = URACES*URACES
      DELRCR = URACER - URACER0
      DELRCS = URACES - URACES0
      VATS = E(2) + XSTERN*E(6)
      WATS = E(3) - XSTERN*E(5)
C
      IF( DABS(URACER) .GT. 0.1) THEN
        DRE  = DR - DATAN2(  VATS,URACER )
       ELSE
        DRE = DR
      ENDIF
C
      IF( DABS(URACER) .GT. 0.1) THEN
        DSSE = DSS - DATAN2( WATS,URACES )
        DSPE = DSP - DATAN2( WATS,URACES )
       ELSE
        DSSE = DSS
        DSPE = DSP
      ENDIF
C
      DRE3   = DRE*DRE*DRE
      DSPE3  = DSPE*DSPE*DSPE
      DSSE3  = DSSE*DSSE*DSSE
      DRDR = DR*DR
      DBDB = DB*DB
      DSDS = DSS*DSS
      DPDP = DSP*DSP
      UUDR = UU*DR
      UUDB = UU*DB
      UUDP = UU*DSP
      UUDS = UU*DSS
      UABW = E(1)*ABS(E(3))
      UABV = E(1)*ABS(E(2))
      WABW = E(3)*ABS(E(3))
      QABQ = E(5)*ABS(E(5))
```

```
      VABV = E(2)*ABS(E(2))
      PABP = E(4)*ABS(E(4))
      RABR = E(6)*ABS(E(6))
      SQRVVWW  = DSQRT(VV+WW)
      VSQRVVWW  = E(2) * SQRVVWW
      WSQRVVWW  = E(3) * SQRVVWW
      WTINH2O  = WT - BOUY
      SINPHI   = DSIN(P(4))
      COSPHI   = DCOS(P(4))
      SINTHETA  = DSIN(P(5))
      COSTHETA  = DCOS(P(5))
C
      IF( (DABS(VATS) .GT. 0.001) .OR. (DABS(WATS) .GT. 0.001)) THEN
       TEMP1 = VATS*VATS
       TEMP2 = WATS*WATS
       TEMP3 = TEMP1+TEMP2
       ARAPPHI2 = TEMP3*2.*VATS*WATS/TEMP3
       ARAPPHI4 = TEMP3*4.*VATS*WATS*(TEMP2 - TEMP1)/(TEMP3*TEMP3)
       BETAS   = DATAN2(DSQRT(TEMP3),E(1))
       PHISTERN = DATAN2(WATS,-VATS)
      ELSE
       ARAPPHI2 = 0.0
       ARAPPHI4 = 0.0
       BETAS   = 0.0
       PHISTERN = 0.0
      ENDIF
C
      IF((DABS(E(3)) .GT. 0.1D-10) .AND. (DABS(E(1)) .GT. 0.01)) THEN
       ALPHA = DATAN2(E(3),E(1))
      ELSE
       ALPHA = 0.0
      ENDIF
C
      IF( (DABS(E(2)) .GT. 0.1D-20) .AND. (DABS(UT) .GT. .01)) THEN
       BETA = DASIN(-E(2)/UT)
      ELSE
       BETA = 0.0
      ENDIF
C
C FOR EFFICIENCY CALL THESE SUBROUTINES ONLY ONCE
C
      IF ( JJJ .EQ. 1)  THEN
       CALL VORTEX
       CALL CROSFLOW
       CALL PROP
```

```
C
      DO 345 IDTAR = 1,10
      CALL TOWDARRY(IDTAR)
345   CONTINUE
     ENDIF
C
     CETA
     ETAM1 = ETA - 1.0
C
C  CALCULATE RIGHT HAND SIDES OF EQUATIONS OF MOTION
C
C  AXIAL FORCES ZERO SPEED MODEL
C
     ZRHS1 = 0.0
C
C LATERAL FORCE ZERO SPEED MODEL
C
     ZRHS2 =  YHVABV*VATS*DABS(VATS)
C
C NORMAL FORCE ZERO SPEED MODEL
C
     ZRHS3 =  ZHWABW*WATS*DABS(WATS)
C
C ROLL MOMENT ZERO SPEED MODEL
C
     ZRHS4 =  KPABP*PABP
C
C PITCH MOMENT ZERO SPEED MODEL
C
     ZRHS5 =  MHWABW*WATS*DABS(WATS)
C
C YAW MOMENT ZERO SPEED MODEL
C
     ZRHS6 = NHVABV*VATS*DABS(VATS)
C
C CALCULATE DTRC HYDRODYNAMIC FORCES
C  HYDRODYNAMIC AXIAL FORCES
C
     DRHS1 =  XQQ*QQ + XRR*RR + XRP*PR + XVR*VR + XWQ*WQ + XVV*VV
    1 + XW*UW + XWW*WW + XQ*UQ
    1 + (XDSSDSS*DSDS + XDSPDSP*DPDP + XDRDR*DRDR +
    1 +  XDBDB*DBDB)*UU
    1 + (XWDSP*DSP + XWDSS*DSS)*UW + (XQDSP*DSP + XQDSS*DSS)*UQ
    1 + (XVDR*UV + XRDR*UR)*DR
C
```

```
C HYDRODYNAMIC LATERAL  FORCE
C
      DRHS2 = YPABP*PABP + YPQ*PQ
     1  + YRU*UR + YPU*UP + YVU*UV + YVABVU*UABV + YVV*VV +
     1  + YWP*WP
     1  + (YDR + YDRN*ETAM1)*UUDR + YVABV*VABV + YRABR*RABR +
     1  + YSTAR*UU
     1  + YVABVR*VSQRVVWW
C
C HYDRODYNAMIC NORMAL FORCE
C
      DRHS3 = ZQU*UQ + ZWU*UW + ZABWU*UABW + ZVP*VP + ZSTAR*UU
     1 + (ZDSS + ZDSSN*ETAM1) * UUDS + (ZDSP + ZDSPN*ETAM1) * UUDP
     1 + ZDB*UUDB
     1 + ZQABQ*QABQ + ZWABW*WABW + ZPR*PR +
     1 + ZWW*DABS(E(3))*SQRVVWW
C
C HYDRODYNAMIC ROLL MOMENT
C
      KBETA = BETAS*BETAS*(UU + VATS*VATS + WATS*WATS)
      DRHS4 =  KPU*UP + KRU*UR + KQR*QR + KWP*WP
     1 + ((KDR + KDRN*ETAM1)*DR + KDSS*DSS + KDSP*DSP + KSTAR)*UU
     1 + KWR*WR + KVU*UV + KPABP*PABP + KI*VATTAIL + ARAPPHI4*K4S
C     1 + KBETA*(K4S*DSIN(4.*PHISTERN) + K8S*DSIN(8.*PHISTERN))
C
C HYDRODYNAMIC PITCH MOMENT
C
      DRHS5 = MQU*UQ + MQABQ*QABQ + MWABW*WABW
     1 + MVP*VP + MRP*PR + MSTAR*UU + MDB*UUDB
     1 + MWU*UW + MWABWR*WSQRVVWW + MABWU*UABW +
     1 + MWW*DABS(E(3))*SQRVVWW
     1 + (MDSS + MDSSN*ETAM1)*UUDS + (MDSP + MDSPN*ETAM1)*UUDP
C
C HYDRODYNAMIC YAW MOMENT
C
      DRHS6 =  NPQ*PQ + NPU*UP + NWP*WP + NSTAR*UU
     1 + NRU*UR + NVU*UV + NVABVR*VSQRVVWW + NABVU*UABV +
     1 +  NVV*VV
     1 + (NDR + NDRN*ETAM1)*UUDR  + NVABV*VABV + NRABR*RABR
C
C CALCULATE BODY FORCES, AND SUM FORCES INDEPENDENT OF ALPHA
OR BETA
C USED FOR BOTH LOW AND HIGH ANGLE OF ATTACK MODELS
C
C BODY AXIAL FORCE
```

```
      BRHS1 = -MASS*( WQ - VR - XG*(QQ + RR) + ZG*PR)
     1  - WTINH2O*SINTHETA + FXP + ARRAY(1)
     1  + XDRE2*DRE*DRE*URUR
     1  + (XDSSE2*DSSE*DSSE + XDSPE2*DSPE*DSPE)*USUS
C
C BODY LATERAL FORCE
C
      BRHS2 = -MASS*(UR - WP + XG*PQ  + ZG*QR )
     1  + WTINH2O*COSTHETA*SINPHI
     1  + CROSS(2) + VORT(2) + ARRAY(2)
     1  + YDRE*( DELRCR*(-XSTERN*E(6) - E(2)) + DR*URUR)
     1  + YDRE3*DRE3*URUR
c    1  + YDRE3*DRE3*URUR
C
C BODY NORMAL FORCE
C
      BRHS3 = -MASS*(VP - UQ + XG*PR - ZG*(PP + QQ))
     1 + WTINH2O*COSTHETA*COSPHI
     1 + CROSS(3) + VORT(3) + ARRAY(3)
     1 + ZDSSE*( DELRCS*(XSTERN*E(5) - E(3)) + DSS*USUS)
     1 + ZDSPE*( DELRCS*(XSTERN*E(5) - E(3)) + DSP*USUS)
     1 + (ZDSPE3*DSPE3 + ZDSSE3*DSPE3)*USUS
C
C BODY ROLL MOMENT
C
      BRHS4 = MASS*ZG*(UR - WP)
     1 - (ZG*WT - ZB*BOUY)*COSTHETA*SINPHI
     1 + (YG*WT - YB*BOUY)*COSTHETA*COSPHI
     1 + QPROP + VORT(4) + ARRAY(4)
     1 + KDRE*( DELRCR*(XSTERN*E(6) - E(2)) + DR*URUR)
     1 + KDRE3*DRE3*URUR
     1 + KDSSE * (DELRCS*(XSTERN*E(5) - E(3)) + DSS*USUS)
     1 + KDSPE * (DELRCS*(XSTERN*E(5) - E(3)) + DSP*USUS)
     1 + (KDSPE3*DSPE3 + KDSSE3*DSPE3)*USUS
C
C BODY PITCH MOMENT
C
      BRHS5 = (-IXX + IZZ)*PR + MASS*(-ZG*(WQ - VR) + XG*(VP - UQ))
     1 - (XG*WT - XB*BOUY)*COSTHETA*COSPHI
     1 - (ZG*WT - ZB*BOUY)*SINTHETA
     1 + CROSS(5) + VORT(5) + ARRAY(5)
     1 + MDSSE * (DELRCS*(XSTERN*E(5) - E(3)) + DSS*USUS)
     1 + MDSPE * (DELRCS*(XSTERN*E(5) - E(3)) + DSP*USUS)
     1 + (MDSPE3*DSPE3 + MDSSE3*DSPE3)*USUS
C
```

```
C BODY YAW MOMENT
C
      BRHS6 = (-IYY + IXX)*PQ - MASS*(XG*(UR - WP))
     1 + (XG*WT - XB*BOUY)*COSTHETA*SINPHI
     1 + (YG*WT - YB*BOUY)*SINTHETA
c    1 + (XG*WT - XB*(BOUY))*COSTHETA*SINPHI
c    1 + (YG*WT - YB*(BOUY))*SINTHETA
     1 + CROSS(6) + VORT(6) + ARRAY(6)
     1 + NDRE*(DELRCR*(-XSTERN*E(6) - E(2)) + DR*URUR)
     1 + NDRE3*DRE3*URUR
C
C SUM ALL FORCES
C
      RHS(1) = BRHS1 + LOFRAC*DRHS1 + UPFRAC*ZRHS1
      RHS(2) = BRHS2 + LOFRAC*DRHS2 + UPFRAC*ZRHS2
      RHS(3) = BRHS3 + LOFRAC*DRHS3 + UPFRAC*ZRHS3
      RHS(4) = BRHS4 + LOFRAC*DRHS4 + UPFRAC*ZRHS4
      RHS(5) = BRHS5 + LOFRAC*DRHS5 + UPFRAC*ZRHS5
      RHS(6) = BRHS6 + LOFRAC*DRHS6 + UPFRAC*ZRHS6

C
      RETURN
      END
```

Appendix B. Trajectory input files.

This appendix presents the geometry limitation file and trajectory command files used to generate the simulation trajectories.

Geometry Limitation File GEOM.LIM

```
  93.57   16.50    0.     XC   YC   ZC   [FT]
  85.275  15.04    0.          XMIN YMIN ZMIN [FT]
  93.576  16.50    0.          XMAX YMAX ZMAX [FT]
   8.00   16.5     0.8125 10.5  D2   HRAD VRAD SLEN [FT]
   0.1    1.625    2.0  1.47    VHOST [FT/SEC] DIA [FT] RHOC [SLUG/FT^3]
ATLMAX
```

Traj_1

2.0 0.04 VELOCITY AND ACCELERATION EXPONENTS
XVEL,YVEL,ZVEL CORRECTION COMMANDS [FT/SEC] [SEC]

P1A	P1T	P2A	P2T	P3A	P3T
0.00	0.00	0.00	0.00	0.00	0.00
0.00	20.00	0.00	600.00	0.00	600.00
0.00	30.00	0.00	700.00	0.00	700.00
0.00	35.00	0.00	750.00	0.00	720.00
0.00	40.00	0.00	800.00	0.00	750.00
0.00	799.00	0.00	850.00	0.00	800.00
0.00	899.00	0.00	860.00	0.00	810.00
0.00	900.00	0.00	870.00	0.00	820.00
0.00	990.00	0.00	880.00	0.00	850.00
0.00	999.00	0.00	900.00	0.00	900.00

ROLL,PITCH,YAW RATE COMMANDS [DEG/SEC] [SEC]

P4A	P4T	P5A	P5T	P6A	P6T
0.00	0.00	0.00	0.00	0.00	0.00
0.00	600.00	0.00	600.00	0.00	20.00
0.00	700.00	0.00	700.00	0.00	25.00
0.00	750.00	0.00	750.00	0.00	28.00
0.00	800.00	0.00	800.00	0.00	750.00
0.00	900.00	0.00	850.00	0.00	800.00
0.00	999.00	0.00	860.00	0.00	810.00
0.00	999.00	0.00	870.00	0.00	820.00
0.00	999.00	0.00	880.00	0.00	850.00
0.00	999.00	0.00	900.00	0.00	900.00

Traj_2

2.0 0.04 VELOCITY AND ACCELERATION EXPONENTS
XVEL,YVEL,ZVEL CORRECTION COMMANDS [FT/SEC] [SEC]

P1A	P1T	P2A	P2T	P3A	P3T
0.00	0.00	0.00	0.00	0.00	0.00
0.00	20.00	0.00	600.00	0.00	600.00
0.00	30.00	0.00	700.00	0.00	700.00
0.00	35.00	0.00	750.00	0.00	720.00
0.00	40.00	0.00	800.00	0.00	750.00
0.00	799.00	0.00	850.00	0.00	800.00
0.00	899.00	0.00	860.00	0.00	810.00
0.00	900.00	0.00	870.00	0.00	820.00
0.00	990.00	0.00	880.00	0.00	850.00
0.00	999.00	0.00	900.00	0.00	900.00

ROLL,PITCH,YAW RATE COMMANDS [DEG/SEC] [SEC]

P4A	P4T	P5A	P5T	P6A	P6T
0.00	0.00	0.00	0.00	0.00	0.00
0.00	600.00	0.00	600.00	0.00	20.00
0.00	700.00	0.00	700.00	-2.00	25.00
0.00	750.00	0.00	750.00	0.00	30.00
0.00	800.00	0.00	800.00	0.00	35.00
0.00	900.00	0.00	850.00	0.00	36.00
0.00	999.00	0.00	860.00	0.00	810.00
0.00	999.00	0.00	870.00	0.00	820.00
0.00	999.00	0.00	880.00	0.00	850.00
0.00	999.00	0.00	900.00	0.00	900.00

Traj_3

2.0 0.04 VELOCITY AND ACCELERATION EXPONENTS
XVEL,YVEL,ZVEL CORRECTION COMMANDS [FT/SEC] [SEC]

P1A	P1T	P2A	P2T	P3A	P3T
0.00	0.00	0.00	0.00	0.00	0.00
0.00	10.00	0.00	600.00	0.00	600.00
0.00	15.00	0.00	700.00	0.00	700.00
0.00	20.00	0.00	750.00	0.00	720.00
-4.00	30.00	0.00	800.00	0.00	750.00
-4.00	799.00	0.00	850.00	0.00	800.00
-4.00	899.00	0.00	860.00	0.00	810.00
-4.00	900.00	0.00	870.00	0.00	820.00
-4.00	990.00	0.00	880.00	0.00	850.00
-4.00	999.00	0.00	900.00	0.00	900.00

ROLL,PITCH,YAW RATE COMMANDS [DEG/SEC] [SEC]

P4A	P4T	P5A	P5T	P6A	P6T
0.00	0.00	0.00	0.00	0.00	0.00
0.00	600.00	0.00	600.00	0.00	20.00
0.00	700.00	0.00	700.00	0.00	25.00
0.00	750.00	0.00	750.00	0.00	28.00
0.00	800.00	0.00	800.00	0.00	750.00
0.00	900.00	0.00	850.00	0.00	800.00
0.00	999.00	0.00	860.00	0.00	810.00
0.00	999.00	0.00	870.00	0.00	820.00
0.00	999.00	0.00	880.00	0.00	850.00
0.00	999.00	0.00	900.00	0.00	900.00

Traj_4

Traj_4 uses Traj_1 with Vhost = 0.01 in Geom.lim

Appendix C. Model Fit Analysis of Variance.

A/L	Variance Source	Degrees of Freedom	Sum of Squares	Mean Square	F Ratio	Prob > F
.68	Model	1	0.04653676	0.046537	4.0022	0.0627
	Error	16	0.18604585	0.011628		
	Total	17	0.23258261			
.84	Model	1	0.13460215	0.134602	2.6603	0.1339
	Error	10	0.50595732	0.050596		
	Total	11	0.64055947			
1.0	Model	1	11.940734	11.9407	25.7911	<0.0001
	Error	70	32.408566	0.4630		
	Total	71	44.349300			
1.16	Model	1	3.2888807	3.28888	88.9794	<0.0001
	Error	16	0.5913961	0.03696		
	Total	17	3.8802768			
1.32	Model	1	4.7664514	4.76645	166.9032	<0.0001
	Error	34	0.9709780	0.02856		
	Total	35	5.9374294			
1.46	Model	1	0.46515718	0.465157	31.1761	<0.0002
	Error	10	0.14920309	0.01492		
	Total	11	0.61436			

Table C-1 ANOVA Table for PTF Effect on Launchway Force

A/L	Variance Source	Degrees of Freedom	Sum of Squares	Mean Square	F Ratio	Prob > F
.68	Model	1	0.04653676	0.046537	4.0022	0.0627
	Error	16	0.18604585	0.011628		
	Total	17	0.23258261			
.84	Model	1	0.13460215	0.134602	2.6603	0.1339
	Error	10	0.50595732	0.050596		
	Total	11	0.64055947			
1.0	Model	1	11.940734	11.9407	25.7911	<0.0001
	Error	70	32.408566	0.4630		
	Total	71	44.349300			
1.16	Model	1	3.2888807	3.28888	88.9794	<0.0001
	Error	16	0.5913961	0.03696		
	Total	17	3.8802768			
1.32	Model	1	4.7664514	4.76645	166.9032	<0.0001
	Error	34	0.9709780	0.02856		
	Total	35	5.9374294			
1.46	Model	1	0.46515718	0.465157	31.1761	<0.0002
	Error	10	0.14920309	0.01492		
	Total	11	0.61436			

Table C-2 ANOVA Table for PTF effect on Launchway Moment